The septin cytoskeleton is associated with distinct myelin structures of the central and peripheral nervous system

Inauguraldissertation

zur
Erlangung der Würde eines Doktors der Philosophie
vorgelegt der
Philosophisch-Naturwissenschaftlichen Fakultät
der Universität Basel

von

Andres Buser

aus Känerkinden (BL)

Basel, 2008

Genehmigt von der Philosophisch-Naturwissenschaftlichen Fakultät
auf Antrag von

Prof. Dr. Nicole Schaeren-Wiemers
Prof. Dr. Markus Rüegg
PD. Dr. Thomas Meier

Basel, den 24. Juni 2008

Prof. Dr. Hans-Peter Hauri

To my parents

Table of contents

1 Acknowledgments 7

2 Abbreviations 8

3 Summary 11

4 Introduction 12
4.1 From polarized transport to the mature myelin sheath 12
4.2 Myelin 12
4.2.1 Myelination 12
4.2.2 Myelinating cells 14
4.2.2.1 Oligodendrocytes 15
4.2.2.2 Schwann cells 16
4.3 Myelin structure and function 17
4.3.1 The nodes of Ranvier 19
4.3.2 Myelin proteins 21
4.3.2.1 MBP, PLP and P0 21
4.3.2.2 MAG and MOG 22
4.3.2.3 MAL 23
4.4 Polarized cells 24
4.4.1 Membrane rafts 25
4.4.2 Polarized sorting and trafficking mechanisms 26
4.4.3 MAL in polarized epithelial cells 28
4.5 Cytoskeleton elements in myelinating cells 29
4.5.1 Schwann cells 29
4.5.2 Oligodendrocytes 30
4.6 The septins 31
4.6.1 Septins in yeast 31
4.6.2 Septin complex formation and structure 33
4.6.3 Septins in the mammalian central nervous system 36
4.6.4 Septins in oligodendrocytes and Schwann cells 37
4.7 The contribution of cytoskeleton elements to subdomain formation in myelinating glial cells 37

5 Motivation and Aim of the Work 39

6 Material and Methods 40
6.1 Custom peptide antibodies 40
6.1.1 Peptide sequences 40
6.1.2 Peptide synthesis and immunization 40
6.1.3 Antibody purification 40

6.1.4 Western blot analysis with custom-made anti-septin antibodies 41
6.2 Other antibodies 41
6.3 Yeast two-hybrid screen 42
6.4 Western blot analysis 42
6.5 Immunohistochemistry 43
6.5.1 Teased peripheral nerve fibers 43
6.5.2 Cryostat sections of fresh frozen human femoralis nerve tissue 43
6.5.3 Cell cultures 43
6.6 Electron microscopy 44
6.7 Immobilization of IgG for Immunoprecipitation 44
6.7.1 SeizeX ProteinA Immunoprezipitation kit (Pierce, USA) 44
6.7.2 ProFound Co-Immunoprecipitation kit (Pierce, USA) 44
6.7.3 Affi-Gel Hz Immunoaffinity kit (Biorad, USA) 45
6.8 Immunoprecipitation 45
6.8.1 Sample preparation 45
6.8.2 Immunoprecipitation 46
6.9 GST pull down assays 46
6.9.1 Sept6 with MAL(1-55)-GST 46
6.9.2 Sept2/ 6/ 7 trimer with MAL(1-24)-GST 47
6.9.2.1 Generation of the MAL(1-24)-GST construct 47
6.9.2.2 Expression and purification of recombinant GST fusion proteins 48
6.9.2.3 GST pull down assay 48
6.10 Light cycler quantitative real-time PCR 49
6.10.1 Primer pairs for real-time PCR 49
6.10.2 Standard curve generation for real-time PCR 51
6.10.3 Total RNA isolation from sciatic nerve tissue 51
6.10.4 Total RNA isolation from cultured cells 51
6.10.5 Reverse transcription reaction 52
6.10.6 Quantitative real-time PCR 52
6.11 Cell culture 52
6.11.1 Standard cell culture 52
6.11.2 Primary cell culture 52
6.11.2.1 DRG/ Schwann cell co-cultures 52
6.11.2.2 Primary oligodendrocytes from neurospheres 53
6.12 RNA interference 54
6.12.1 Target sequences 54
6.12.2 Generation of retroviral RNAi constructs 55
6.12.2.1 RNAi hairpin oligonucleotide sequences 55
6.12.2.2 Annealing of hairpin oligonucleotides 55
6.12.2.3 Ligation and transformation 55
6.12.2.4 Production of retroviral stocks 56
6.12.3 Retroviral infection 56
6.13 Generation of mCherry tagged Sept2 constructs 57

6.13.1 Subcloning of the mCherry sequence into the retroviral pMX vector ... 57
6.13.2 Subcloning Sept2 wild type into the pMX-mCherry vector ... 58
6.13.3 Subcloning the S51N Sept2 mutant sequence into the pMX-mCherry vector ... 58
6.13.4 Mutation elimination in the pMX-S51N-mCherry construct ... 59
6.13.5 Production of retroviral stocks ... 61

7 Results ... 62
7.1 The cytoskeleton protein Sept6 interacts with the myelin protein MAL ... 62
7.1.1 Sept6 is a potential interaction partner of MAL ... 62
7.1.2 Verification of the Sept6 / MAL interaction by GST pull down ... 63
7.1.3 The Sept2/ 6 / 7 complex does not interact with MAL ... 63
7.1.4 Sept6 and MAL are co-targeted to myelin fractions ... 64
7.2 The MAL^{null} phenotype is not replicated in Sept6^{null} mice ... 65
7.3 Sept11 compensates for loss of Sept6 in CNS myelin ... 66
7.4 Oligodendrocytes express and developmentally regulate a complex septin scaffold ... 67
7.5 A distinct septin scaffold is upregulated during PNS myelination ... 70
7.6 Discrete septin complexes interact with myelin membranes ... 73
7.6.1 Sample preparation for immunoprecipitation ... 73
7.6.2 Co-immunoprecipitation for Sept6 using proteinA sepharose ... 74
7.6.3 Co-immunoprecipitation for Sept6 using activated agarose ... 75
7.6.4 Co-immunoprecipitation for Sept2 ... 76
7.6.5 A septin scaffold differentially interacts with myelin membranes ... 81
7.7 The incorporation of septins into myelin is not dependant on MAL ... 82
7.8 Accumulation of septins in non-compact myelin structures ... 83
7.9 Sept6 and MAL co-localize in the Schwann cell cytoplasm ... 85
7.10 Disturbance of the septin cytoskeleton by RNA interference ... 86
7.10.1 Myelinating DRG/ Schwann cell co-cultures ... 86
7.10.2 Retroviral RNAi constructs targeting Sept2 and Sept7 ... 88
7.10.3 Control infected co-cultures myelinate normally ... 89
7.10.4 Downregulation of Sept2 has no impact on myelination ... 90
7.10.5 Downregulation of Sept7 may impair Schwann cell survival ... 90
7.11 A dominant negative approach to disturb the septin cytoskeleton ... 92

8 Discussion ... 94

9 Outlook ... 102

10 References ... 104

11 Curriculum vitae ... 116

1 Acknowledgments

This work was performed in the Neurobiology laboratory of the Department of Biomedicine at the University Hospital Basel under the supervision of Prof. Nicole Schaeren-Wiemers.

First, I want to thank Nicole for giving me the opportunity to do my PhD thesis in her laboratory. Especially, I thank Nicole for providing me all the support needed but also for giving me the freedom and confidence to find my own ways in science.

I further want to thank Frances Kern and Beat Erne for their continuous support. I specially thank Beat for his great support concerning all aspects of microscopy and for his thoughts how scientific analysis should be done. I thank Frances for helping through difficult times which were not few during my thesis and for many helpful discussions.

I also thank all other members of the lab, Thomas Zeis, Jochen Kinter, Anna Stalder, Eva Herrero-Herranz, Marie-Francoise Ritz, Thomas Lazzatti, Daniela Schmid and Svenja Zitzling for generating a rich and friendly atmosphere.

Special thanks go to my collaborators Hauke Werner and Klaus-Armin Nave from the Department of Neurogenetics of the MPI for Experimental Medicine in Göttingen, Germany. The work of Hauke was the basis for the septin project and his suggestions and critics were always very constructive and helpful.

Finally, I want to thank my parents for their continuous help and support.

2 Abbreviations

β-Gal	β-D-galactosidase
BSA	bovine serum albumin
Caspr	contactin associated protein
CBB	coomassie brilliant blue
CDC#	cell division cycle protein #
Cdk5	cyclin-dependant kinase 5
CNS	central nervous system
C-terminal	carboxy terminal
CreERT	inducible cre recombinase
Cx32	connexin 32
DAPI	4,6-Diamidin-2-phenylindol-dihydrochlorid
DDTM	n-dodecyl-β-D-thiomaltopyranoside
DIG	detergent insoluble glycolipid-enriched complex
DM20	small isoform of the proteolipid protein
DMEM	Dulbecco's modified eagle medium
DMSO	dimethylsulfoxide
dNTP	deoxynucleotide triphosphate
DRG	dorsal root ganglion
DSS	disuccinimidyl suberate
E#	embryonic day #
EAE	experimental autoimmune enzephalomyelitis
EGF	epidermal growth factor
EGTA	ethylene glycol tetraacetic acid
EM	electron microscopy
f-actin	filamentous actin
FBS	fetal bovine serum
FGF	fibroblast growth factor
FRT	Fisher rat thyroid cells
GAL4	positive regulator for the gene expression of the galactose induced genes of S. cerevisiae
GFP	green fluorescent protein
GLAST	glutamate aspartate transporter
GPI	glycosylphosphatidylinositol
GPM6B	glycoprotein M6B
GST	glutathione-S-transferase
GTP	guanosine triphosphate
GTPase	GTP hydrolyzing enzyme
HA	hemaglutinine
HEPES	4-(2-hydroxyethyl)-1-piperazineethanesulfonic acid
His	histidine

HIS-3	imidazoleglycerol-phosphate dehydratase, catalyzing the sixth step in histidine biosynthesis
Hz	hydrazide
IF	intermediate filament
IgG	immunoglobulin G
IP	immunoprecipitation
IPTG	isopropyl-ß-D-thiogalactopyranoside
kD	kilo Dalton
LacZ	ß-D-galactosidase
Leu	leucine
L-MAG	large myelin-associated glycoprotein isoform
MAG	myelin-associated glycoprotein
MAL	myelin and lymphocyte protein
MAP	microtubule-associated protein
MBP	myelin basic protein
MDCK	Madin-Darby canine kidney cells
MEM	minimum essential medium
MF	microfilament
MOG	myelin oligodendrocyte glycoprotein
mRNA	messenger ribonucleic acid
MT	microtubule
NF	neurofilament
Nfc	neurofascin
NGF	nerve growth factor
NGS	normal goat serum
Nr-CAM	neuronal cell adhesion molecule
N-terminal	amino terminal
null	null mutant
o.n.	over night
O2A	oligodendrocyte-type 2 astrocyte precursor
OD	optical density
OPC	oligodendrocyte precursor cell
OSP	oligodendrocyte-specific protein
OTG	octyl-ß-D-1-thioglucopyranoside
P#	postnatal day #
P0	protein zero
PBS	phosphate-buffered saline
PCR	polymerase chain reaction
PDGF	platelet derived growth factor
Pen/Strep	penicilline/streptomycine
PFA	paraformaldehyde
PLP	proteolipid protein
PMP22	peripheral myelin protein 22

PMSF	phenylmethylsulfonylfluorid
PNS	peripheral nervous system
PVDF	polyvinylidene difluoride
RISC	RNA-induced silencing complex
RNA	ribonucleic acid
RNAi	small double-stranded RNA induced interferrence
RT	room temperature
SAP	shrimp alkaline phosphatase
SCP	Schwann cell precursor
SDS	sodium dodecyl sufate
SDS-PAGE	sodium dodecyl sulfate polyacrylamide gel electrophoresis
Sec6/8	exocyst complex
Sept	septin
S-MAG	short myelin-associated glycoprotein isoform
SNARE	soluble N-ethylmaleimide-sensitive-factor attachment receptor
SPF	specific pathogen free
TAE	tris-acetate-EDTA buffer
Taq	thermus aquaticus DNA polymerase
TBS	tris-buffered saline
TGN	trans-Golgi network
Trp	tryptophan
TTBS	tris-buffered saline with 0.1% Tween-20
WB	Western blot
wt	wild type

3 Summary

Rapid conduction of nerve impulses in the nervous system of higher vertebrates is made possible by ensheathment of nerve fibers by the specialized plasma membrane structure myelin. Consequently, failure of myelination or damage to the myelin sheath leads to severe pathology as seen in multiple sclerosis. During myelination oligodendrocytes and Schwann cells are challenged to build up and maintain a highly complex multilaminar plasma membrane structure. It is well-known that myelin membranes are divided into subdomains with distinct protein and lipid composition. Nevertheless, it is unclear how these domains are generated and then maintained throughout the adult. Especially the mechanisms of interaction between cytoskeleton elements and membrane structures in the developing and adult myelin sheath are still unknown. In this work, the interaction of the cytoskeleton protein septin 6 (Sept6) and the myelin and lymphocyte protein MAL is demonstrated. Septins are enriched in myelin membranes which is unique for cytoskeleton elements. Most important, the loss of Sept6 in myelin is compensated by its closest homolog Sept11 which clearly points to a functional role of septins in the myelin compartment. A detailed analysis of the septin protein family in myelinating cells was performed here. It was shown that septins are coordinately regulated during differentiation and myelination in Schwann cells and oligodendrocytes. On the protein level particular septins were identified to be differentially enriched in myelin membranes. They form distinct stoechiometric complexes interacting also with actin. We propose that septin/myelin membrane complexes play an important role in myelination. Septins might be crucial in the formation and maintenance of myelin subdomains as well as in the transport of myelin components. In line with this, a possible site of interaction between Sept6 and MAL was identified in the Schwann cell cytoplasm. There, Sept6 and MAL might be important for sorting and trafficking processes crucial for the targeting of myelin components into the emerging and adult myelin sheath. Sept6-deficient mice, however, did not disclose alterations in myelin ultrastructure and protein composition besides the upregulation of Sept11. But, it is well-known that the septin cortex is very robust and that homologous isoforms might compensate for the loss of single septins. In line with this, it is shown here that myelinating Schwann cells tolerate the loss of Sept2, which might be due to such compensation mechanisms. The function of Sept7 in myelination could not be elucidated, since downregulation in *in vitro* myelinating cultures led to unspecific effects probably on cytokinesis and cell survival. Nevertheless, this first comprehensive study on septins in oligodendrocytes and Schwann cells generated valuable data critical for further analysis of septin function in myelin. This study provides insight into the composition of the septin cytoskeleton, its regulation during myelination and its interaction with myelin membranes. Understanding the role of the septin cytoskeleton in myelin formation and maintenance may reveal new insights in the mechanisms of myelination and remyelination in health and disease.

4 Introduction

4.1 From polarized transport to the mature myelin sheath

Myelination is the basis for fast and efficient conduction of nerve impulses in the nervous system of higher vertebrates. The myelin sheath is a uniquely complex and elaborate plasma membrane structure interacting with nerve processes, the axons. Its morphological buildup goes far beyond the imagination of what a single cell is capable of doing perhaps only comparable with the generation of axons of long-projecting motor neurons. Despite of decades of research it is still largely unknown how myelinating cells succeed in constructing and maintaining the myelin sheath. Recently, parallels of differential sorting and trafficking of membrane components in polarized epithelial cells and myelinating cells were appreciated. The concepts of polarized transport mechanisms in myelinating cells are, therefore, avidly discussed. Especially the role of cytoskeleton elements in this respect is matter of interest since these elements are crucial for all transport processes but also for the structuring of membranes. In this work, the role of a cytoskeleton protein family, the septins, in myelinating cells is described.

4.2 Myelin

4.2.1 Myelination

Rapid conduction of nerve impulses in the nervous system of higher vertebrates is made possible by ensheathment of nerve fibers by the specialized plasma membrane structure myelin. Myelinating cells wrap plasma membrane extensions up to 50 fold around the axon and tightly pack the respective membrane layers excluding the cytoplasm. The resulting insulation minimizes loss of electrical signals caused by transverse diffusion. Additionally, ion channels contributing to the propagation of the action potential are clustered at specialized axonal segments, the nodes of Ranvier, lowering the energy demand for action potential firing (Waxman and Ritchie, 1993). In consequence faster and more efficient nerve conductance is achieved with smaller axon diameters (for review see Waxman, 1980). This is indeed important for the built up of the nervous system of higher vertebrates since myelinated fast firing nerves can be more tightly packed than non-myelinated fibers which axon diameters have to be much larger to reach comparable conduction velocities. Consequently, failure of myelination or damage to the myelin sheath results in slowed signal propagation or even conduction block leading to severe pathology as seen in multiple sclerosis and other primary demyelinating diseases.

During myelination, oligodendrocytes and Schwann cells are challenged to build up and maintain a highly complex multilaminar plasma membrane structure. This implies changing the expression pattern of multiple genes with the prominent upregulation of a distinct myelination program as well as redistribution of cytoskeleton elements and polarization of the membrane structures. Indeed Schwann cells and oligodendrocytes

establish and maintain distinct membrane subdomains with different protein and lipid content (Kim and Pfeiffer, 1999; Simons et al., 2000). A schematic overview about the different myelin compartments with some of the molecules that are specifically enriched in either domain is illustrated in Figure 1. Myelin structure and domains are introduced in detail in chapter 4.3. The rate of membrane production in the period of highest myelinating activity demands specialized cytoskeleton elements for trafficking and transport of vesicles as well as structural support for the emerging myelin sheath. Many aspects concerning the process of myelination are still unclear. Recently, concepts of how distinct subdomains contributing to functionality along myelinated axons are generated are emerging (for review see Poliak and Peles, 2003; Salzer, 2003).

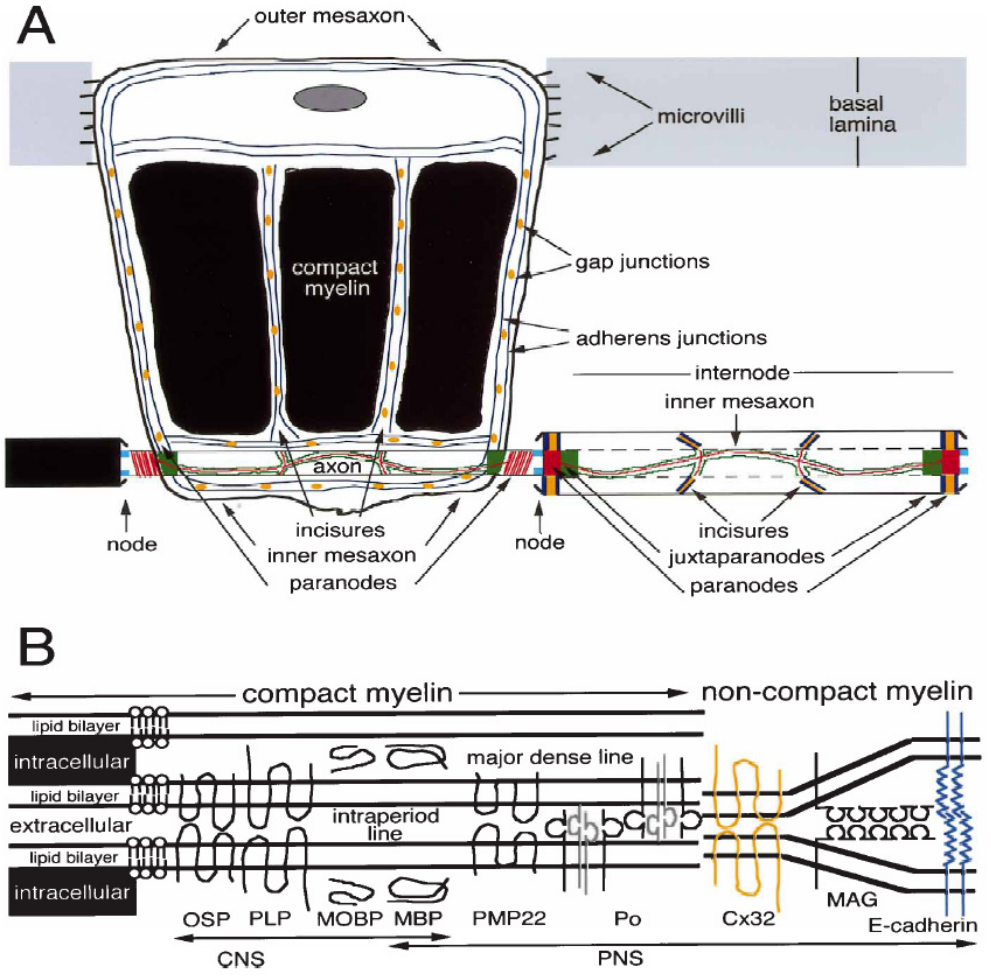

Figure 1 Schematic drawing of a myelinated nerve segment in the PNS
(A) The membrane compartment of a myelinating Schwann cell is presented as “enrolled” sheath. Different subcompartments like the compact myelin and the non-compact myelin, the incisures and the paranodes, are depicted. (B) Both the compact as well as the non-compact myelin compartments have distinct sets of molecules selectively enriched. The major myelin proteins are discussed in more detail in chapter 4.3.2 (copied from Arroyo and Scherer, 2000).

4.2.2 Myelinating cells

The myelinating cells of the central and peripheral nervous system, the oligodendrocytes and Schwann cells respectively are basically confronted with a very similar task. Although there are differences in respect of how these cells enwrap the axons, the structural outcome is very comparable (Figure 2). Both cell types need to synthesize vast amounts of myelin membrane with the respective proteins and lipids, correctly target and transport the building blocks and integrate them into the emerging myelin sheath. This process involves an orchestrated interplay of vesicular transport systems with the cytoskeleton tracks and scaffolds to target the respective structures. After completion of myelination the myelin sheath has to be conserved throughout live respecting the established subdomains and compartments.

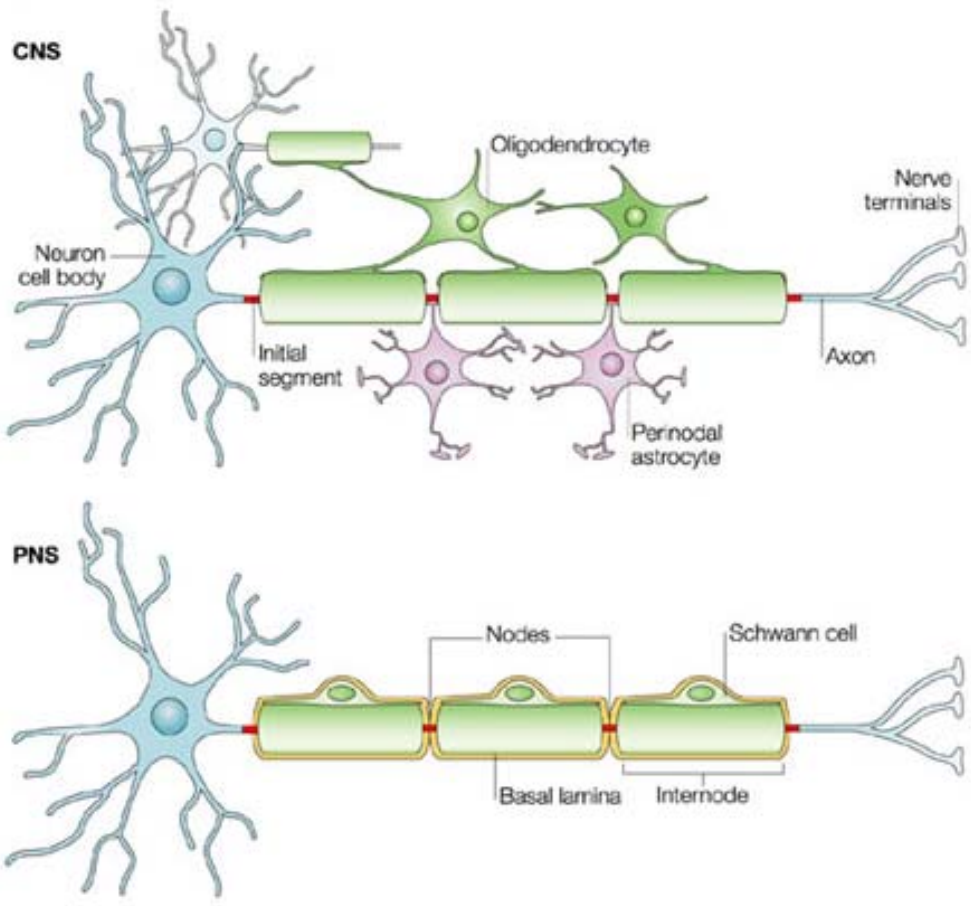

Figure 2 Myelinating cells
Oligodendrocytes in the CNS and Schwann cells in the PNS myelinate fast conducting axons. Oligodendrocytes are capable of forming multiple myelin sheaths whereas Schwann cells form one single myelinated internode (copied from Poliak and Peles, 2003).

4.2.2.1 Oligodendrocytes

Oligodendrocytes derive from pluripotent glial precursor cells generated in restricted regions of the neural tube (Warf et al., 1991), and then precede through a differentiation program that will ultimately lead to myelinating oligodendrocytes (Figure 3). The first identifiable glial precursors, the glial restricted precursor cells, can be isolated from the entire rostrocaudal axis. From there they proceed to progressively more restricted precursor cells. The earliest well characterized cell of the oligodendrocyte lineage are bipolar A2B5+ precursors (Raff et al., 1984). They are critically dependant on PDGF as their major growth factor. In fact, high expression of PDGFαR is a marker for the oligodendrocyte lineage (Pringle et al., 1992). Correct number of progenitor cells is controlled by regulating cell proliferation and survival (Barres et al., 1992). These immature so-called O2A progenitors still show stem cell like characteristics in that they can give rise to all neural cell types, in particular oligodendrocytes, astrocytes and neurons (Kondo and Raff, 2000). During maturation the A2B5+ cells begin to express the O4 antigens e.g. galactosulfatite but retain their bipolar morphology (Pfeiffer et al., 1993). The next stage is characterized by a loss of precursor antigens (e.g. A2B5) and the expression of galactocerebroside detectable as O1 antigens (Raff et al., 1978). O1+ cells stop proliferation and gain a multibranched morphology (Figure 3, premyelinating oligodendrocyte). At this stage they are determined into the oligodendrocyte fate and will ultimately mature or undergo apoptosis (Barres et al., 1992). Continuing maturation, they begin to express the first myelin genes such as MBP and PLP and elaborate their membrane sheaths; *in vivo* they will begin to form multiple internodes (Figure 2). Finally, mature oligodendrocytes are characterized by high expression of late myelin genes like MOG or MAL (Schaeren-Wiemers et al., 1995; Scolding et al., 1989). Importantly, oligodendrocytes can undergo most of their maturation program autonomically. They can express all major myelin genes in pure cultures without neurons, and build large membranes with normal myelin protein composition (Pfeiffer et al., 1993).

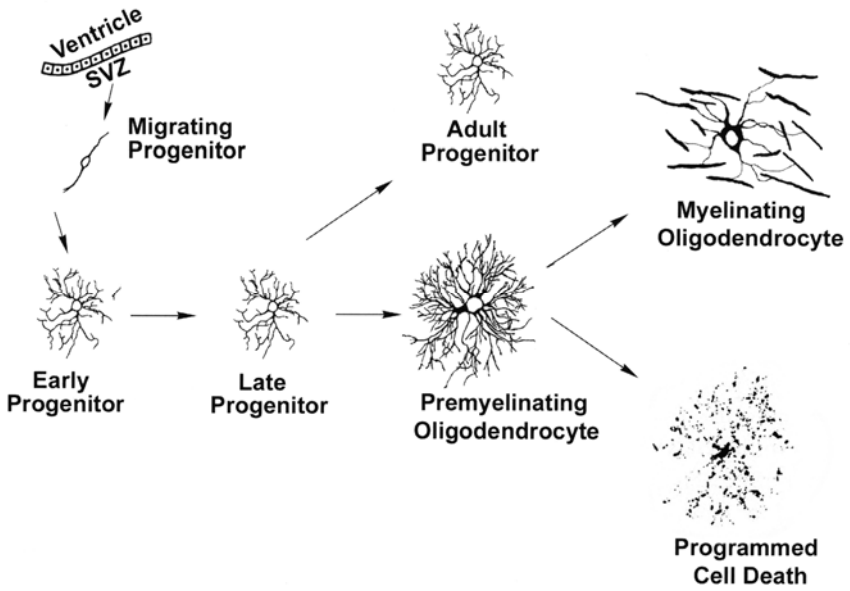

Figure 3 The oligodendrocyte lineage
Oligodendrocytes derive from pluripotent progenitor cells. During differentiation they proceed from early to late progenitors and premyelinating oligodendrocytes. The premyelinating oligodendrocyte will either myelinate or undergo apoptosis if they are not associated with an axon (adapted from Trapp et al., 1997).

4.2.2.2 Schwann cells

Schwann cell precursor cells (SCPs) are generated from neural crest cells (Figure 4). From there they migrate along the developing peripheral nerves in intimate contact to the axons. The survival of SCPs is critically dependant on axonal derived signals like neuregulin-1 type III (Garratt et al., 2000). Conversely, SCPs seem to provide axons with survival factors important for both sensory and motor neurons (Britsch et al., 2001; Riethmacher et al., 1997). SCPs seem to be unifated in that they are destined to become only Schwann cells in normal development. The transition of SCPs to Schwann cells was determined to peak at E16 in rodents. Mature Schwann cells have lost their extrinsic dependency on neuregulin for survival and established autocrine survival circuits (Jessen et al., 1994; Meier et al., 1999). Following this, the immature Schwann cell intermediate stage splits into the future myelinating Schwann cells and non-myelinating Schwann cells. The myelinating Schwann cells form a one-to-one relationship to axons and ultimately myelinate. At this stage of development, neuregulin-1 type III expressed on the axons triggers myelination and regulates Schwann cell membrane growth and, thus, myelin sheath thickness to match the axon caliber (for review see Nave and Salzer, 2006). Non-myelinating Schwann cells ensheathe a bundle of smaller caliber axons with a double plasma membrane layer the so-called Remark bundles (for review see Jessen and Mirsky, 1999). In this respect the fate of the Schwann cell is determined by the axon that is associated and

instructs the glia cell either to myelinate or not. As mentioned, Schwann cells loose their extrinsic dependency on axonal signals and can, therefore, also survive and dedifferentiate after loss of their axon. This ability enables Schwann cells to remyelinate regenerating peripheral nerves after injury (Fawcett and Keynes, 1990). *In vitro*, Schwann cells do not differentiate autonomously like oligodendrocytes. The transcription factor Krox20 which is the main instructor for the myelination program is only expressed upon contact with axons (Nagarajan et al., 2001; Parkinson et al., 2002; Zorick et al., 1996; Zorick et al., 1999). Therefore, isolated Schwann cells do not express myelin markers and dedifferentiate in culture to gain a SCP like stage.

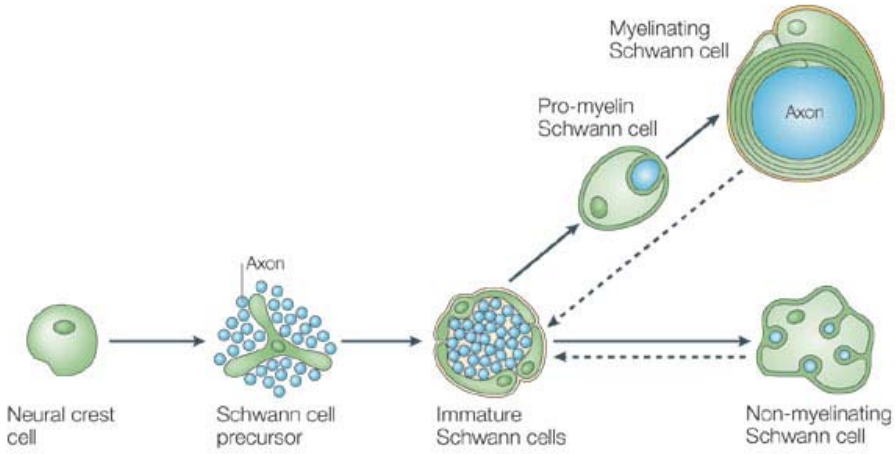

Figure 4 The Schwann cell lineage
Schwann cells derive from neural crest cells. They migrate along the peripheral nerve tracts as Schwann cell precursors. At E18 immature Schwann cells populate the entire length of peripheral nerves in intimate contact with axons. Depending on the axon the Schwann cell will either myelinate or form Remark bundles of non-myelinated axons (copied from Jessen and Mirsky, 1999).

4.3 Myelin structure and function

The myelin sheath critically depends on its complex structure for normal function (for review see Poliak and Peles, 2003; Salzer, 2003). During myelination the respective glial cells wrap their plasma membranes around the axons. During this process, the cytoplasm between the membrane layers is excluded leading to a compact packing of both the intracellular and extracellular leaflets of the membranes visible by electron microscopy (Figure 5). The cytoplasmic leaflets contact to form the major dense line whereas the packed extracellular leaflets form the minor dense lines. Consequently, the compact myelin sheath is seen in cross section as a circular consecution of electron dense (major dense line) and light lines (minor dense line or intraperiod line).

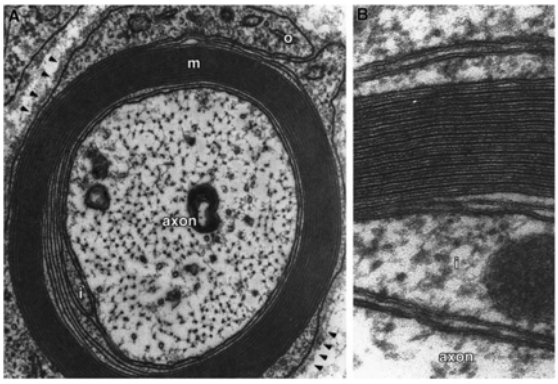

Figure 5 The ultrastructure of the myelin sheath
A cross-section of a myelin sheath is visualized by electron mycroscopy. The compact myelin structure (m) is composed of alternating major dense and intraperiod lines (copied from Revel and Hamilton, 1969).

Besides the compact myelin compartment (Figure 6A) which makes up the majority of the myelin sheath also several non-compact myelin compartments exist (Figure 6B and C). At the lateral ends where opposing internodes form the nodes of Ranvier, the myelin membranes split up to form cytoplasm filled paranodal loops attaching to the axons (Figure 6B). The adaxonal compartment, the innermost membrane wrap contacting the axon, also comprises cytoplasmic channels possibly enabling signal transduction between axon and glia. Finally, in the PNS the compact myelin is interrupted by cytoplasmic channels spiraling down to the axon, the Schmidt-Lanterman incisures (Figure 6C). In addition, Schwann cells form a snake-skin like network of cytoplasmic channels surrounding the myelin sheaths known as the Cajal bands (Court et al., 2004). The non-compact myelin compartments are believed to be important for nourishing the myelin sheath as well as providing structural components and signaling platforms for axon-glia crosstalk.

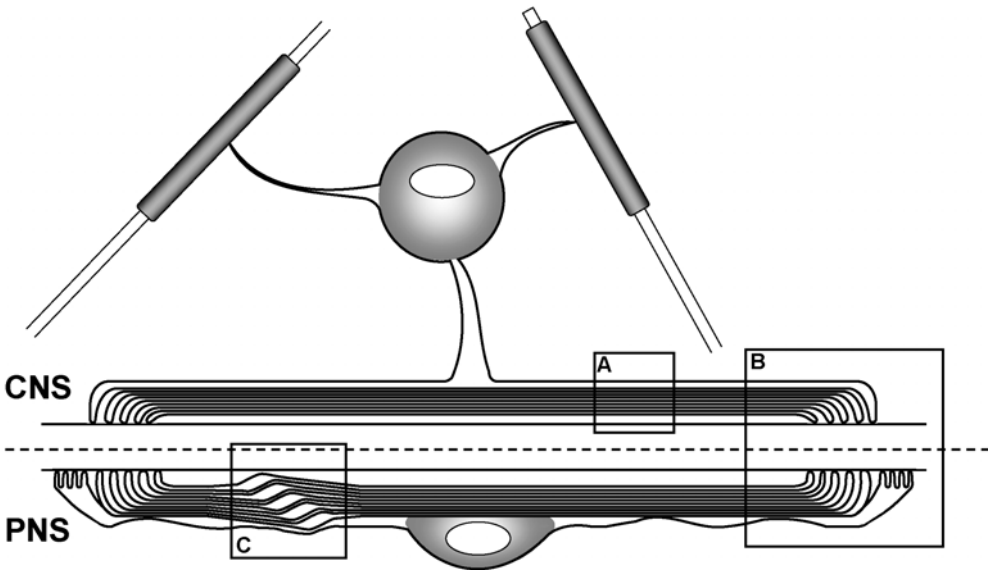

Figure 6 The compact and non-compact myelin compartments of a myelin sheath
The myelin sheath is composed of compact and non-compact myelin compartments. (A)The majority of the internode is compact myelin. (B) At the lateral ends of the internodes the myelin membranes split up to form cytoplasm filled paranodal loops and microvilli. (C) Schwann cells also form regions of non-compact myelin, the Schmidt-Lanterman incisures, within compact myelin domains.

Oligodendrocytes are capable of forming multiple internodes each of which is formed by one plasma membrane extension. Depending on the region and type of myelinated axons, oligodendrocytes myelinate between few to up to 40 axons. Interestingly, they seem to be capable of recognizing the “future size” of their target axons. This is of importance since large caliber axons also acquire thicker myelin sheaths. Oligodendrocytes myelinating large caliber axons (e.g. in the brainstem) will form fewer internodes whereas oligodendrocytes myelinating small caliber axons as in the optic nerve will form many internodes (Fanarraga et al., 1998). Oligodendrocytes do not form Cajal bands but have a single longitudinal cytoplasmic channel along the whole myelin sheath connecting the perinuclear and paranodal cytoplasm. This channel contains microtubules, mitochondria, smooth endoplasmic reticulum and vesicles. Schwann cell internodes are distinct from oligodendrocyte internodes not only by having Schmidt-Lanterman incisures and Cajal bands. In contrast to oligodendrocytes Schwann cells form a complex extracellular matrix, the basal lamina, containing laminins and collagens (Bunge, 1993; Scherer, 1996). The outmost lateral loops of the Schwann cell membrane form microvilli contacting the nodal axolemma (Ichimura and Ellisman, 1991; Raine, 1982). Microvilli have a distinct set of ion channels and structural components which might be necessary for forming functional nodes of Ranvier and for normal electrical signal processing (Devor et al., 1993; Howe and Ritchie, 1990).

4.3.1 The nodes of Ranvier

The nodes of Ranvier were already appreciated 1928 by Ramón y Cajal by silver staining and described to comprise different compartments (Cajal, 1928). Both CNS and PNS nodes of Ranvier fulfill the same function but still are not identical in terms of ultrastructure. The nodes of Ranvier can be subdivided into three parts crucial for the renewal of the action potential: the nodal, paranodal and juxtaparanodal regions (Figure 7A). At the centre or nodal region voltage-gated sodium channels are clustered and ultimately are responsible for propagation of the action potential (Ellisman and Levinson, 1982). The clustering of sodium channels critically depends on intact nodal architecture (Rios et al., 2003; Rosenbluth et al., 2003). The axonal segment underlying the node is highly specialized with a distinct submembranous cytoskeleton containing spectrin, f-actin and ankyrin (Arroyo and Scherer, 2000; Kordeli et al., 1990). Additionally, adhesion molecules like Nr-CAM and Neurofascin186 are clustered at the node and seem to interact with glial proteins in the microvilli (for review see Poliak and Peles, 2003). Since oligodendrocytes are not forming microvilli, the CNS nodes are not covered by oligodendrocyte membranes. Instead, glial processes formed by astrocytes contact the nodes but do not form tightly adherent structures like seen in the PNS nodes (Black and Waxman, 1988).
At the lateral end of compact myelin the tight membrane packing is split up to form the paranode. Cytoplasm filled loops contact the paranodal axolemma stabilized to the axon and each others by junction complexes (Figure 7B). At the contact site of paranodal loops with the axolemma septate-like junctions are formed which are

believed to enforce the adhesion of the opposing membranes (Bhat et al., 2001; Boyle et al., 2001). On the axonal site a complex of the adhesion molecules Caspr and contactin accumulate at the paranode where they are proposed to interact with glial Neurofascin155 in the paranodal loops.
The tight junction between the paranodal loops and the axolemma seem to have a function in restraining potassium channels to the juxtaparanode but not on clustering sodium channels at the nodal region (for review see Mitic and Anderson, 1998). Paranodal loops are comparable to other non-compact myelin compartments like Schmidt-Lanterman incisures, but contain more cytoplasm and have a complex cytoskeleton scaffold.
The juxtaparanode cannot be identified as morphological structure, but is defined as 10-15 nm wide area adjacent to the paranode. Functionally important is the clustering of delayed rectifying potassium channels, which are important for the excitability of the nodes (Rasband et al., 1998). With the exception of some molecular components, the juxtaparanodes do not differ much from the remaining internodal region.

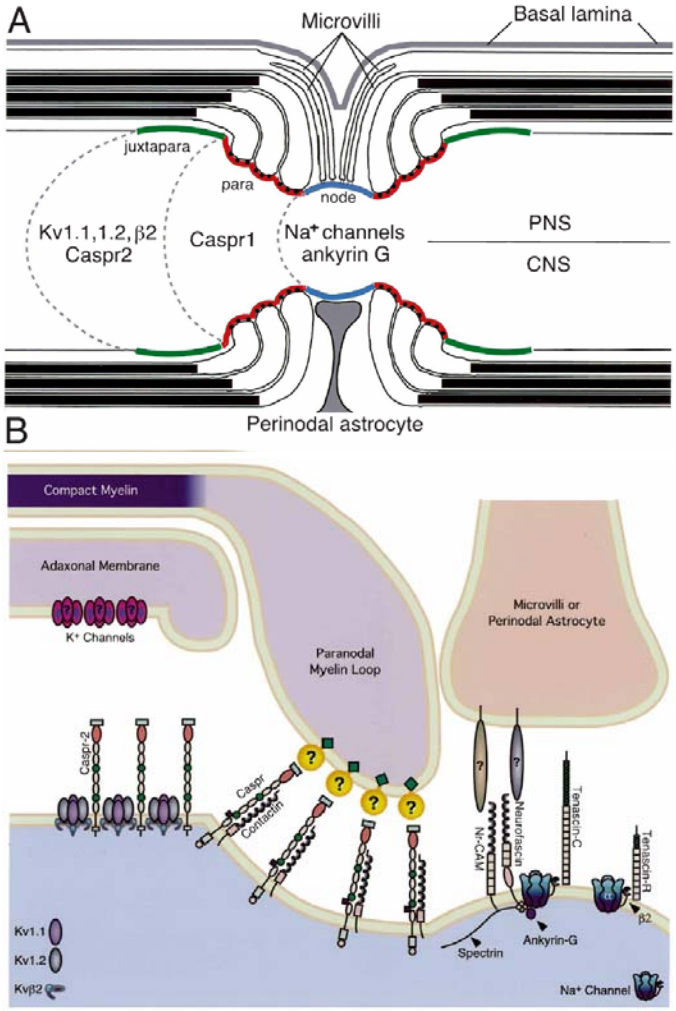

Figure 7 The node of Ranvier
(A) The compartments of the node of Ranvier, the nodal, the paranodal and juxtaparanodal regions are depicted.
(B) A complex set of adhesion molecules, cytoskeleton elements and membrane receptors are important for nodal integrity and correct localization of ion channels (copied from Arroyo and Scherer, 2000).

4.3.2 Myelin proteins

The myelin membrane comprises a regular consecution of membrane layers with defined periodicity. Clearly, there must be organizing elements integrating into the compact myelin layers to mediate the adhesion of the membranes. Interestingly, the total myelin protein content is represented to very large proportions by a small number of major myelin proteins. They are believed to determine the ultrastructural constants of the myelin spirals as defining the intraperiod line or the major dense line.

4.3.2.1 MBP, PLP and P0

Myelin accounts for 20-25% of the dry weight of the brain. The myelin basic protein (MBP) together with proteolipid protein (PLP) account for 80% of the total protein content in myelin (Braestrup and Squires, 1977; Squires and Brastrup, 1977). PLP is largely specific for CNS myelin (Trotter et al., 1981), whereas protein zero (P0) is exclusively expressed in PNS myelin where it comprises 60% of total protein (Greenfield et al., 1973). Because of their abundance these were among the first myelin proteins analyzed in the nervous system (Takahashi et al., 1985). It was evident from studies with specific antibodies that both MBP and PLP are exclusively localized to myelin (Agrawal et al., 1977; Hartman et al., 1982).

The primary function of these three proteins is believed to be to support the structure of the myelin sheath. P0 seems to stabilize the intraperiodal line in PNS myelin. This is achieved by homophilic interaction of P0 molecules from adjacent membrane layers. High resolution structure of P0 suggests that it may form a tetramer on the membrane which can then interact with a second tetramer from the apposing membrane layer (Shapiro et al., 1996).

PLP and its alternatively spliced minor isoform DM20 contributes to 50-60% of the total CNS intra-membrane protein and is, therefore, an excellent candidate for structural maintenance in myelin. Nevertheless, PLP/DM20-deficient mice show only very subtle phenotypes (Garbern et al., 1999). In contrast, a PLP/DM20 and OSP/Claudin-11 double-deficient mouse line has severe neurological deficits and markedly abnormal myelin compaction (Chow et al., 2005) which was not obvious in the single null mice. OSP/Claudin-11 and PLP are both structurally related tetraspan proteins and might therefore compensate for the loss of each other.

MBP owes its name to the fact that it contains a very high percentage of basic residues which are believed to be important for the interaction with the phospholipids of the membrane. MBP might be necessary for compaction and maintenance of the myelin sheath by connecting the inner leaflets of myelin membranes (Omlin et al., 1982). However, this role of MBP is questioned since a spontaneous mutation in the MBP locus, resulting in almost complete absence of MBP, can still form grossly normal myelin structures in the PNS (Kirschner and Ganser, 1980). Data from other studies suggest that MBP might interact with cytoskeleton elements which will be discussed later. Interestingly, MBP mRNA was shown to be distributed along myelinated internodes, whereas transcripts encoding for PLP and P0 remain

localized around the nuclei of the myelinating cells (Trapp et al., 1987). Further studies in oligodendrocyte cell cultures demonstrated that MBP mRNA gradually moved into the oligodendrocyte processes over time. Later experiments showed that MBP is synthesized on free polysomes very close to where it is incorporated into the myelin.
Taken these data together the exact role of the major myelin proteins MBP, PLP and P0 is still not fully understood. Seemingly, compensation mechanisms masking loss of function mutation hinder the analysis of myelin proteins tremendously.

4.3.2.2 MAG and MOG

MAG is the major CNS glycoprotein and thought to be involved in neuron-glia interaction. Both MAG and MOG belong to the Ig superfamily of proteins which potentially interact with carbohydrates of target structures. MAG is expressed upon first contact with axons (Quarles, 1983) and is subsequently upregulated towards myelination. MAG is restricted to non-compact myelin including the periaxonal location. A number of studies implicated MAG in the development, maintenance and repair of the myelin sheath and axon-glia interaction. Seemingly, MAG might have a role in axon glial interaction during development and in the adult (Sternberger et al., 1979). Alternative splicing gives rise to two MAG isoforms, the large L-MAG and the short S-MAG. Besides having properties of a cell adhesion molecule, MAG might also be a transmembrane receptor. L-MAG is thought to be able to signal extracellular cues to the inside since L-MAG has phosphorylation sites, but their precise function is not known. Interestingly, S-MAG binds tubulin potentially linking the axonal surface to the glial cytoskeleton (Kursula et al., 2001). It was also shown that the microtubule associated protein MAP1B can bind to MAG (Franzen et al., 2001) strengthening the concept that MAG might be important for cytoskeleton interactions. MAG-deficient mice are viable but show a delay in CNS myelination (Bartsch et al., 1997; Li et al., 1994; Montag et al., 1994) and subtle defects in normal myelin structure as well as secondary effects on neurons. Although MAG was intensely investigated, its exact role in development and in the adult is still matter of debate.

MOG was discovered as an immunological target in experimental autoimmune encephalomyelitis (EAE). It was further recognized that MOG is a glycoprotein expressed by oligodendrocytes (Linington et al., 1984). Immunization against MOG is frequently used as a model for inflammatory demyelinating diseases like multiple sclerosis. MOG is a minor constituent of CNS myelin and has some features that clearly distinguish it from the major myelin components MBP, PLP and MAG. MOG localizes exclusively to the outermost surface of the oligodendrocyte membrane structures (Brunner et al., 1989). The topographic organization of MOG in the lipid bilayer was for long a matter of debate. Kroepfl and colleagues demonstrated in 1996 that MOG is a type I transmembrane protein. Although containing two potential transmembrane domains only one spans the plasma membrane (Kroepfl et al., 1996). Later work suggested that the second hydrophobic region is interacting with

the plasma membrane leaving two short cytoplasmic stretches (della Gaspera et al., 1998). The extracellular loop of MOG was modeled and predicts a Ig-like domain (Hjelmstrom et al., 1998; Mesleh et al., 2002). It is believed that MOG might be important as an adhesion molecule since it is highly enriched on the surface of the myelin sheath. There, it might interact with the extracellular matrix or mediating adhesion between neighboring myelinated axons (for review see Schachner and Martini, 1995). Nevertheless, MOG-deficient mice do not show a phenotype despite insensitivity to MOG-mediated EAE (Delarasse et al., 2003). Interestingly, there might be a link between MOG and microtubular integrity since treatment with anti-MOG antibodies can lead to depolymerization of microtubules in oligodendrocytes (Dyer, 1993; Dyer and Benjamins, 1990; Dyer and Matthieu, 1994). These results are in line with speculations about potential receptor functions of MOG. Besides being an Ig-like protein, its raft association points to a role in signaling cascades (Lisanti et al., 1995). There, it might be involved in lipid/protein sorting as well as in signal transduction pathways (Kim and Pfeiffer, 1999).

4.3.2.3 MAL

MAL is a highly hydrophobic proteolipid that was first discovered in cells of the immune system, the T-lymphocytes (Alonso and Weissman, 1987). MAL is expressed in intermediate and late stage T-cells. Its name derived from the fact that it was identified as being expressed by both **M**OLT-4 (stage II thymocytes) and HPB-**A**LL **l**ymphocyte cells (stage II/III). Later, differential screens identified MAL being expressed in rat primary oligodendrocytes (Kim et al., 1995; Schaeren-Wiemers et al., 1995) and in polarized epithelial cells (Frank, 2000; Magyar et al., 1997; Zacchetti et al., 1995). The already introduced abbreviation “MAL” was further used as **m**yelin **a**nd **l**ymphocyte protein (Schaeren-Wiemers et al., 1995). Its strongest expression is found in myelinating cells both of the CNS and PNS, and the MAL protein is incorporated into compact myelin as a minor myelin protein (Frank et al., 1998). Interestingly, MAL was also shown to be present in non-compact myelin structures which differs from the major myelin proteins MBP, PLP and P0 (Erne et al., 2002). First insights into the potential molecular functions of the MAL protein derived from the fact that MAL is incorporated into glycolipid-enriched membrane fractions the so-called rafts (Frank et al., 1998; Kim et al., 1995; Martin-Belmonte et al., 1998; Millan et al., 1997; Zacchetti et al., 1995). Zacchetti and colleagues localized MAL in vesicular structures in the apical cytoplasm of polarized Madin-Darby canine kidney (MDCK) cells and proposed that MAL might be a candidate component in vesicular trafficking systems (Zacchetti et al., 1995). In polarized tissue like kidney and stomach epithelial, MAL is localized exclusively on the apical surface of the cells suggesting a role of MAL in raft dependant polarized sorting and trafficking mechanisms (Frank et al., 1998). In line with these findings, alterations of MAL levels in MDCK cells had effects on protein and membrane transport (Cheong et al., 1999). The role of MAL in polarized sorting is discussed in more detail in chapter 4.4.3.

In the nervous system MAL is expressed both in oligodendrocytes and Schwann cells (Schaeren-Wiemers et al., 1995). Interestingly, the timing of expression during development is different in the CNS compared to the PNS pointing to distinct functions in both systems (Frank et al., 1999). In oligodendrocytes MAL is expressed late during myelination. It appears several days after the onset of MBP and PLP expression and probably coincides with the expression of the late myelin marker MOG. In the PNS MAL is already expressed embryonically (E17) in Schwann cell precursors long before myelination initiates. This suggests that MAL might have a function in Schwann cell differentiation (Schaeren-Wiemers et al., 1995). Both MAL-deficient and MAL-overexpressing mice were generated and analyzed for defects in CNS and PNS myelination (Frank et al., 2000; Schaeren-Wiemers et al., 2004). In both models overall myelin formation appeared normal. Nevertheless, distinct phenotypes appeared both in the CNS and the PNS. In MAL-deficient mice a defect was described for the CNS nodes of Ranvier. The paranodal loops were found to be detached from the nodal axolemma and the electron dense protein accumulation known as septate junctions were lost from some paranodal loops but not all. Most strikingly, the paranodal marker Caspr was dispersed in MAL-deficient mice compared to clusters in the wild type animals (Schaeren-Wiemers et al., 2004). Suggested function from other cell types indicate that MAL might be important to target specific components which are important for axon-glia interaction to the paranodal loops, and therefore, maintain the integrity of the junctions. The PNS nodes of Ranvier were seemingly not altered. MAL-overexpressing mice, in the PNS, showed a defect in axonal sorting (Frank et al., 2000) and in the regulation of myelination initiation (Schaeren-Wiemers, unpublished). These effects are not yet understood but might be attributed to a signaling defect in MAL-overexpressing mice due to altered lipid raft composition. Clearly, the role of MAL is best understood in polarized sorting mechanisms. These results may be applicable to the myelinating glia. Yet, the exact role of MAL influencing sorting and trafficking in oligodendrocytes and Schwann cells has to be demonstrated. Undoubtedly, these processes involve cytoskeleton elements. Therefore, the identification of the link between the raft associated protein MAL and the cytoskeleton might reveal new concepts of how MAL and related lipid raft associated proteins exert their function on the molecular level.

4.4 Polarized cells

The concept of polarized transport and trafficking mechanisms originates from and is best studied in epithelial cells but was adapted to approach the generation of distinct subdomains in myelinating cells. Here, models of raft-dependant and independent polarized transport machineries will be introduced. First, the concept of membrane rafts, and subsequently, polarized transport mechanisms and their importance in myelinating cells will be discussed.

4.4.1 Membrane rafts

Particular aspects of polarized sorting mechanisms depend on detergent-insoluble glycolipid-enriched complexes (DIGs) or glycolipid-enriched microdomains (GEMs) floating within the plasma membrane and, therefore, called membrane rafts. For decades membrane bilayers were thought to be unstructured and that membrane bound molecules were able to diffuse unconfined in the two-dimensional membrane plane (Singer and Nicolson, 1972). However, it became evident that not only different lipid species are asymmetrically distributed between the cytoplasmic leaflet and the exoplasmic leaflet of the membrane (Simons et al., 2000; van Meer and Simons, 1988) but there is also a lateral structuring in the two-dimensional lipid plane (Kusumi and Sako, 1996). In this view, specific lipids form clusters together with cholesterol into micro-domains, the membrane rafts, which display different physico-chemical properties compared to the surrounding plasma membrane. The proposed spingolipid/cholesterol raft is described as follows (Figure 8). Sphingolipids associate laterally and form lipid clusters. Their head groups occupy more space than their hydrocarbon chains. Consequently, voids are formed in the membrane bilayer which are filled by cholesterol (Simons and Ikonen, 1997). These densely-packed spingolipid/cholesterol assemblies may serve as platforms for specific protein transport and for intracellular and transmembrane signaling. In the last years considerable dispute emerged about the issue if rafts exist also *in vivo* or if they are an isolation artifact (for review see Munro, 2003). In a recent Keystone Symposium on membrane rafts the following consensus definition emerged: ”Membrane rafts are small (10-200nm), heterogeneous, highly dynamic, sterol- and sphingolipid-enriched domains that compartmentalize cellular processes. Small rafts can sometimes be stabilized to form larger platforms through protein-protein and protein-lipid interactions” (Pike, 2006). Today, rafts are considered to be organizing platforms for diverse cellular functions like cell adhesion, signaling, sorting and trafficking processes.

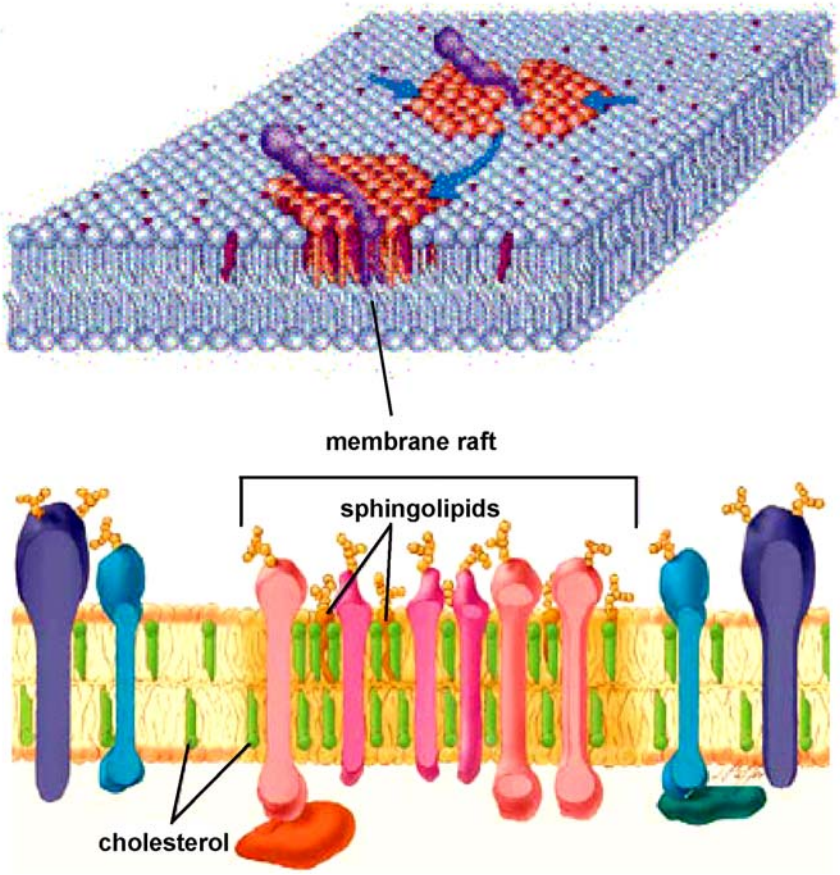

Figure 8 Schematic illustration of membrane rafts
Membrane or lipid rafts are specialized structures floating in the membrane bilayer. Sphingolipids associate laterally and incorporate cholesterol to form membrane rafts. Particular membrane bound proteins can enrich specifically in membrane rafts (adapted from Anderson and Jacobson, 2002 and NIGMS, 2005).

4.4.2 Polarized sorting and trafficking mechanisms

The plasma membrane of epithelial cells is polarized into an apical and a basolateral compartment (Einarson et al., 1982 and Figure 9). These membrane domains exert different functions reflected also in a different protein and lipid composition. The apical domain is enriched in sphingolipids whereas the basolateral domain has a high content of glycerolipids and phosphatidylcholine (Simons et al., 2000; van Meer, 1989). The two domains are separated physically by diffusion restricting tight junctions at their interface. How these distinct domains are generated and maintained in terms of transport and integration of newly synthesized components is issue of intense studies. Epithelial cells have two distinct transport mechanisms both contributing to generate polarity, a direct pathway and an indirect pathway (Mostov et al., 1992; Weimbs et al., 1997). The direct pathway integrates apical and basolateral proteins into separate transport vesicles and directly delivers them to their respective compartment (Figure 9). The indirect pathway sorts both apical and basolateral components to the basolateral membrane and subsequently redirects apical proteins

to the apical membrane by specific transcytosis (Figure 9). The signal for sorting transmembrane proteins to either compartment is intrinsic to the respective proteins. Basolateral sorting signals are usually integrated into the cytoplasmic domain of the proteins but also their tertiary structure can provide the targeting information (Matter and Mellman, 1994). The GPI anchor is the best described targeting signal integrating GPI-anchored proteins into apically sorted rafts (Brown and Rose, 1992; Simons and Ikonen, 1997). Besides this, also the transmembrane segments can promote membrane raft association and apical targeting (Barman and Nayak, 2000). Also N- and O-linked oligosaccharides and specific amino acids may function as apical sorting signals (Benting et al., 1999; Rodriguez-Boulan and Gonzalez, 1999). Microtubules and microfilaments as well as motor proteins from the kinesin and dynein family are important to translocate the transport vesicles for both direct and indirect pathways (Hirokawa, 1998; Kamal and Goldstein, 2000). After having reached its destination the transport vesicle fuses using specific recognition and fusion machineries. Besides proteins, also lipids integrate differentially into different membrane domains. It was appreciated that newly synthesized sphingolipids were preferentially transported to the apical membrane (Simons et al., 2000). Based on this it was proposed that glycosphingolipids specifically cluster in the Golgi membrane and are then transported to the apical surface. Along with them, proteins destined for the apical plasma membrane may be co-transported to their target compartment. Additionally, clustered glycosphingolipids together with cholesterol (membrane rafts) are present in caveolae, small invaginations of the plasma membrane devoid of clathrin coats. These caveolae might have a role in endocytosis and transcytosis both of which are important for basolateral sorting processes (Ghitescu et al., 1986; Tran et al., 1987). Therefore, sphingolipid membrane rafts seem to be involved in membrane trafficking.

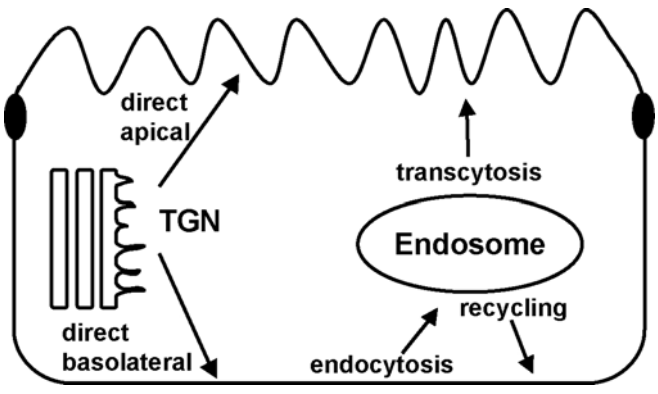

Figure 9 Scheme of polarized cells
Polarized cells feature an apical and a basolateral membrane domain separated by tight junctions (black ellipses). The direct pathway sorts components from the trans-Goligi network (TGN) directly to their respective domain. Endocytotis and transcytosis remove components from the membrane and can redirect them to the correct localization (indirect pathway).

In myelinating cells sorting and transport mechanisms are investigated and are considered to stand in the center of understanding how myelin internodes are generated and maintained. Importantly, myelin proteins have targeting sequences which are functional in polarized sorting in epithelial cell lines. As example the large isoform of MAG (L-MAG) was targeted to both apical and basolateral compartments, whereas the short isoform S-MAG was targeted to the apical domain of MDCK cells (Minuk and Braun, 1996). For MOG, a potential basolateral sorting signal was identified and indeed MOG is targeted to the basolateral compartment in MDCK cells (Kroepfl and Gardinier, 2001). In contrast, PLP is integrated into the apical domain and a 13 amino acids signal sequence at its N-terminus is sufficient to target LacZ to the myelin sheath *in vivo* (Kroepfl and Gardinier, 2001; Wight et al., 1993). Controversially, P0 was targeted not to the apical but to the basolateral domain in MDCK cells, and deletion of its cytoplasmic domain led to apical targeting. The latter results demonstrate that the situation of myelinating cells cannot be easily modeled in simple polarized epithelial cells. Therefore, the identified signal sequences must be studied during the process of myelination itself. Up to day little is known about the specific molecules and their interactions in sorting and targeting machineries in myelinating cells. Therefore, concepts established in other cells are used to speculate about the situation in oligodendrocytes and Schwann cells.
Some studies provided evidence how proteins are sorted and transported in PNS internodes. Trapp and colleagues analyzed the targeting of P0 (compact myelin), MAG (non-compact myelin) and laminin (plasma membrane) to their respective domain (Trapp et al., 1995). First, they demonstrated that P0 and MAG were incorporated into different transport vesicles as they exit from the TGN and were transported along the internode on microtubules. Furthermore they showed that P0 and MAG were not mistargeted upon disruption of microtubules but accumulated in the cytoplasm as distinct entities (Trapp et al., 1995). They conclude that microtubules have no direct role in targeting of distinct vesicles but that most likely specific ligand receptor interaction at the target domains is responsible to correctly incorporate respective vesicles.

4.4.3 MAL in polarized epithelial cells

As described in chapter 4.3.2.3, MAL was identified to be present in membrane rafts of vesicular structures in the apical cytoplasmic domain of MDCK cells (Zacchetti et al., 1995). Therefore, it was speculated that MAL might have a role in polarized sorting and transport mechanisms. Interestingly, if overexpressed in insect cells MAL caused the formation of intracellular vesicles. This suggests that MAL might have a role in formation of glycolipid-enriched vesicles (Puertollano et al., 1997). Following this, several functional experiments led to the conclusion that, indeed, MAL is crucial for sorting and transport of apical components. Cheong and colleagues analyzed the effect of altering MAL levels in MDCK cells by overexpression and antisense techniques. They stated that increased levels of MAL led to increased apical transport and expansion of the apical surface (Cheong et al., 1999). In contrast,

reduced levels of MAL caused accumulation of apical surface markers like the influenza virus hemaglutinin (HA) in the post-Golgi compartments. The basolateral surface marker E-cadherin was not influenced leading to the concept that MAL must be important for apical transport mechanisms. Another study analyzed the role of MAL in Fischer rat thyroid (FRT) cells. These cells sort GPI-linked proteins to their basolateral compartment under normal conditions. Also in these FRT cells the correct transport of apical markers was dependant on normal MAL levels independent if they were raft associated or not (Martin-Belmonte et al., 2000). Frank and colleagues draw the parallel to myelinating cells since the apical compartment is enriched in specific glycosphingolipids, e.g. galactosylceramide and sulfatide which are also enriched in myelin (for review see Frank, 2000). MAL co-purifies with these glycosphingolipids in detergent insoluble complexes suggesting a role of MAL in subdomain formation of myelinating cells. Nevertheless, the situation in myelin structures is much more complex than simple apical vs. basolateral. Therefore, polarized sorting mechanisms from epithelial cells can provide general concepts but myelin specific protein sorting and trafficking probably needs much more elaborated systems.

4.5 Cytoskeleton elements in myelinating cells

Protein and lipid transport in all cells is dependant on cytoskeleton elements. Golgi derived vesicles travel along microtubule and microfilament tracks to reach their destination. There, they interact with specified target recognition systems and ultimately fuse. The role of cytoskeleton elements here is crucial and was to some extend studied in both Schwann cells and oligodendrocytes.

4.5.1 Schwann cells

Initially, Schwann cells polarize their plasma membrane into two domains the abaxonal and the adaxonal membrane. The abaxonal membrane is crucial for synthesis of the basal lamina (Bunge et al., 1986; Eldridge et al., 1987). The adaxonal compartment is enriched in MAG and in direct contact with the axon (Trapp et al., 1984). The polarization of Schwann cell membranes into distinct domains is dependant on cytoskeleton elements. Indeed, the transport of myelin proteins in Golgi-derived vesicles is dependant on microtubules (Trapp et al., 1995). The role of cytoskeleton elements, in particular microtubules (MTs) and microfilaments (MFs), has been studied in the mature myelin sheath. In myelinated internodes tubulin tracks emanate from perinuclear Golgi rich regions (Kidd et al., 1994). The majority of microtubules is polarized with their plus ends away from the perinuclear region and might serve as tracks for vesicular transport of myelin components. Still also minus end directed MTs are found with the implication that both minus and plus end directed transport might contribute to myelin formation in Schwann cells (Kidd et al., 1994). The presence of the microfilament components f-actin and spectrin was shown in all non-compact myelin compartments where they co-localize with MAG

(Trapp et al., 1989). Additionally, an extensive intermediate filament (IF) network was found in the cytoplasmic compartments by immunoreactivity for vimentin (Trapp et al., 1995). Still the role of the Schmidt-Lanterman incisures for protein and lipid turnover is not clear. Nevertheless, it is believed that non-compact myelin compartments and specially Schmidt-Lanterman incisures might be the hotspot where vesicle dependant turnover takes place. The microvilli and paranodal Schwann cell cytoskeleton is thought to be crucial for correct initiation and maintenance of the axonal nodal specialization. Still, in comparison to the cytoskeleton specialization of the nodal axolemma, the molecular makeup of the microvilli and paranodal cytoskeleton is still poorly understood.

4.5.2 Oligodendrocytes

Whereas Schwann cells only form one internode, oligodendrocytes extend multiple extensions to many internodes. Each internode has to be separately established and later on maintained. The respective myelin building blocks have to be transported and sorted through specific sorting mechanisms (for review see Pfeiffer et al., 1993). The primary and secondary processes of oligodendrocytes are filled with numerous organelles such as mitochondria and ER as revealed by EM (Barry et al., 1996). This arrangement of cellular organelles points to the local synthesis of myelin component in the processes (Barry et al., 1996). Still, they have to be correctly targeted and transported to integrate into the emerging myelin sheath. During myelination opposing myelin membrane layers become compacted leaving narrow cytoplasmic channels rich in microtubules. In culture, oligodendrocytes form flat membrane sheaths with comparable channels containing an extensive network of MTs and MFs but lacking IFs (Pfeiffer et al., 1993; Song et al., 2001; Wilson and Brophy, 1989). Vimentin as prominent IF is only present in OPCs but no longer expressed in mature oligodendrocytes (Barry et al., 1996). Microfilaments are present throughout the cytoplasm in the cell body and all processes. They are necessary in various processes to generate meshwork's contributing to mechanical force and this is also true for oligodendrocytes (Simpson and Armstrong, 1999). Particular enrichment of MFs can be seen at the leading edges of processes and branching sites (Song et al., 2001). The MT network is abundant in the cell body and all processes, but does not extend into the most distal tips of leading edges (Song et al., 2001). MTs in oligodendrocyte processes are thought to provide the tracks for directed vesicular and organelle transport. They are preferentially polarized with their plus end towards the cell periphery (Lunn et al., 1997). In nocodazole treated cells with disrupted MT network, the morphology and transport processes are disturbed (Carson et al., 1997; Lunn et al., 1997). Since oligodendrocytes can be cultured *in vitro* the identification and characterization of oligodendrocyte microtubule associated proteins (MAPs) was much more successful than for Schwann cells. In oligodendrocytes various MAPs in particular MAP2 and tau are expressed and developmentally regulated (Richter-Landsberg and Gorath, 1999). Tau proteins are already expressed in OPCs and later on enriched at branching points and at the ends of mature oligodendrocytes

processes. Interestingly, oligodendrocytes switch the expression pattern of tau isoforms from splice variants with three MT binding domains to four towards maturation (Richter-Landsberg and Gorath, 1999). The different MAPs contribute to MT dynamics and stabilization to adjust the cytoskeleton during the different stages of differentiation and myelination. This might reflect the need for more stable MT tracks in more mature stages to stabilize the oligodendrocyte processes.

4.6 The septins

Septins are a family of cytoskeleton proteins which were identified in yeast as temperature sensitive mutants of cytokinesis (Hartwell, 1971). Septin mutants in yeast are demarcated by elongated mother-bud necks and multinucleated cells resulting from impaired septation. The phenotype was traced to four homologous genes CDC3, CDC10, CDC11 and CDC12 which were later termed septins. With the exception of plants, septins are well conserved throughout species (Pan et al., 2007). Interestingly, the number of isoforms and the complexity of splice variants increases tremendously from yeast to mammals. In humans, currently 14 septins are described showing multiple alternative splicing with tissue specificity of their expression (Hall et al., 2005). After the initial discovery in cytokinesis they where subsequently found in diverse tissues and additional functions of septins were soon discussed. Today, septins are thought to be involved in many cellular processes like cytokinesis, vesicular transport mechanisms and vesicle fusion as well as being important regulators of the other cytoskeleton systems, the microfilaments and microtubules (Kartmann and Roth, 2001; Kinoshita, 2003b). The presence of septins in myelinating cells has been demonstrated recently (Roth, 2006; Taylor et al., 2004).

4.6.1 Septins in yeast

Septin research in yeast looks back on four decades of investigation. After their discovery in 1971 as mutants of cytokinesis they were shown to localize to the mother-bud neck (Figure 10). S. cerevisae features an asymmetric division by polarized membrane growth at a distinct membrane location leading to the emergence of a bud. When the bud has reached the respective size and contains all subcellular elements as well as its nucleus, then, the daughter cell is separated from the mother cell by septation using an actomyosin contractile ring. During polarized bud growth, septins form a highly ordered filamentous structure known as the septin collar at the mother-bud junction (Byers and Goetsch, 1976; Kim et al., 1991). Septin mutants completely impair cytokinesis whereas disturbance of the contractile actomyosin ring only delays septation. This lead to the view that septins must act upstream of the later (Kim et al., 1991; Vallen et al., 2000). Septins were soon shown to interact abundantly among themselves. As mentioned, the S. cerevisiae septins co-localized at the mother-bud neck (Ford and Pringle, 1991; Haarer and Pringle, 1987; Kim et al., 1991) and mutation of one septin isoform leads to the loss of the

others from the neck (Ford and Pringle, 1991; Haarer and Pringle, 1987; Kim et al., 1991) suggesting that all yeast septins have to be present to form a functional complex. During the yeast cell cycle septins initially localize at the presumptive bud site as a ring structure. During polarized bud growth the septin ring expands to a collar at the mother bud neck (Figure 10). Coinciding with cytokinesis, the septin collar splits into two separate rings one of which will persist in each cell after division (Ford and Pringle, 1991; Kim et al., 1991). An interesting feature of septins is that they form a membrane bound barrier preventing the free diffusion of RNA and proteins between the emerging daughter cell and the mother cell (Takizawa et al., 2000). Recently, it was shown that a septin dependant diffusion barrier also compartmentalizes the ER between the mother and the daughter cell (Luedeke et al., 2005). None of the septins contains a transmembrane domain which implicates that septins interact with other membrane bound proteins or lipids. Besides organizing themselves, septins were also shown to localize specific elements required for septation like chitin synthase III to the mother-bud neck (DeMarini et al., 1997). Taken together, septins form a highly dynamic filament scaffold at the mother-bud neck organizing subsequent protein integration required for establishing a diffusion barrier and ultimately for the septation of the cells.

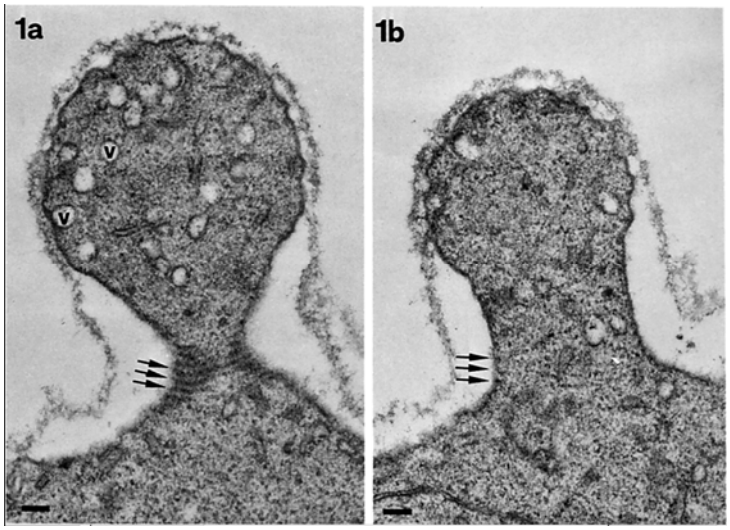

Figure 10 The septin collar
Electron micrograph of the emergind daughter cell in budding yeast. Septins form a filamentous ring structure at the mother bud neck (1a arrows). Septin mutants lack this septin collar (1b arrows) and cannot complete cytokinesis (copied from Byers and Goetsch, 1976).

4.6.2 Septin complex formation and structure

Septins are cytoplasmic proteins of intermediate molecular weight between 30kD and 75kD which display over 26% homology along the entire sequence (for review see Longtine et al., 1996). Overall septin domain structure can be divided in three regions (Figure 11). In a central region the homology is highest and this domain contains a P-loop consensus sequence indicating a GTP binding cassette (Hall and Russell, 2004; Saraste et al., 1990). GTPase activity *in vitro* could only be attributed to some septins and the function of the GTPase motif is still unclear (Field et al., 1996; Frazier et al., 1998). In contrast, the N-terminus is highly variable. The C-terminus implies predicted coiled-coil motifs for most septins but not all (Kartmann and Roth, 2001; Longtine et al., 1996).

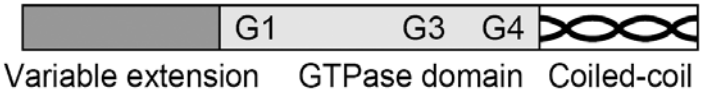

Figure 11 The septin protein domains
Septin proteins contain a central GTPase domain with a G1, G3 and G4 cassette. The G1 cassette contains a P-loop motif responsible for nucleotide binding. The N-terminal domains are highly variable among different septins. The C-terminal regions contain predicted coiled-coil stretches for most but not all septins (copied from Field and Kellogg, 1999).

The septin gene family comprises 2 isoforms in C.elegans, 3 isoforms in drosophila and 12 or more isoforms in mammals (Figure 12). For human septins it was reported that the septin transcripts undergo multiple alternative splicing potentially generating dozens of different polypeptides (Hall et al., 2005). To form higher order structures septins form heteromeric complexes with distinct stoechiometry. The prototype septin complex was isolated from Drosophila by immunoprecipitation and contained three septin isoforms in 1:1:1 relation (Field et al., 1996). Thereafter, the ultimate building blocks of septin structures were analyzed to be a tetramer for the nematode, a hexamer for mammalian and drosophila complexes and a octa- or decamer for fungal complexes (for review see Barral and Kinoshita, 2008). For mammalian complexes single isoforms are replaceable in the hexameric building block. This is due to higher complexity and redundancy among the septin family in mammals. Here, different combinations of septins are believed to fulfill different functions but still it is unclear how this might be achieved. Native and recombinant septin complexes can be purified and polymerized as 8nm thick filaments of variable length (Figure 13, Field et al., 1996; Frazier et al., 1998; Hsu et al., 1998).

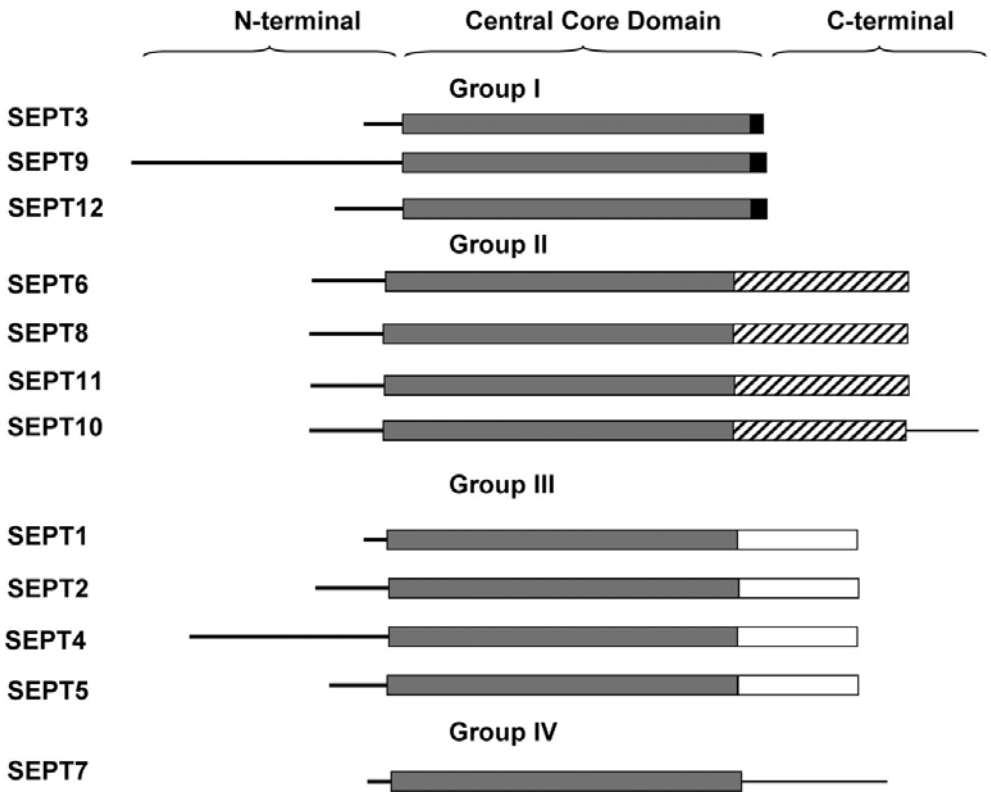

Figure 12 The septin protein family
The septin protein family can be grouped according to the sequence homology. Four subgroups are currently discussed (copied from Martinez and Ware, 2004).

In mammals the septin family was grouped into four subgroups according to sequence homology (Figure 12, Kartmann and Roth, 2001). This classification so far parallels with the compatibility of the proteins to form recombinant complexes in insect cells (Kinoshita, 2003a). Seemingly, for a stable septin complex one member of each subgroup has to be integrated. In line with this, a septin complex model was proposed. In the fundamental SeptX/ 6/ 7 complex with a stoechiometry of 1:1:1 (X : 1, 2, 4, 5), Sept6 is probably replaceable with Sept11, Sept8 and Sept10. Since being unique in terms of not having homologous isoforms, Sept7 might be crucial for all septin complexes. The role of Sept3, Sept9 and Sept12 in complex formation has to be further analyzed (Kinoshita, 2003a). Thereafter, other septins might be incorporated at sub-stoechiometric quantities. The *in vivo* composition of septin structures is still not well understood.

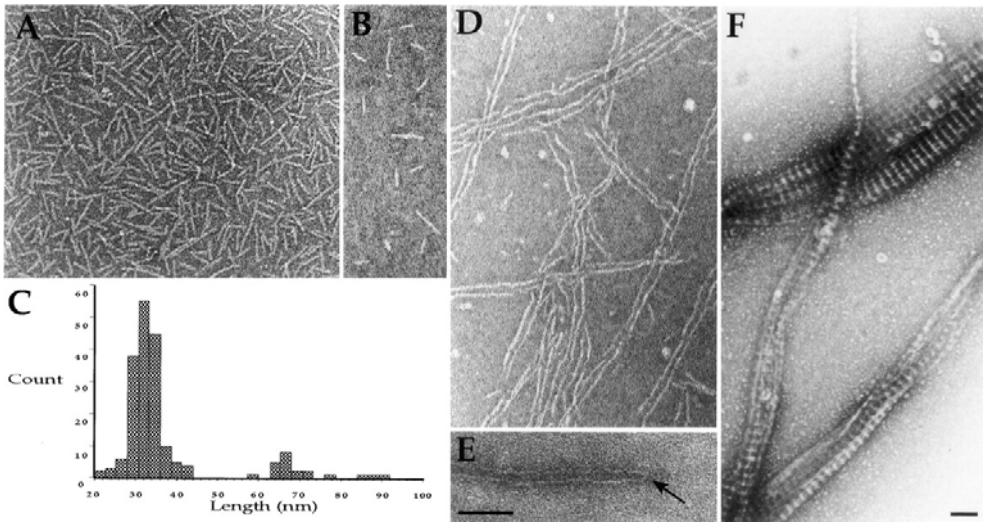

Figure 13 Septins form filaments *in vitro*
Purified yeast septins form filaments *in vitro* as analyzed by electron microscopy. Depending on ionic strength variable filament lengths can be achieved (copied from Frazier et al., 1998).

In vivo septin assemblies were originally discovered at the yeast mother-bud neck as 10nm filaments circumfering the neck (Byers and Goetsch, 1976). The first ultrastructural data about septin filaments derived from EM studies. There, septin filaments appeared as consecutions of short filament segments with obscure polarity (Hsu et al., 1998; Kinoshita et al., 2002). These filaments can laterally assemble into higher order structures forming curved bundles, rings or coils. Rapid-freeze and deep-etch EM techniques showed that septins can also form ordered gauzes or scaffolds at the cell cortex (Rodal et al., 2005). Importantly, septins might use existing actin bundles as templates for assembly (Kinoshita et al., 2002). *In vitro* septin assembly is not coupled to robust nucleotide exchange or hydrolysis and the role of the GTP cassette in septin assembly and function is still matter of debate. *In vivo*, septins seem to rearrange abundantly probably controlled by diverse binding factors and covalent modifications.
Comparable to the situation for actin, tubulin and intermediate filament proteins, crystallization of septins complexes was very challenging. Recently, the Wittinghofer group succeeded in crystallizing and reconstructing the human Sept2/ 6 /7 complex with atomic resolution (Figure 14). Surprisingly, they demonstrated that septins do not interact among themselves through their coiled-coil domains but rather the GTPase domains and stretches of their N-terminal domains (Sirajuddin et al., 2007). The coiled-coil domains were not visible in the crystal indicating that their orientation was flexible. The hexameric nature of the septin core unit was verified. Additionally, the polymerization of septins to filaments can be achieved by adding further hexamers in a linear fashion. Clearly, the septin filaments have no polarity which was also

concluded from other studies (John et al., 2007). According to the proposed model, septins might interact among themselves with the GTPase domains and with other proteins with the coiled-coil domain but the latter remains to be demonstrated.

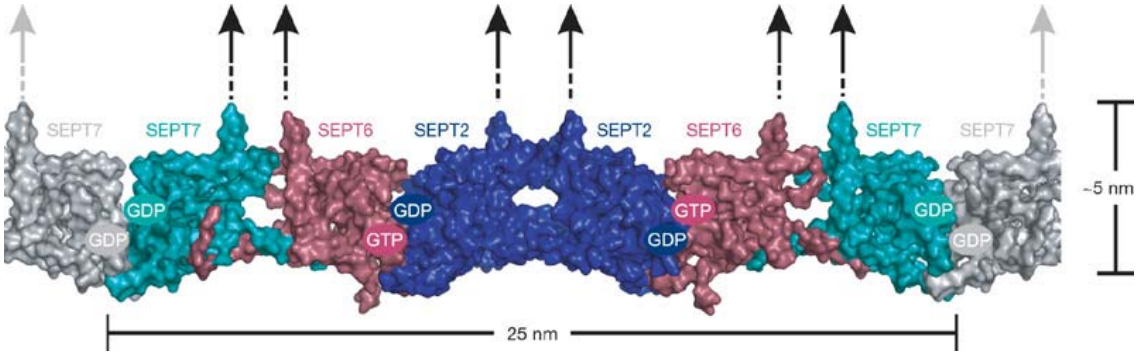

Figure 14 Ultrastructure of the human Sept2/ 6/ 7 complex
The crystal structure of the human Sept2/ 6/ 7 complex has been solved. Importantly, septins interact via their GTPase domains. The coiled-coil domains (depicted as arrows) seem to be flexible and radiate laterally from the septin filament (copied from Sirajuddin et al., 2007).

4.6.3 Septins in the mammalian central nervous system

After the initial discovery in yeast septin homolog's were soon found in higher animal species like Drosophila (Neufeld and Rubin, 1994) and ultimately in both mouse and human tissue (Nakatsuru et al., 1994; Nottenburg et al., 1990). A role in cytokinesis was demonstrated both for Drosophila and in mammalian cells (Kinoshita et al., 1997; Neufeld and Rubin, 1994; Surka et al., 2002). Since septins are also abundantly expressed in non-dividing tissues like the nervous system, additional functions besides cytokinesis are readily studied and described. Septins are thought to be important in cell polarity, cell cortex compartmentalization, vesicle transport and regulation of the actin and tubulin cytoskeleton and they also seem to be involved in numerous pathological conditions (Hall and Russell, 2004; Kartmann and Roth, 2001; Kinoshita, 2003b). In 1998, Hsu and colleagues identified a brain septin complex interacting with the exocyst or Sec6/8 complex (Hsu et al., 1998). The Sec6/8 complex in yeast is crucial for directed vesicle integration into distinct plasma membrane regions. In neurons, the exocyst complex seems to display a comparable role targeting vesicles to specific sites during neurite outgrowth and synaptic assembly (Hazuka et al., 1999; Hsu et al., 1999). Further support for a role of septins in vesicle targeting derived from the fact that septins interact with the SNARE protein syntaxin (Beites et al., 1999). SNARE proteins are thought to be crucial for the thermodynamically unfavorable approach of two membrane bilayers necessary for mediating vesicle fusion. It is believed that distinct vesicle bound SNAREs interact with target SNAREs on the membrane and that this system might provide specificity

for vesicle targeting (Sollner et al., 1993). Importantly, Sept5 did not only bind to syntaxin but by that inhibited exocytosis. This suggests that septins might regulate the availability of free SNAREs for fusion of vesicles (Beites et al., 1999). Recently, Amin et al. demonstrated that the inhibitory function of Sept5 on syntaxin and thereby exocytosis is regulated by phosphorylation through Cdk5 (Amin et al., 2008). Taken together, these data suggest that septins may be important for vesicle targeting by interacting with the exocytosis machinery and by regulating the availability of free fusion sites in neurons. Besides regulating exocytosis septins may also be involved in regulating spine morphology. Sept7 was identified to localize to the bases of dendritic spines in mature hippocampal neurons (Xie et al., 2007). Importantly, neurons deficient for Sept7 displayed altered spine morphology. Additionally, alterations in Sept7 expression lead to changes in dendrite arborization (Tada et al., 2007; Xie et al., 2007). Besides having a presynaptic role in vesicle targeting septins might also exert a postsynaptic function since numerous septins were isolated from postsynaptic density fractions. Undoubtedly, septins might reveal new concepts for the highly polarized neurons and their extensive vesicular systems. Besides in neurons, septins may also have a role in astrocytes. Kinoshita and colleagues showed that Sept2 co-localized with the glutamate transporter GLAST in Bergmann glia. Dominant negative mutants of Sept2 reduced the glutamate uptake via GLAST by internalization of the glutamate transporter (Kinoshita et al., 2004).

4.6.4 Septins in oligodendrocytes and Schwann cells

Very recently, it became evident that septins may also have a role in myelinating glia. Indeed, several proteomic screens for myelin and myelin-associated components revealed members of the septin family being incorporated into myelin fractions (Roth, 2006; Taylor et al., 2004). Additionally, recent work on the null mutant of the main CNS myelin component proteolipid protein (PLP) revealed that distinct septin isoforms were lost in myelin of these mice (Werner et al., 2007). In humans, mutations in the Sept9 gene were associated with hereditary neuralgic amyotrophy, a recurrent painful brachial plexus neuropathy (Kuhlenbaumer et al., 2005). These data suggest a role for septins in myelinating cells.

4.7 The contribution of cytoskeleton elements to subdomain formation in myelinating glial cells

In most mammalian cells interaction of the cytoskeleton with the plasma membrane is involved in regulating shape and movement (Niggli and Burger, 1987; Stossel, 1982; Weber et al., 1999). The mediators between the membrane and cytoskeleton elements are diverse and range from signaling receptors to membrane lipids. It is well-known that myelin membranes are divided into subdomains with distinct protein and lipid composition. Nevertheless, it is unclear how these domains are generated and then maintained throughout the adult. Especially the mechanisms of interaction

between cytoskeleton elements and membrane structures in the developing and adult myelin sheath are not fully resolved. Data from several studies suggests that myelin components might interact with the cytoskeleton. Dyer and colleagues provided evidence that CNPase can directly interact with f-actin and MTs and that MBP domain organization might result from interaction with MTs (Dyer and Benjamins, 1989a). Furthermore, they demonstrated that antibodies against galactocerebroside resulted in disruption of MT integrity and fusion of previously separated MBP domains (Dyer and Benjamins, 1989b). Wilson and Brophy showed interaction of CNPase and MBP with cytoskeleton fractions after detergent extraction (Wilson and Brophy, 1989). This implies an intimate crosstalk between myelin and cytoskeleton elements crucial for proper structuring of myelin membrane domains. In line with this, oligodendrocytes derived from the shiverer mouse which lack most of the MBP expression display altered MT morphology in culture (Dyer et al., 1997). The precise cascade of proteins involved in the transduction of the interaction between the myelin components and the cytoskeleton remain unknown. Furthermore, the situation in mature internodes might be much more complex and involve more elements than during oligodendrocyte differentiation and initiation of myelination. Septins might be intriguing in this context since they abundantly interact both with the plasma membrane and the tubulin and actin cytoskeleton. In fact this interface between cytoskeleton elements and plasma membrane structures is unique and might be important to establish membrane subdomains (Barral et al., 2000; Martin and Konopka, 2004). The septin gene family gives rise to a complex set of different isoforms and transcript variants. The septin cortex of a cell can then form higher order structures like filaments and scaffolds by heteromeric assembly and interact focally with other cytoskeleton elements and membrane structures. The abundance of different building blocks opens up a myriad of levers for regulating the cytoskeleton/membrane interface of a given cell. In this respect, septins are intriguing mediators of cortex organization and might be crucial in the highly polarized myelinating cells the oligodendrocytes and Schwann cells. Many aspects of how these cells generate their distinct subdomains and organize complex membrane structures are not known. The study of septin function in myelinating cells might provide answers to these questions and help to understand the structuring of complex membrane systems.

5 Motivation and Aim of the Work

Myelination is a uniquely complex and fascinating process. Oligodendrocytes and Schwann cells synthesize vast amounts of myelin membranes. They establish and maintain diverse subcompartments which are crucial for correct structuring of myelin internodes and functionality. Despite of decades of research, it is still not known how myelinating glia specifically transport and integrate myelin building blocks into the emerging myelin sheath. It is known that myelin membranes are divided into subdomains with distinct protein and lipid composition. How these domains are generated and maintained throughout the adult is currently heavily investigated. Cytoskeleton elements interacting with membrane components could generate and sustain such structural domains. Data from a yeast two hybrid screen suggested that the myelin and lymphocyte protein MAL may interact with septin 6 (Sept6) a member of a diverse cytoskeleton protein family, the septins. MAL is a mediator of compartmentalization in polarized cells and was already studied for its role in protein sorting and transport processes. In the myelin internode, MAL localizes both to the compact myelin compartment as well as non-compact compartments which is unique for myelin proteins. This suggests that MAL, indeed, might have a role in protein and lipid transport in myelinating cells. An interaction between MAL and the cytoskeleton, here the septins, opens up new concepts how myelin membrane domains are generated. Therefore, this work was aimed to verify and characterize the interaction between MAL and Sept6. Additionally, we aimed to analyze the septin gene family in myelinating cells. Not much was known about septins and their function in the nervous system, and no data on septins existed for oligodendrocytes and Schwann cells. Recent studies have only revealed the presence of septins in myelin but did not disclose their distribution and function. This work aimed to investigate the septin family in oligodendrocytes and Schwann cells with focus on their expression pattern, interaction with myelin structures and localization. Additionally, the downregulation of specific septin isoforms and the use of dominant negative septin mutants in myelinating DRG/ Schwann cell co-cultures to study septin function *in vitro* were planed.

6 Material and Methods

6.1 Custom peptide antibodies

Custom peptide antibodies against Sept2, Sept6 and Sept7 were generated. For each protein a peptide sequence from the N-terminus as well as one from the C-terminus was chosen for immunization.

6.1.1 Peptide sequences

Sept2 N-terminal: MSKQQPTGFINPETP + C
Sept2 C-terminal: C + QGGDSDSGALGQHV
Sept6 N-terminal: AADIARQVGEDCRT
Sept6 C-terminal: AGGSQTLKRDKEKKN + C
Sept7 N-terminal: SVSARSAAAEERSVNC
Sept7 C-terminal: C + EAQQRILEQQNSSRT

6.1.2 Peptide synthesis and immunization

Peptides were synthesized and used for immunization by Eurogentec, Belgium (DoubleXP protocol). 5mg of each peptide was coupled to hemocyanin. Two SPF rabbits for each protein were immunized with both peptides (4 injections: day 0, day 14, day 28, day 56; 4 bleeds: day 0, day 38, day 66 and day 87). Generated antisera were purified using the respective peptide column as described below. Specificity of the antibodies was tested with Western blot analysis (chapter 6.1.4).

6.1.3 Antibody purification

The respective peptide column was washed with 10mM Tris pH7.5 until the detector signal was stable. 3ml of serum was diluted to 10ml with 10mM Tris pH7.5 and loaded thrice onto the column. Unbound proteins were cleared by washing the column with 10mM Tris pH7.5 until the detector signal was on baseline. The column was first washed with 6ml 500mM NaCl in 10mM Tris pH7.5 and further with 10mM Tris pH7.5. Specific antibodies were eluted by applying 100mM glycine-HCL pH 2.5. Ten 2ml fractions were collected and neutralized at once with 150µl 1M Tris-HCl pH 8.0. Fractions with elevated OD_{280} absorption were collected and concentrated in Centricon dialysis units (Millipore, USA) and dialyzed 1:1000 to PBS. Protein concentration was determined by the Bradford method.

6.1.4 Western blot analysis with custom-made anti-septin antibodies

The purified N- or C-terminus specific antibodies were characterized by Western blot analysis. 20μg myelin proteins were loaded on a 5-15% SDS-PAGE gradient gel. The Western blot analysis was performed as described in chapter 6.4. All septin antibodies were diluted 1:1000 and incubated with the membrane o.n. at 4°C. The N-terminus specific septin antibodies revealed single bands at the calculated molecular weight of 41kD for Sept2, 49kD for Sept6 and 51kD for Sept7 (Figure 15). All C-terminus specific antibodies did not generate specific bands. The N-terminus specific septin antibodies were, therefore, used for further applications.

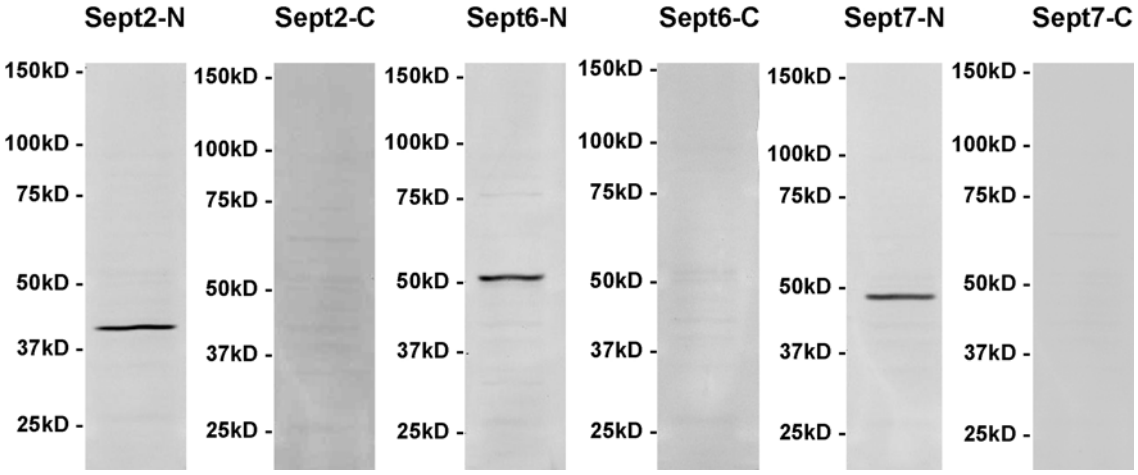

Figure 15 Myelin membranes were enriched by density gradient centrifugation. 20μg protein per lane was loaded on 5-15% SDS-PAGE gradient gels. The N-terminus specific as well as the C-terminus specific antibodies for Sept2, Sept6, Sept7 were used for Western blot analysis. The N-terminus specific antibodies generated single bands at expected molecular weight.

6.2 Other antibodies

The Sept4 antibody was purchased from Santa Cruz Biotechnology (sc-20179, USA). Sept8, Sept9 and Sept11 antibodies were kindly provided by Koh-Ichi Nagata (Institute for Developmental Research, Aichi, Japan). Monoclonal and polyclonal anti-Caspr antibodies and anti-Gliomedin antibody were kindly provided by Elior Peles (The Weizmann Institute, Rehovot, Israel). The MBP antibody was purchased from Millipore (MAB386, USA). Anti-tubulin antibody was from Invitrogen (A11126, USA), and anti-beta-actin from Sigma (USA). Phalloidin-Alexa555 was purchased from Invitrogen (USA). Monoclonal anti-O1 and anti-O4 antibodies were kindly provided by Martin Schwab (Brain Research Center, University of Zurich, Switzerland). Polyclonal anti-MAL antibody was generated and characterized in the lab.

6.3 Yeast two-hybrid screen

The yeast two-hybrid screen was performed using the yeast strain CG-1945 harboring HIS3 and β-Gal as reporter genes (Fields and Song, 1989; Stegmuller et al., 2003). As bait, cDNA encoding the N-terminal cytoplasmic domain of MAL (amino acid 1-24, Schaeren-Wiemers et al., 1995) was subcloned into the pGBT9 vector (GAL4 DNA-binding domain vector, Clontech). Using the lithium acetate method, yeast was transformed sequentially with pGBT9-MAL and a postnatal (6 weeks) mouse brain MATCHMAKER cDNA library in pACT2 (GAL4 activation domain, Clontech). About 1 million transformants were screened. Transformants were grown on SD medium-Leu-Trp-His plates with 5mM 3-amino-1,2,4-triazole. Robustly growing colonies were tested for β-galactosidase gene activity: yeast were grown on SD-Leu-Trp-His, transferred onto reinforced nitrocellulose membrane (Schleicher and Schuell, Germany), submerged in liquid nitrogen, and placed on a Z-buffer/X-gal-soaked Whatman (Z-buffer: 60mM Na_2HPO_4, 40mM NaH_2PO_4, 5mM KCl, 1mM $MgSO_4$, pH 7; Z-buffer/X-gal solution: 100ml Z-buffer, 0.27ml β-mercaptoethanol, 1.67ml 20mg/ml X-gal stock solution). Blue color was allowed to develop for 30'. DNA sequencing revealed two independent clones of Sept6 that both included the complete open reading frame. The specificity of the MAL-Sept6 interaction was confirmed by nutritional selection and β-galactosidase test of yeast co-transformed with pGBT9-MAL and isolated pACT2-Sept6, while pACT2-myc or isolated library plasmids served as negative controls. Unspecific interactions of pACT2-Sept6 were excluded by co-transformation of yeast with pGBT9 constructs expressing cytoplasmic domains of the unrelated transmembrane proteins PLP or GPM6B.

6.4 Western blot analysis

Appropriate amounts of protein were diluted in dilution buffer (33mM Tris pH6.8, 0.2% SDS) and incubated with 4x protein sample buffer (100mM Tris pH 6.8, 2% SDS, 50% glycerol, bromphenolblue, 20% β-mercaptoethanol) for 1hr at 37°C. Proteins were separated on 5-20% SDS-PAGE gradient gels and transferred onto PVDF membranes at 50V for 1.5hr at RT. Unspecific binding sites were blocked with 3% Top-Block (Sigma, USA) for 2hrs at RT and incubated with primary antibodies o.n. at 4°C. After four washes with TTBS (20mM Tris pH 7.5, 0.5mM NaCl, 0.1% Tween20) for 5' at RT, membranes were incubated with fluorescent-coupled secondary antibodies for 1hr at RT. After four washes with TTBS and two with TBS for 5' at RT, the membranes were scanned with the Odyssey system (LI-COR Biosciences, USA). The scan resolution was 84μm and the intensity was set to 5.0 for both channels.

6.5 Immunohistochemistry

6.5.1 Teased peripheral nerve fibers

Teased fibers were prepared as follows. The sciatic nerves of adult mice were prefixed 5' in Zamboni fixation solution (2% PFA, 0.18% picric acid in Soerensen phosphate buffer pH 7.3) prior to removal from the animals. After excision, the sciatic nerves were further fixed in Zamboni solution for 10' and washed twice for 15' in PBS (PBS Instant Dulbecco, pH 7.4, Biochrom AG, Germany). After teasing, the fibers were dried on gelatin-chromalaun coated slides for 2hrs on a 37°C hot plate, and frozen at -20°C for storage. For immunohistochemistry, the teased fibers were permeabilized in acetone (-20°C) for 10', and then washed in PBS (4°C) for 10'. Tissue samples were incubated for 1hr in blocking buffer (PBS, 1% glycine, 4% NGS, 0.1% TritonX-100) and subsequently incubated with primary antibodies o.n. at 4°C. Afterwards, the fibers were washed in PBS at RT for 15' and incubated with fluorochrome-coupled secondary antibodies for 30' at RT. The teased fibers were washed for 15' in PBS and 10' in water before embedding in Fluorosafe (Calbiochem, Germany).

6.5.2 Cryostat sections of fresh frozen human femoralis nerve tissue

Cryostat sections of fresh frozen human femoralis nerves (10μm) were mounted on gelatin-chromalaun coated slides and fixed for 90' with 10% buffered formalin solution. Delipidation was performed o.n. in 70% ethanol. Unspecific binding sites were blocked for 90' at RT in blocking buffer (PBS, 1% glycine, 4% NGS, 0.1% TritonX-100). Primary antibodies were incubated at 4°C for 70hrs and fluorochrome-coupled secondary antibodies 30' at RT. Confocal fluorescent images were acquired on a Carl Zeiss LSM510 microscope.

6.5.3 Cell cultures

Cells were washed twice with ice cold PBS and fixed with 4% PFA in PBS for 15' at RT. Following three washes with PBS for 5', the cells were treated with methanol for 15' at -20°C. After two washes with PBS for 5', the cells were incubated with blocking buffer (PBS, 5% BSA, 1% NGS, 0.2% TritonX-100) for 1hr at RT. The cells were incubated with primary antibodies o.n. at 4°C. The cells were washed three times with PBS for 15' and incubated with fluorochrome-coupled secondary antibodies for 1hr at RT. Finally, the cells were washed three times with PBS for 15', twice with water and embedded in Moviol.

For the O1 (galactosylceramide) and O4 (sulfatide) epitopes, life stainings were performed as follows. If the cell culture medium did not contain 10% FBS unspecific binding sites were saturated with corresponding medium supplemented with 10% FBS for 30' in the incubator prior to staining. The cells where incubated with undiluted

O1 or O4 supernatant for 30' at RT, washed twice with PBS and then processed as described above for fixation and further staining.

6.6 Electron microscopy

The optic nerves of adult mice were fixed in Karnovsky solution (3% paraformaldehyde, 3% glutaraldehyde, 0.1M Cacodylatbuffer) at RT for 20'. Afterwards, the samples were postfixed with osmium tetroxide, dehydrated and embedded in EPON. Ultrathin sections of 70-80nm were contrasted by PB-Citrate and uranyl-acetat. Sections were imaged with a transmission electron microscope (Morgagni 268 D; FEI).

6.7 Immobilization of IgG for Immunoprecipitation

6.7.1 SeizeX ProteinA Immunoprezipitation kit (Pierce, USA)

The coupling of IgG samples to proteinA sepharose was performed according to the manufacturer's instructions. In short, 400µl proteinA sepharose was added to a filter tube and washed twice with binding/wash buffer (0.14M NaCl, 8mM sodium phosphate, 2mM potassium phosphate, 10mM KCl, pH 7.4). The purified antibody (100-150µg) was added to the sepharose and incubated 1hr at RT with end-over-end mixing. The beads were then washed thrice with binding/wash buffer. The filter was placed into a new collection tube and 400µl binding/wash buffer was added. A provided 2mg disuccinimidyl suberate (DSS) aliquot was dissolved with 80µl dimethylsulfoxide (DMSO). 25µl DSS in DMSO was supplemented to the bead suspension and incubated 1hr at RT on a rocker. The beads were washed five times with 500µl elution buffer (pH 2.8, contains primary amine), twice with binding/wash buffer and stored in binding/wash buffer with 0.1% sodium azide.

6.7.2 ProFound Co-Immunoprecipitation kit (Pierce, USA)

The coupling of IgG samples to aldehyde-activated beaded agarose was performed according to the manufacturer's instructions. In short, 200µl AminoLink plus coupling gel 50% slurry were washed twice with coupling buffer (0.14M sodium chloride, 8mM sodium phosphate, 2mM potassium phosphate, 10mM KCl, pH 7.4). The antibody sample (600-700µg) was added to the beads. 3µl 5M sodium-cyanoborohydride (provided with the kit) was added to the slurry and incubated with end-over-end mixing for 4hrs at RT. The beads were washed twice with coupling buffer. Afterwards, 400µl quenching buffer (1M Tris-HCl, pH 7.4) supplemented with 4µl 5M Na-cyanoborohydride was added to the beads. The quenching reaction was incubated for 30' at RT with end-over-end mixing. The beads were washed four times with wash solution (1M NaCl), twice with coupling buffer and stored in coupling buffer with 0.1% sodium azide.

6.7.3 Affi-Gel Hz Immunoaffinity kit (Biorad, USA)

The coupling of IgG samples to hydrazide-agarose beads was performed according to the manufacturer's instructions. Buffer exchange was performed as follows. The upper and bottom cap of Econo-Pac 10DG columns (provided in the kit) were removed and excess buffer on top was poured off. The columns were washed with 20ml 1xHz coupling buffer and the antibody samples were applied to the columns. Then, 2ml 1xHz coupling buffer was added to the columns. 0.5ml elution fractions were collected and further 2ml 1xHz coupling buffer was applied while collecting fractions. The OD_{280} of collected fractions was measured and antibody containing fractions were pooled. Following this, the IgG samples were oxidized as follows. 1.2ml water was added to one vial of sodium periodate (25mg, provided in the kit). 3/10 volume sodium periodate stock solution was added to the IgG samples and the tubes were wrapped in aluminum foil to protect them from light. The samples were incubated with end-over-end mixing for 1hr at RT. The oxidation reaction was stopped by buffer exchange over Econo-Pac 10DG columns as described above. For coupling, 800µl Affi-Gel Hz gel was applied to a 5ml tube and allowed to settle. The supernatant was removed and the beads were washed twice with 2ml coupling buffer. 1ml coupling buffer was added and the beads were divided into two 2ml tubes. Oxidized IgG samples were added to the gel and rotated end-over-end for 24hrs at RT. The beads were washed once with 1ml 500mM NaCl in PBS, twice with 2ml PBS with 0.1% sodium azide and stored in PBS with 0.1% sodium azide.

6.8 Immunoprecipitation

6.8.1 Sample preparation

All steps were carried out at 4°C if not otherwise stated. Sciatic nerves from 4 adult mice or rats were homogenized in lyses buffer (PBS, 2mM $MgCl_2$, 0.5% DDTM (Anatrace, USA), aprotinin, leupeptin, pepstatinA, PMSF) and incubated for 30' with end-over-end mixing. Insoluble components were separated by centrifugation at 18'000g for 30'. The supernatant was diluted 1:2 with PBS, 2mM $MgCl_2$ and used for immunoprecipitation.

For CNS myelin samples, myelin fractions were prepared as follows. The mice were decapitated and the brains transferred to 15ml tubes. 3ml solution A (250mM sucrose, 10mM HEPES, 2mM EGTA pH 7.4) containing protease inhibitors (aprotinin, leupeptin, pepstatinA, PMSF) was added to the tissue and the samples were homogenized with a polytron. 5.8ml solution C (2M sucrose, 10mM HEPES, 2mM EGTA pH 7.4) was added to obtain a 1.4M sucrose containing homogenate. These samples were mixed gently by inversion. A sucrose gradient was set up in Beckmann tubes (13x51mm) as follows. 1ml of solution C was added into the tubes and overlain by 8.5ml of homogenate. 2.2ml solution B (750mM sucrose, 10mM HEPES, 2mM EGTA pH 7.4) and 0.75ml solution A were added subsequently to the tubes. Afterwards, the tubes were centrifuged in a free swing out rotor type TST41.14 for

20hrs at 4°C and 25'000rpm (100'000g). The myelin membrane fractions were collected at the top of the gradient and transferred to new 15ml tubes. These samples were diluted with 10mM Hepes, 2mM EGTA pH 7.4 up to 13ml and centrifuged at 100'000g at 4°C for 2hrs. The resulting myelin membrane pellet was resuspended in 10mM Hepes, 2mM EGTA pH 7.4.
For detergent extraction, 3 to 4.5mg of myelin proteins were incubated with an equal volume of extraction buffer (PBS, 2mM $MgCl_2$, 2% DDTM, aprotinin, leupeptin, pepstatinA, PMSF) and homogenized with a syringe. The samples were then incubated for 30' with end-over-end mixing before centrifugation at 18'000g for 30'. The supernatant was diluted 1:4 with PBS, 2mM $MgCl_2$ and subjected to immunoprecipitation.

6.8.2 Immunoprecipitation

All steps were performed at 4°C in the cold room if not otherwise stated. Sepharose beads (20µl settled) with 40µg covalently coupled antibody were incubated with blocking buffer (3% BSA in PBS, 2mM $MgCl_2$, 0.5% DDTM) for 15' and washed once with washing buffer (PBS, 2mM $MgCl_2$, 0.5% DDTM). Equal volumes of sciatic nerve or myelin detergent extract were incubated with sepharose beads with either anti-septin antibody or control IgG for 4hrs with end-over-end mixing. Beads were washed three times with washing buffer for 10'. Bound proteins were eluted with elution buffer (100mM Tris pH 6.8, 0.6% SDS) at 37°C for 15'. The eluted proteins were separated on 5-20% SDS-PAGE gradient gels and either stained with the Colloidal Blue kit (Invitrogen, USA) or subjected to Western blot analysis. Protein bands were excised and subjected to tryptic digest. The masses of the resulting peptides were measured by electro spray ionization and matched to the Mascot database (Matrix Science Inc., USA, Paul Jenö, Mass Spectrometry Facility, Biocenter, University Basel).

6.9 GST pull down assays

6.9.1 Sept6 with MAL(1-55)-GST

The MAL(1-55) N-terminal GST fusion construct or GSTTM1 was generated in the lab by Christoph Berger. Recombinant Sept6 was expressed in COS7 cells as follows. COS7 cells were transfected with the full length Sept6 sequence under the control of the CMV promoter (construct generated earlier in the lab, pcDSept6). Mock transfected cells were used as negative control. Plasmids were transfected with the Effectene transfection reagent (Qiagen, Germany). $1.2x10^6$ cells were seeded on a 100mm cell culture plate. The next day, 12µg DNA was diluted to 491µl with EC buffer. 96µl Enhancer was added and the mix was incubated for 5' at RT. Afterwards, 60µl Effectene was added and the transfection mix was incubated for 10' at RT. Meanwhile, the cells were washed once with PBS (Sigma, USA). The transfection mix was diluted with 10ml DMEM (Sigma, USA), 10% FCS (Sigma, USA), Pen/Strep

(Sigma, USA) and added to the cells. After 24hrs the cells were washed with PBS and incubated with new medium for further 24hrs for protein expression. COS7 cells from one 100mm plate per pull down were trypsinized 5' at 37°C. The trypsine reaction was stopped by addition of DMEM containing 10% FBS. After three washes with ice cold PBS the cells were resuspended in 100µl PBS containing protease inhibitors (aprotinin, leupeptin, pepstatinA, PMSF). Lyses was performed by addition of 100µl lyses buffer (PBS, 2mM $MgCl_2$, 2% DDTM (Anatrace, USA), 2% OTG (Sigma, USA)) and the samples were incubated with end-over-end mixing for 30' at 4°C. The samples were centrifuged at 18'000g for 30' to pellet insoluble material. The supernatant was diluted 1:2 with PBS, 2mM $MgCl_2$ and subjected to the GST pull down. For the pull down assay, 20µl glutathione-sepharose 75% slurry was washed twice with PBS and incubated with 50µg GST or MAL(1-55)-GST protein for 1hr at RT. The beads were washed three times with PBS and once with cold washing buffer (PBS, 2mM $MgCl_2$, 0.25% DDTM, 0.25% OTG) prior to incubation with samples. The COS7 cell extracts were incubated with loaded beads o.n. at 4°C. Afterwards, the beads were washed three times with washing buffer for 15' at 4°C. Bound proteins were eluted with elution buffer (100mM Tris pH 6.8, 0.6% SDS) at 37°C for 15' and analyzed with SDS-Page and Western blot analysis.

6.9.2 Sept2/ 6/ 7 trimer with MAL(1-24)-GST

6.9.2.1 Generation of the MAL(1-24)-GST construct

The N-terminal 24 amino acid fragment of MAL was amplified with the following primer pair:

5'HT-N-MAL: 5'-GATCCATGGCTCCGGCAGCGGCTTC-3'
3'HT-N-MAL: 5'-GATCCATGGAGTCAGGGAAGGTGGTGAAGACCGAGAAG-3'

The PCR reaction contained 38.5µl water, 5µl 10x buffer, 2µl dNTP (Promega, USA), 1.5µl of each primer and 0.5µl Taq polymerase (Roche, Switzerland). The PCR program implied an annealing temperature of 70°C and 40 cycles. The PCR fragment was purified using the Qiagen Nucleotide Removal kit (Qiagen, Germany) and digested with NcoI (88µl sample, 10µl buffer D (Roche), 2µl NcoI (Roche), 37°C for 4hrs). After digestion and purification with the Nucleotide Removal kit (Qiagen, Germany) the fragment was cloned in NcoI digested dephosphorylated pETGEXCT. The vector was prepared as follows. 10µg pETGEXCT vector was digested with NcoI as above and purified with the Qiagen PCR Purification kit (Qiagen, Germany). The purified digested vector was then dephosphorylated with shrimp alkaline phosphatase (30µl DNA, 50µl water, 10µl SAP buffer, 10µl SAP enzyme (Promega, USA), 37°C for 20'). Finally, the vector was purified with the PCR Purification kit. The ligation reaction was set up by mixing 7µl PCR fragment with 1µl vector, 1µl ligation buffer and 1µl T4 DNA ligase (Roche, Switzerland) and incubated at RT for 4hrs. The

ligation mix was used for transfection into DH5α by adding 2μl ligation mix to 50μl chemically competent bacteria. After incubation on ice for 30', bacteria were heat shocked at 42°C for 1' transferred on ice and supplemented with 250μl SOC medium. Ampicilline restistence was expressed for 1hr at 37°C prior to plating on agar plates. Colonies were screened with PCR with the 5'T7 and 3'HT-N-MAL primer (annealing temperature 54°C, 40 cycles). Positive clones were inoculated with 6ml LB medium containing ampicilline. Plasmids were prepared according to the Qiagen Mini Prep kit (Qiagen, Germany). The sequences were verified by sequencing (Microsynth, Switzerland) and one clone with correct sequence was chosen for protein synthesis.

6.9.2.2 Expression and purification of recombinant GST fusion proteins

One colony from a freshly prepared agar plate was inoculated with 20ml 2xYT medium supplemented with ampicilline (AppliChem, Germany) for both GST and N-MAL-GST clones. This starter cultures were incubated o.n. at 37°C with shaking. The next morning 500ml 2xYT with ampicilline were inoculated 1:100 with starter culture. The cultures were grown for 2.5hrs with shaking until they reached an OD_{600} > 0.6. At this point the expression of recombinant fusion protein was induced by addition of 1:500 100mM IPTG (AppliChem, Germany). The cultures were further incubated for 6hrs with shaking. After this, the cultures were centrifuged at 4000g for 15' and the pellets were frozen at –80°C until purification of the GST proteins. After thawing, each pellet was completely resuspended in 50ml B-PER solution (Pierce, USA) supplemented with one tablet Complete Protease Inhibitor Cocktail (Roche, Switzerland). The lyses of the bacteria was completed by incubation for 2hrs at RT with end-over-end mixing. Afterwards, the samples were centrifuged at 6000g for 30' at 4°C. Meanwhile 2ml Glutathione-Sepharose 4B (Amersham, UK) was washed twice with 50ml PBS. The bacterial supernatant was added to the sepharose and incubated for 2hrs at RT with end-over-end mixing. The beads were washed thrice with 50ml PBS and subsequently transferred to disposable columns (Amersham Pharmacia Biotech Inc., USA) with 5ml PBS. Bound GST proteins were eluted with 9ml 10mM glutathione in 50mM Tris pH 8.0. The samples were dialyzed twice 1:100 to PBS and concentrated with Centricon filter units (Millipore, USA). Protein concentration was determined with the Bradford method. The protein samples were diluted to 0.5μg/μl with PBS and aliquoted to 100μl for use in the GST pull down.

6.9.2.3 GST pull down assay

Purified Sept2/ 6/ 7 trimer was kindly provided by Prof. Ian Macara (Center for Cell Signaling, University of Virginia, USA).

20μl glutathione-sepharose 75% slurry was washed twice with PBS. 50μg of GST protein or MAL(1-24)-GST was added to the sepharose and incubated at RT for 1hr. The beads were washed once with PBS and the unspecific binding sites were blocked with blocking buffer (3% BSA in PBS, 2mM $MgCl_2$, 0.5% DDTM (Anatrace,

USA), 0.5% OTG (Sigma, USA)) for 15' at 4°C. Thereafter, the beads were washed once with washing buffer (PBS, 2mM $MgCl_2$, 0.5% DDTM, 0.5% OTG) prior to incubation with septin trimer. The purified Sept2/ 6/ 7 trimer was diluted in washing buffer (125μg to 500μl) added to the loaded beads and incubated o.n. at 4°C. Afterwards, the beads were washed three times with washing buffer for 15' at 4°C. Bound proteins were eluted by boiling in Laemmli buffer for 5' and analyzed with SDS-PAGE and Western blot analysis.

6.10 Light cycler quantitative real-time PCR

6.10.1 Primer pairs for real-time PCR

Primer pairs for Light cycler quantitative PCR were designed with the Clone Manager program (Table 1). Suitable primer pairs were chosen to overlap exon/intron junctions to avoid amplification of genomic DNA. Each primer alone and the PCR product were blasted using the NCBI blast server to exclude unspecific DNA amplification.

Primer name	Gene accession number	Sequence
5'Sept1	NM_017461.1	5'-TGCTGCCTCTACTTCATCTCAC-3'
3'Sept1		5'-ATCCCTCACCACTTCACAAGAC-3
5'Sept2	NM_010891.1	5'-GTGCCTGTCATTGCGAAAGC-3'
3'Sept2		5'-GGTCTTGGGTCACTTCCTGTAG-3'
5'Sept3	NM_011889.1	5'-AACACTGGTCAACACCCTCTTC-3'
3'Sept3		5'-GCGTTTCTTCCTGGCAATGTTC-3'
5'Sept4	NM_011129.1	5'-ACTGCTGCCTGTACTTCATCTC-3'
3'Sept4		5'-TGCTTTCCTTTAGGGCTTGGTC-3'
5'Sept5	NM_213614.1	5'-TCAGACCTGGAGCCACAGAG-3'
3'Sept5		5'-TCGTAGCCCACTGGAATCGG-3'
5'Sept6	NM_019942.2	5'-TCCTACCATGACTCCCGAATCC-3'
3'Sept6		5'-CATTGATCTCGCTCACCGACTC-3'
5'Sept7	NM_009859.2	5'-GTACAGGTGGAGCAATCCAAAG-3'
3'Sept7		5'-GTTGGCATTCCTCTGGTGTAAG-3'
5'Sept8	NM_033144.1	5'-TGGGCGAAACTGGGATTGG-3'
3'Sept8		5'-GGTGGGCGTGATGAAGTAGAG-3'
5'Sept9	NM_017380.1	5'-ACTGCTGCCTCTACTTCATC-3'
3'Sept9		5'-TCTGCGTCCTCATCAAACTC-3'
5'Sept10	NM_001024911.1	5'-GGCGTCAGGTAGCAGCATTAG-3'
3'Sept10		5'-GGCAGCAGGAAAGTGACCAAG-3'
5'Sept11	NM_001009818.1	5'-CCAGCAAACCAAGAAGGACAAG-3'
3'Sept11		5'-AAGCGACATACAAGGGACAGAC-3'
5'Sept12	NM_027669.1	5'-TGACAAGTGCTGGGACCCTATC-3'
3'Sept12		5'-ATCCTGCTCCTGAAGGCATCTC-3'
5'Krox20	NM_010118.1	5'-TCTACCCGGTGGAAGACCTC-3'
3'Krox20		5'-CAGGGTACTGTGGGTCAATGG-3'
5'Oct6	NM_011141.1	5'-AGCCGCTGCTCAACAAGTG-3'
3'Oct6		5'-CTTCTCCAGTTGCAGGCTGTC-3'
5'MAL	NM_010762.4	5'-GTGAGACTTCCTGGATCACAC-3'
3'MAL		5'-CATGGACCACGTAGATCAGA-3'
5'MBP	NM_010777.3	5'-GGTCCAGGCTTCCTTTGTTTTCTT-3'
3'MBP		5'-TGTCCAGCGTGTTCTCCTAAGTCC-3'
5'CNP	NM_009923.1	5'-TGTGCCCACCCTTTCTTTTCC-3'
3'CNP		5'-CAATGACCCAGCCCTTTTATTACC-3'
5'P0	NM_008623.4	5'-CCTCTCAGGTCACGCTCTATG-3'
3'P0		5'-GCCCGCTAACCGCTATTTC-3'
5'40S	NM_029767.1	5'-CGTGAGGTTTGGAGGGTCAAG-3'
3'40S		5'-TGTGACGTTGGCGGATGAG-3'
5'60S	NM_009438.3	5'-GGAAGTACCAGGCAGTGACAG-3'
3'60S		5'-GCAGGCATGAGGCAAACAG-3'

Table 1 5' and 3' primers used for quantitative real-time PCR are displayed together with the respective gene accession number. The 60S and 40S genes were used for normalization and quality control.

6.10.2 Standard curve generation for real-time PCR

PCR was performed on cDNA derived from P4 brain total RNA with respective primer pairs (see chapter 6.10.1). Specific PCR products were purified on TAE-gels and the bands were isolated with the Qiagen Gel Extraction kit (Qiagen, Germany). The PCR fragments were cloned into the pCR2.1-TOPO vector using the TOPO-TA Cloning kit (Invitrogen, USA) according to the manufacturer's instructions. The sequences were verified by sequencing (Microsynth, Switzerland). For standard curve generation a dilution series with defined cDNA copy numbers was established. A standard curve was generated by fitting the crossing points of the 10^5, 10^4 and 10^3 copy number dilutions into a logarithmic regression. The copy number of a given gene in a mRNA pool was then determined by fitting the measured crossing point of the sample into the respective standard curve.

6.10.3 Total RNA isolation from sciatic nerve tissue

Total RNA from sciatic nerves was isolated with the RNA Lipid Tissue kit (Qiagen, Germany) according to the manufacturer's instructions. Sciatic nerves from four C57Bl/6 mice per preparation were used for RNA extraction. The sciatic nerves were homogenized in 1ml Qiazol lyses reagent (Qiagen, USA) with a polytron. After homogenization, the samples were incubated at RT for 5'. Thereafter, 200µl chloroform was added and the tubes were shaken vigorously for 15''. After 3' at RT, the samples were centrifuged at 12'000g for 15' at 4°C. The aqueous phase was further processed. One volume of 70% ethanol was added and the samples were loaded on Rneasy Mini Spin Columns (Qiagen, Germany). After centrifugation (13'000rpm, 15'') the columns were washed once with the high salt buffer RW1 and twice with RPE (Qiagen, Germany) to remove remaining ions from the columns. The columns were centrifuged once empty in new collection tubes to get rid of the ethanol. Finally, the RNA was eluted twice with 30µl water.

6.10.4 Total RNA isolation from cultured cells

Total RNA from cultured cells was isolated with the RNA Micro kit (Qiagen, Germany) according to the manufacturer's instructions. About $4x10^4$ cells (one 60mm plate) were used for RNA extraction. Cells were scraped off with 350µl buffer RLT (RNA Micro kit, Qiagen, Germany) supplemented with β-mercaptoethanol. Afterwards, the cell suspension was homogenized with a polytron for 10''. One volume of 70% ethanol was added and the samples were loaded on Rneasy Micro Spin Columns (Qiagen, Germany). After loading, the columns were washed twice with the high salt buffer RW1, once with buffer RPE and once with 80% ethanol to remove remaining ions. The columns were dried by centrifugation empty in new collection tubes for 5' at max speed. The RNA was eluted with 14µl water.

6.10.5 Reverse transcription reaction

1μg total RNA per sample was subjected to reverse transcription. 20μl reactions were set up as follows. RNA was either precipitated by ethanol or used directly depending on purity of the samples. The RNA samples were diluted to 11.5μl with water. 1μl of OligodT primer (Promega, USA) was added and the samples were incubated at 65°C for 5' to resolve secondary RNA structures. The samples were then placed on ice. The reactions were supplemented with 4μl transcription RT buffer, 2μl dNTP mix (Promega, USA), 1μl Rnase inhibitor (Roche, Switzerland) and 0.5μl Transcriptor reverse transcriptase (Roche, Switzerland). The samples were incubated at 55°C for 30' for the RT reaction followed by 85°C for 5' for inactivation of the RT enzyme. The cDNA was diluted 1:25 with 10mM Tris pH8.0 and used for the Light Cycler reaction.

6.10.6 Quantitative real-time PCR

2.5μl sample or standard was applied to a capillary (Roche, Switzerland). The PCR mix containing 0.5μl water, 0.5μl of each primer and 1μl SybrGreenII (Roche, Switzerland) was added to the capillaries. The capillaries were closed and centrifuged shortly at 4000rpm. The quantitative PCR program implemented 50 cycles with an annealing temperature of 65°C. Determined mRNA copy numbers were normalized to the mRNA copy number of the 60S ribosomal protein subunit L13a.

6.11 Cell culture

6.11.1 Standard cell culture

COS7 and NIH3T3 cells were cultured in DMEM (Sigma, USA), 10% FBS (Sigma, USA), Pen/Strep (Sigma, USA) on standard tissue culture plates and split 2-3 times per week 1:5 or 1:10 according to the cell density.

6.11.2 Primary cell culture

6.11.2.1 DRG/ Schwann cell co-cultures

Dissociated mouse DRG/ Schwann cell co-cultures were generated basically as described earlier (Carenini et al., 1998). DRG's were isolated from E13 embryos and dissociated by trypsinization with 0.25% trypsine solution (Sigma, USA) for 45' at 37°C. MEM containing 10% FBS was applied to stop the tryptic digest. The cells were separated by trituration through FBS coated fire polished Pasteur pipettes with four strokes and seeded on poly-L-lysine (Sigma, USA) and collagen (Cell Systems Biotechnologies, Germany) coated cover slips. One embryo was seeded onto eight 12mm glass cover slips in 24 well plates (BD, Falcon). Cells were grown in MEM (Invitrogen, USA) supplemented with 0.4% glucose, 10% FBS (Sigma, USA) and

50ng/ml NGF (Sigma, USA). Myelination was induced four days after dissection by addition of 50μg/ml L-ascorbic acid (Sigma, USA). The medium was renewed every 2-3 days. After 4 weeks in culture, myelination was observed in all wells.

6.11.2.2 Primary oligodendrocytes from neurospheres

Neurospheres were obtained from E13 mouse embryos according to the protocol provided by Prof. Wendy Macklin (Pedraza et al., 2008). The brain was dissected and the cerebellum removed. The tissue was homogenized by trituration with a 1000ml Gilson pipette tip with 25 strokes. Afterwards, the cell suspension was passed through a 70μm cell strainer (BD, USA). The cell suspensions from two brains were pooled and plated in T25 tissue culture flasks (BD, USA) without coating in 8ml DMEM/F12 (Invitrogen, USA) supplemented with L-glutamine (Sigma, USA), B27 supplement (Invitrogen, USA) and 20ng/ml EGF (Sigma, USA). The resulting neurosphere cultures were passaged every 2-3 days at a ratio of 1:3. Oligodendrocyte precursor cells (OPCs) were obtained from passage two of the neurosphere cultures. The neurospheres were collected by centrifugation and resuspended in 5ml DMEM/F12, L-glutamine, B27, 20ng/ml FGF (Peprotech, USA), 20ng/ml PDGF (Peprotech, USA). The cells were triturated with a blue 5ml disposable pipette (BD, USA) with 7 strokes and passed through a 70μm cell strainer. The cell suspension from one T25 tissue culture flask was seeded into one poly-D-lysine (Sigma, USA) coated T75 tissue culture flask (BD, USA). After 4-7 days proliferating OPCs were abundant. For OPC isolation and enrichment, the T75 plates were shaken at 120rpm for 30' at 37°C to remove dead cells and debris. The plates were further shaken at 200rpm for 6-8 hours to detach the OPCs from the surface. The OPC suspension was recovered and subjected to a differential adhesion assay to reduce the astrocytes in the cultures. The cell suspension was incubated on untreated Petri dishes for 30' in the incubator. The astrocytes attached to the Petri dish surface and, therefore, their number was reduced in the final culture. The cell suspension containing the OPCs was recovered and the cells were counted for further experiments. For RNA isolation, 200'000 OPCs were seeded onto poly-L-ornithine (Sigma, USA) coated 60mm cell culture plates (BD, USA) in 5ml DMEM/F12, L-glutamine, B27, 20ng/ml PDGF/FGF. Differentiated oligodendrocytes were obtained by switching the medium to SATO (Bottenstein and Sato, 1979) supplemented with 1% horse serum.

6.12 RNA interference

ShRNA retrovirus constructs were made as follows. Reported effective target sequences for Sept2, Sept7 and MAG were subcloned into a modified pSRG retroviral system (provided by Ivo Spiegel, The Weizmann Institute, Rehovot, Israel). This construct expresses GFP for infection control under the control of the PGK promoter and the hairpin RNA sequence under the control of the H1 promoter (Brummelkamp et al., 2002a; Brummelkamp et al., 2002b).

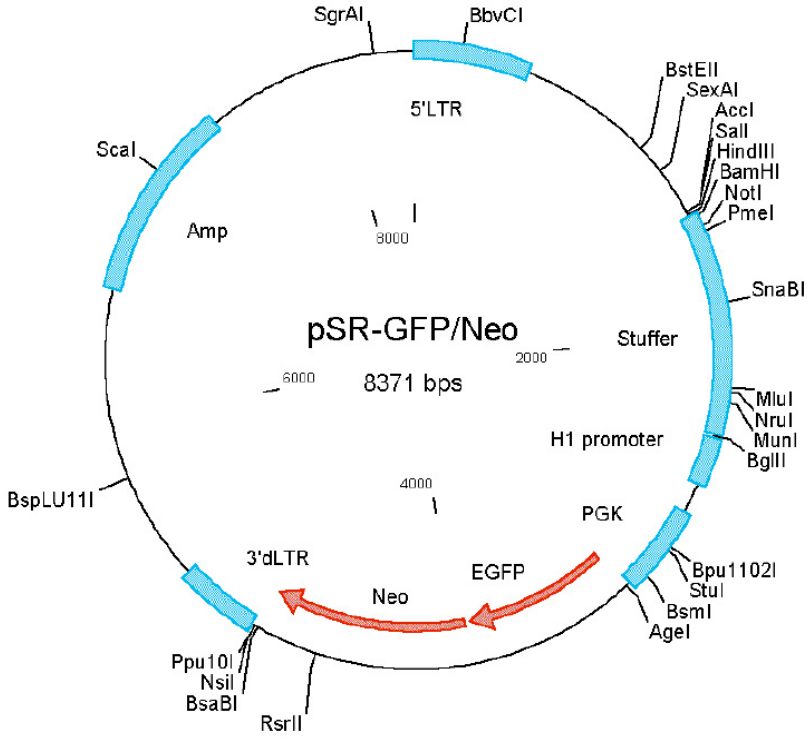

6.12.1 Target sequences

Sept2:	5'-GAAUAUUGUGCCUGUCAUUG-3'	(Kinoshita et al., 2002)
Sept7:	5'-AGAAAGCUAGCAGCAGUGAC-3'	(Kinoshita et al., 2002)
MAG:	5'-CAUGGCGUCUGGUAUUUCA-3'	(Eshed et al., 2005)

(The MAG construct was kindly provided by Ivo Spiegel, The Weizmann Institute, Rehovot, Israel)

6.12.2 Generation of retroviral RNAi constructs

6.12.2.1 RNAi hairpin oligonucleotide sequences

Sept2 sense primer (5'-3'):
gatccccGAATATTGTGCCTGTCATTGttcaagagaCAATGACAGGCACAATATTCttttta

Sept2 antisense primer (5'-3'):
agcttaaaaaGAATATTGTGCCTGTCATTGtctcttgaaCAATGACAGGCACAATATTCggg

Sept7 sense primer (5'-3'):
gatccccAGAAAGCTAGCAGCAGTGACttcaagagaGTCACTGCTGCTAGCTTTCTttttta

Sept7 antisense primer (5'-3'):
AgcttaaaaaAGAAAGCTAGCAGCAGTGACtctcttgaaGTCACTGCTGCTAGCTTTCTggg

6.12.2.2 Annealing of hairpin oligonucleotides

The primers were purchased from Microsynth (Switzerland) and diluted to 3mg/ml in water. The annealing reaction contained 48μl annealing buffer (50mM Hepes, 100mM NaCl pH 7.4) and 1μl of sense and antisense primers respectively.

Annealing: 94°C, 5' → 75°C, 10' → 72°C, 10' → 65°C, 10' → 62°C, 10' → RT

6.12.2.3 Ligation and transformation

The annealed hairpin sequences were cloned into HindIII/BglII digested pSuper vector. The plasmid was digested as follows. 10μg vector (30.8 μl), 57.2μl water, 10μl 10x buffer B (Roche, Switzerland) was supplemented with 2μl HindIII (Roche, Switzerland) and incubated at 37°C for 1hr. Following this, 2μl BglII (Roche, Switzerland) was added to the reaction and the samples were incubated for further 2hrs at 37°C. After the digestion the plasmid was purified with the Qiagen PCR Purification kit (Qiagen, Germany). The ligation reaction implemented 14.5μl water, 0.5μl digested pSuper plasmid (HindIII/BglII), 2μl annealed oligonucleotides, 2μl 10x ligation buffer, 1μl T4 DNA ligase (Roche, Switzerland) and was incubated for 4hrs at 16°C. After ligation 1μl BglII was added to each sample and the digestion was performed for 30' at RT to decrease religation of digested vector (the BglII site is destroyed upon successful ligation). The constructs were transfected into DH5α by adding 2μl ligation mix to 50μl chemically competent bacteria. After incubation on ice for 30', the bacteria were heat shocked at 42°C for 1', transferred on ice and supplemented with 250μl SOC medium. Ampicilline resistance was expressed for 1hr at 37°C prior to plating on agar plates. Colonies were screened with PCR with the

5'T7 and 3'T3 primers (for PCR program see chapter 6.13.1). Positive clones were inoculated and plasmids were prepared according to the Qiagen Mini Prep kit (Qiagen, Germany). The sequences were verified by sequencing and one correct clone per construct was chosen for further use.

6.12.2.4 Production of retroviral stocks

Retroviral stocks were produced in the Helper virus-free Phoenix-Eco packaging cell line (as described by G. Nolan, Stanford, CA, USA) with calcium phosphate co-precipitation transfection as follows. The cell culture medium for virus production was DMEM (Sigma, USA), 10% FBS (Sigma, USA), Pen/Strep (Sigma, USA). For virus production poly-L-ornithine (Sigma, USA) coated plates were used for better adherence of the cells. $5.5x10^6$ cells were seeded per 100mm plate the afternoon prior to transfection. The next morning, 9ml new medium was applied to the cultures. All reagents were brought to RT before use. 28μg DNA was diluted to 1291μl with water. 208μl 2M $CaCl_2$ was added to the DNA. 1.5ml 2xHBS pH 7.00 was added to a 8ml tube. While vortexing slowly the DNA/$CaCl_2$ solution was added drop wise to the 2xHBS. Afterwards, the mixture was incubated for 15' to allow Ca-phosphate precipitate formation. Meanwhile, 6μl 50mM chloroquine (Sigma, USA) was added per 100mm cell culture plate to neutralize the lysosomal pH. After the completion of precipitate formation the transfection mix was gently spread onto the cells. After 6hrs the cells were washed gently with PBS and 10ml new medium was applied. 48h after transfection the viral supernatant was recovered, centrifuged at 500g for 5', aliquoted and snap frozen in liquid nitrogen.

6.12.3 Retroviral infection

Retroviral infection of cell cultures was performed as follows. One day after plating, undiluted viral stock was supplemented with 8μg/ml polybrene and left on the cells for 2hrs. Afterwards, the viral supernatant was removed and the appropriate medium for further culturing was applied. For DRG/ Schwann cell co-cultures this procedure was repeated the second and third day after plating.

6.13 Generation of mCherry tagged Sept2 constructs

6.13.1 Subcloning of the mCherry sequence into the retroviral pMX vector

The DNA sequence for the red fluorescent protein mCherry was kindly provided by Prof. Tsien (UCSD, San Diego, USA). Primers to amplify the mCherry sequence were extended with the recognition sequences of the restriction endonucleases BamHI and NotI for cloning into the pMX retroviral backbone (kindly provided by Ivo Spiegel, The Weizmann Institute, Rehovot, Israel). Additionally, a HindIII recognition sequence was introduced in the 5' primer for further cloning. The PCR reaction contained 20.95µl water, 2.5µl 10x buffer, 0.5µl dNTP mix (Promega, USA), 0.5µl of each primer and 0.05µl Tag polymerase (Biolabs, USA). Following the PCR reaction the respective DNA band was isolated from a TAE gel, purified with the Gel Extraction kit (Qiagen, USA) and subjected to restriction digestion.

5' primer: 5'-GAT**GGATCC**GAC**AAGCTT**ATGGTGAGCAAGGGCGAGGAG-3'
BamHI HindIII

3' primer: 5'-GAT**GCGGCCGC**TTACTTGTACAGCTCGTCCATGCC-3
NotI

PCR Program: 94°C, 56°C, 72°C → 94°C, 54°C, 72°C → 94°C, 52°C, 72°C → 72°C
5x 5x 20x

The purified PCR fragment as well as the pMX vector were digested sequentially with BamHI (Roche, Switzerland) and NotI (Roche, Switzerland). The restriction reactions contained 10µl 10x restriction buffer, 2µl of enzyme, the DNA sample (purified PCR reaction or 10µg vector) and water up to 100µl and was incubated at 37°C for 4hrs. Following purification with the PCR Purification kit (Qiagen, USA) the digested mCherry DNA fragment was ligated into the digested pMX vector. The ligation reaction was set up by mixing 7µl mCherry fragment, with 1µl digested pMX vector, 1µl 10x ligation buffer and 1µl T4 DNA ligase (Roche, Switzerland) and incubated at 16°C for 4hrs. Thereafter, the construct was transfected into DH5α by adding 2µl ligation mix to 50µl chemically competent bacteria. After incubation on ice for 30' the bacteria were heat shocked at 42°C for 1', transferred on ice and supplemented with 250µl SOC medium. Ampicilline resistance was expressed for 1hr at 37°C prior to plating on agar plates. Colonies were screened with PCR as described above. Single positive clones were inoculated with 6ml LB medium supplemented with ampicilline (AppliChem, Germany) and incubated o.n. at 37°C with shaking. Plasmids were isolated with the Qiagen Mini Prep kit (Qiagen, Germany) according to the manufacturer's instructions. The DNA sequence was verified by sequencing (Microsynth, Switzerland) and one clone without mutation was chosen for further use.

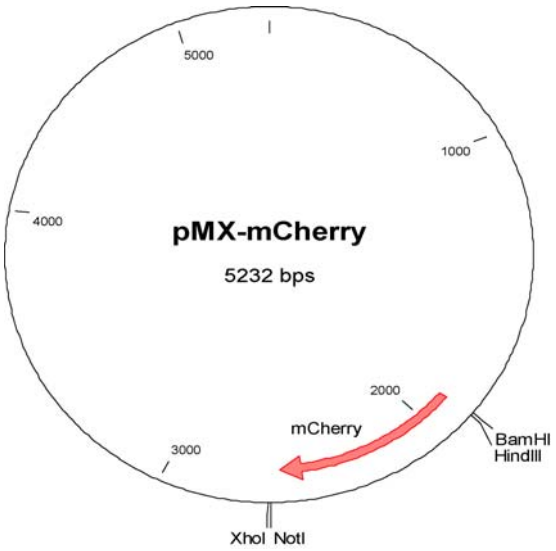

The resulting pMX-mCherry vector could further be used to tag any protein N-terminally or C-terminally using BamHI/HindIII or NotI/XhoI respectively.

6.13.2 Subcloning Sept2 wild type into the pMX-mCherry vector

The DNA sequence of Sept2 was amplified with primers extended with the recognition sequences of the restriction endonucleases BamHI and HindIII. The PCR reaction was performed as described in chapter 6.13.1. Afterwards the DNA band corresponding to the Sept2 sequence was isolated from a TAE gel and purified with the Gel Extraction kit (Qiagen, USA). The PCR product and the pMX-mCherry vector were digested with BamHI and HindIII. The restriction reaction contained 10µl 10x restriction buffer, 2µl of each enzyme, the DNA sample (purified PCR reaction or 10µg vector) and water up to 100µl and was incubated at 37°C for 4hrs. After digestion, the DNA was purified with the PCR Purification kit (Qiagen, USA). The purified Sept2 fragment was ligated into the pMX-mCherry vector and transfected as described in chapter 6.13.1. One clone with the correct sequence was chosen for further use.

5' primer: 5'-GAT**GGATCC**ATGTCTAAGCAACAACCAACTCAG-3'
BamHI

3' primer: 5'-GAT**AAGCTT**GCCCACATGCTGCCCGAGAGC-3'
HindIII

6.13.3 Subcloning the S51N Sept2 mutant sequence into the pMX-mCherry vector

The DNA sequence of the dominant negative Sept2 mutant S51N was kindly provided by Prof. Hsu Shu (Rutgers University, Piscataway, USA). The DNA

sequence of Sept2-S51N was amplified with primers extended with the recognition sequences of the restriction endonucleases BamHI and HindIII. The PCR reaction was performed as described in chapter 6.13.1. The DNA band corresponding to the Sept2-S51N sequence was isolated from a TAE gel and purified with the Gel Extraction kit (Qiagen, USA). The PCR product and the pMX-mCherry vector were digested with BamHI and HindIII. The restriction reaction contained 10µl 10x restriction buffer, 2µl of each enzyme, the DNA sample (purified PCR reaction or 10µg vector) and water up to 100µl and was incubated at 37°C for 4hrs. Thereafter, the DNA samples were purified with the PCR Purification kit (Qiagen, USA). The purified Sept2 fragment was ligated into the pMX-mCherry vector and transfected as described in chapter 6.13.1. Unexpectedly, the sequencing of the pMX-S51N-mCherry construct as well as the original construct from Prof. Shu revealed several additional mutations downstream of S51N. Therefore, these undesired mutations were eliminated as described in the following chapter.

5' primer: 5'-GAT**GGATCC**ATGTCTAAGCAACAACCAACTCAG-3'
BamHI

3' primer: 5'-GAT**AAGCTT**GCCCACATGCTGCCCGAGAGC-3'
HindIII

6.13.4 Mutation elimination in the pMX-S51N-mCherry construct

A PfoI restriction site lies downstream of the S51N mutation (Figure 16). A second PfoI restriction site is located on the pMX-mCherry vector upstream of the multiple cloning site (not shown), and therefore, PfoI could be used to replace the DNA region containing the undesired mutations with the wild type sequence. However, the restriction analysis demonstrated that the PfoI restriction site downstream of the S51N mutation was not functional. PfoI allows all 4 bases on position 4 of its recognition sequence (TCC**X**GGA) according to the distributor (Fermentas, Canada). However, the sequence TCC**T**GGA (downstream of S51N) was not recognized by this enzyme whereas the sequence TCC**G**GGA on the pMX vector was efficiently recognized. Therefore, the PfoI sequence downstream of S51N was mutated to the functional sequence TCC**G**GGA by a PCR based mutagenesis strategy (Figure 16). This lead to a silent mutation at the respective base triplet in the Sept2 open reading frame. Two primer pairs binding at the PfoI site were designed. Two further primers were designed to bind at the 5' end and the 3' end of Sept2 respectively. The PCR reaction was performed as described in chapter 6.13.1. The PCR products were purified with the PCR Purification kit (Qiagen, USA). The purified fragment A was digested with PfoI and BamHI. The purified fragment B was digested with PfoI and HindIII. The pMX-mCherry vector was digested with BamHI and HindIII. The restriction reactions contained 10µl 10x restriction buffer, 2µl of enzymes, the DNA sample (purified PCR reaction or 10µg vector) and water up to 100µl and was

incubated at 37°C for 4hrs. All digested fragments were purified with the PCR Purification kit (Qiagen, USA). The fragments A and B were co-ligated into the digested pMX-S51N-mCherry vector by mixing 3.5µl fragment A, 3.5µl fragment B, 1µl vector, 1µl 10x ligation buffer, 1µl T4 DNA ligase (Roche, Switzerland) and incubation for 4hrs at RT. The ligation was transfected into bacteria as described in chapter 6.13.1. Finally, the construct was sequenced to verify the correct sequence of the construct.

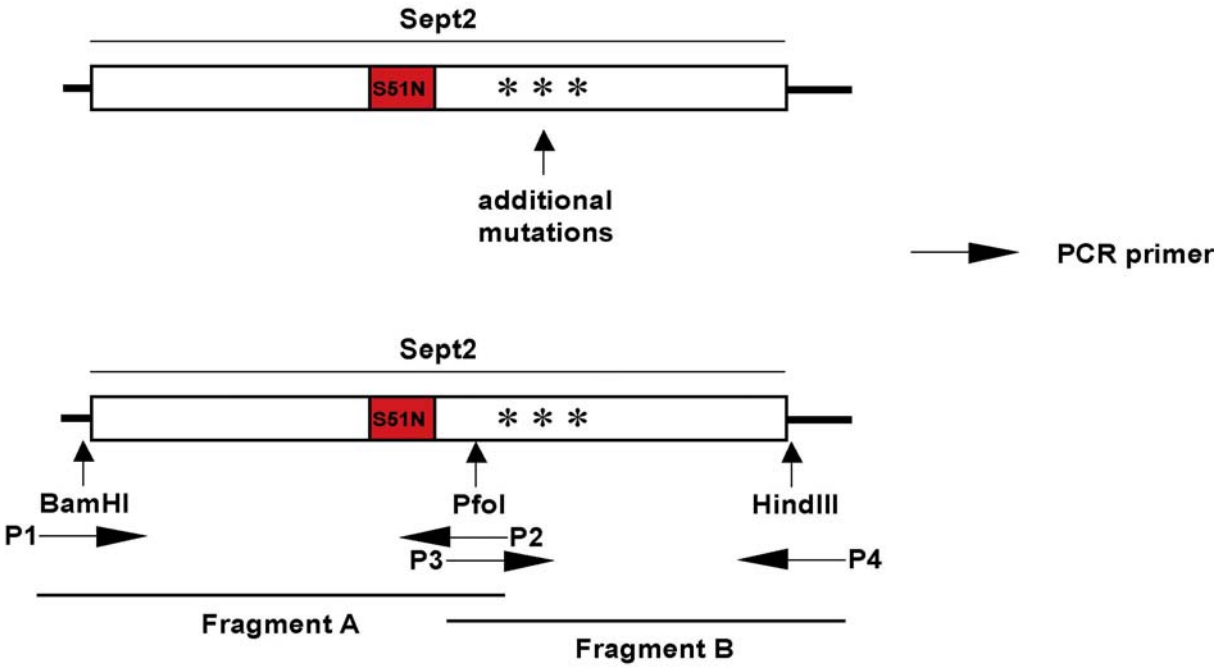

Figure 16 Sequencing of the original Sept2-S51N sequence from Prof. Shu revealed besides the desired S51N mutation additional mutations (asterix). These unwanted mutations were eliminated by performing a PCR reaction with the primers P1 and P2 on the original Sept2-S51N sequence of Prof. Shu and with the primers P3 and P4 on the wild type Sept2 sequence. The resulting fragments A and B were co-ligated into the pMX-mCherry vector using the BamHI and HindIII restriction sites.

P1: 5'-GAT**GGATCC**ATGTCTAAGCAACAACCAACTCAG-3'
BamHI

P2: 5'-GAG**TCCCGGA**ATAATTCTTTCTGGGTAGAGAT-3'
PfoI

P3: 5'-GAG**TCCGGGA**GCTGCAGAGAAAATTGAAAGA-3'
PfoI

P4: 5'-GAT**AAGCTT**GCCCACATGCTGCCCGAGAGC-3'
HindIII

6.13.5 Production of retroviral stocks

The retroviral supernatants were produced in the Helper virus-free Phoenix-Eco packaging cell line as described in chapter 6.12.2.4.

7 Results

7.1 The cytoskeleton protein Sept6 interacts with the myelin protein MAL

7.1.1 Sept6 is a potential interaction partner of MAL

The myelin and lymphocyte protein (MAL) is a raft-associated proteolipid predominately expressed by myelinating glia. MAL is involved in apical sorting and transport mechanisms of polarized epithelial cells (for review see Frank, 2000). Its association with glycosphingolipids in myelin membranes suggests a role in the formation as well as the maintenance of myelin subcompartments. Additionally, MAL is necessary for correct localization of particular myelin components which are important for axon-glial interactions in the adult CNS (Schaeren-Wiemers et al., 2004). Because polarized sorting and trafficking as well as subcompartment formation require cytoskeleton elements, we were interested in possible intracellular interaction partners of MAL. In collaboration with Hauke Werner (Department of Neurogenetics, Max-Planck-Institute of Experimental Medicine, Göttingen, Germany), a yeast two-hybrid screen with the intracellular N-terminal domain of MAL as bait with focus on cytoskeleton elements was performed. Septin 6 (Sept6), a member of the septin cytoskeleton protein family, was identified as a potential intracellular binding partner of MAL (Figure 17).

pGBT9	pACT2	-Leu/-Trp	-Leu/-Trp/-His	B-GAL
MAL	Sept6	+	+	+
PLP	Sept6	+	-	-
GPM6B	Sept6	+	-	-
MAL	c-myc	+	-	-

Figure 17 The N-terminal intracellular domain of MAL was used to screen a cDNA library for brain specific interaction partners of MAL. The pGBT9 vector harbored the GAL4 DNA-binding domain and pACT2 the GAL4 activation domain. PLP and GPM6B (glycoprotein M6B) were used as negative controls since they display significant structural homology to MAL. HIS3 and β-GAL were used as reporter genes. Robustly growing colonies were tested for β-GAL activity. Only co-transfection of pGBT9-MAL and the isolated pACT2-Sept6 led to β-GAL positive colonies.

7.1.2 Verification of the Sept6 / MAL interaction by GST pull down

The interaction between MAL and Sept6 was verified by a GST pull down assay. Sept6 was produced in COS7 cells and the cell lysate was subjected to GST-pull down. The DNA sequence of the N-terminal 55 amino acid fragment of MAL was fused to the sequence of glutathione-S-transferase (GST). GST alone was used as negative control. Recombinant proteins were expressed in E.coli and purified with glutathione-coupled sepharose. A defined amount of recombinant protein was loaded on glutathione-sepharose beads for the pull down assays. Sept6 was specifically co-purified from a COS7 cells lysate with the N-terminal 55 amino acids fragment of MAL whereas GST alone did not (Figure 18). These data demonstrate that Sept6 binds to the N-terminus of MAL verifying the yeast two-hybrid screen.

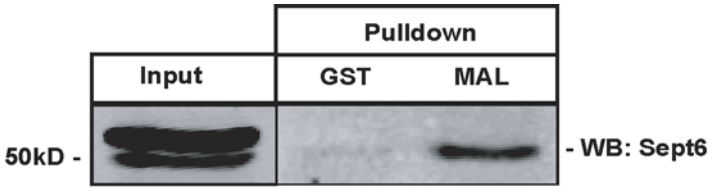

Figure 18 The Sept6 full length sequence under the control of the CMV promoter was transfected into COS7 cells. The cell lysate was used in a GST pull down assay. 50μg of recombinant GST-MAL or GST alone were loaded on glutathione-sepharose beads and probed for interaction against Sept6.

7.1.3 The Sept2/ 6 / 7 complex does not interact with MAL

Septins form heteromeric complexes which seem to be fundamental for septin protein stability and for function. We wanted to further characterize the interaction between MAL and septins by using a physiological brain septin complex (Sept2/ 6/ 7) expressed and purified from E.coli (kindly provided by Prof. Ian Macara, Center for Cell Signaling, University of Virginia, USA). The septin complex was incubated with a N-terminal 24 amino acids fragment of MAL fused to GST and then precipitated on glutathione-coupled sepharose. This fragment corresponds to the intracellular N-terminal domain of MAL which was also used as bait for the yeast two hybrid screen. The Sept2 /6 / 7 complex could not be co-purified together with MAL (Figure 19). Different buffer conditions were used but did not lead to successful enrichment of the septin complex compared to the negative control. This is in contrast to the observation that Sept6 alone could be co-purified with MAL (Figure 18). A possible explanation is that the Sept6 domain which interacts with MAL is masked in the Sept2 /6 /7 complex suggesting that Sept6 alone or a Sept6 complex of another composition might be responsible for interaction with MAL.

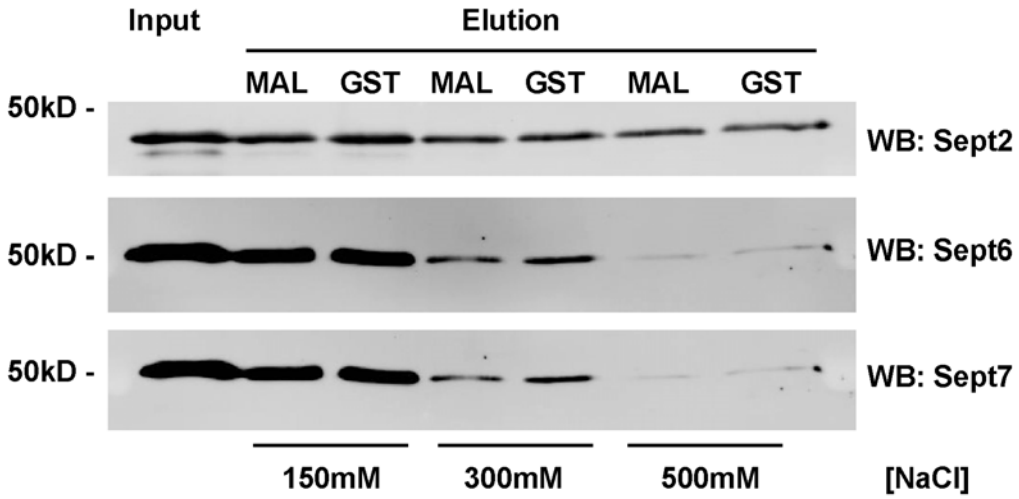

Figure 19 Purified Sept2/ 6 /7 protein complex samples were incubated with the N-terminal intracellular MAL fragment coupled to GST. GST alone was used as negative control. Different ionic strength ([NaCl]) buffers were tested to optimize the pull down for specific protein interactions. No difference between the MAL-GST and the GST alone was evident.

7.1.4 Sept6 and MAL are co-targeted to myelin fractions

Sept6 was shown to interact with MAL in a yeast two-hybrid screen as well as in a GST pull down assay. Septins are cytoplasmic proteins which localize and interact with plasma membranes by interactions with proteins and lipids. MAL is predominantly localized to myelin fractions and we, therefore, asked if septins and in particular Sept6 are interacting with myelin membranes. For this, myelin membrane fractions were analyzed for co-purifying septins. Myelin membranes were enriched and separated from astrocytic and neuronal plasma membranes by density gradient centrifugation. Equal amounts of protein from crude homogenate, myelin membrane fraction and plasma membrane fraction were loaded on SDS-PAGE gradient gels and analyzed by Western blot. As expected the myelin protein MAL was targeted to the myelin membrane fraction (Figure 20). Sept6 was highly enriched in the myelin fraction suggesting interaction with the myelin membranes (Figure 20). Comparably, Sept2 and Sept7 were incorporated into the myelin membrane fraction suggesting that several components of the septin cytoskeleton might interact with myelin membranes. For Sept7, two protein bands could be detected one of which seems to be more prominent in myelin fractions. The two bands might correspond to differentially spliced isoforms since two splice isoforms were described for the human Sept7 gene (Nakatsuru et al., 1994). Both Sept7 splice isoforms were also detected in plasma membrane fractions. These data show that both MAL and Sept6 were highly enriched in myelin membranes. The interaction between the raft associated myelin protein MAL and the septin cytoskeleton opens up new concepts in the context of an interface between cytoskeleton elements and myelin subdomains.

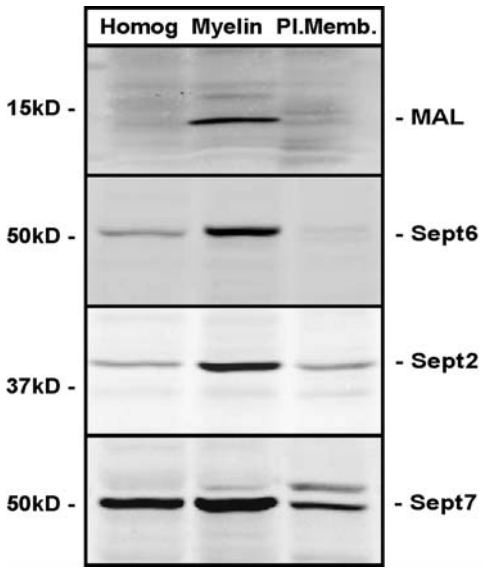

Figure 20 The integration of septins and MAL into myelin membrane fractions was tested by Western blot analysis. Myelin membranes were separated from plasma membranes by density gradient centrifugation. 20μg of crude brain homogenate, myelin membrane fraction and plasma membrane fraction was loaded on SDS-PAGE gels. MAL was enriched in the myelin fraction as reported earlier. Accordingly, Sept2, 6 and 7 were co-purified with myelin membranes.

7.2 The MAL^{null} phenotype is not replicated in Sept6^{null} mice

MAL-deficient mice display structural alterations in paranode organization at the node of Ranvier. The paranodal loops, which are normally tightly connected to the axon, are detached from the nodal axolemma (Schaeren-Wiemers et al., 2004). This suggests that MAL is involved in the stabilization of the paranodal junctions. Although lack of MAL leads to reduced incorporation of particular paranodal components, it is not known how MAL contributes to the nodal architecture. Since we showed that MAL interacts with Sept6, we asked whether the paranodal alteration in MAL-deficient mice was due to an impairment of the septin cytoskeleton and further cytoskeleton elements. We, therefore, analyzed the Sept6^{null} mouse (Ono et al., 2005) for changes in myelin ultrastructure (performed by Beat Erne, Neurobiology, Department of Biomedicine and Neurology, University Hospital Basel, Pharmacenter, Basel, Switzerland). Electron microscopy analysis revealed changes neither in the nodal architecture nor in other myelin compartments like the compact myelin and the Schmidt-Lanterman incisures. Notably, in Sept6 deficient mice the paranodal loops where tightly connected to the axolemma and no detached loops where found (Figure 21).

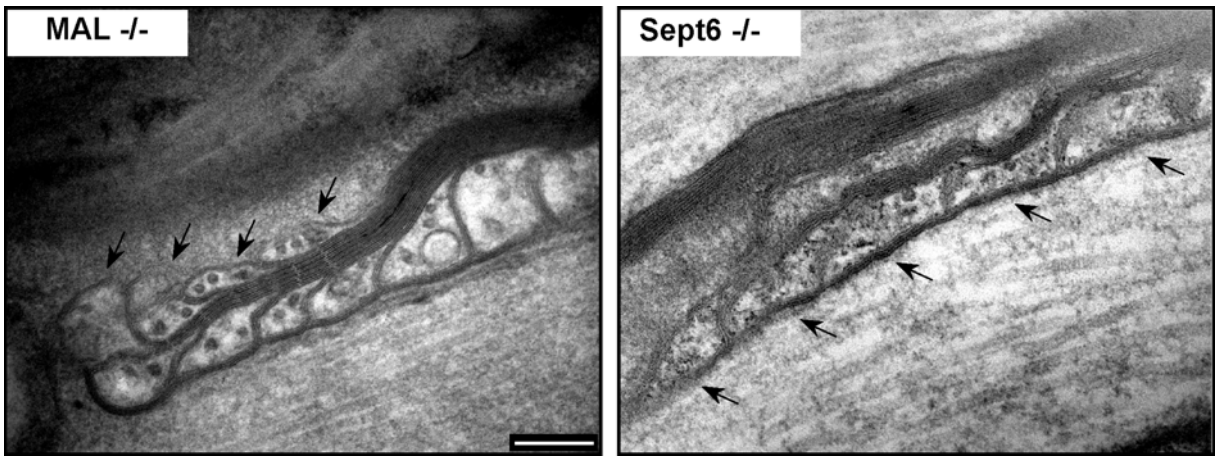

Figure 21 The integrity of the paranodal organization in Sept6-deficient mice was analyzed by EM. The reported MAL^{null} phenotype (2004 Schaeren-Wiemers et al.) characterized by detached paranodal loops (arrows) was not replicated in the Sept6^{null} mouse. Bar 200nm.

7.3 Sept11 compensates for loss of Sept6 in CNS myelin

Next, myelin preparations of Sept6 deficient mice were analyzed for changes in protein composition. Neither the expression level of MAL nor of other myelin proteins analyzed (e.g. CNP, MBP, Neurofascin155) were altered (Figure 22). Septins are a complex family of proteins which display significant sequence homology to each other. It was already reported that homologous septins may compensate for the loss of single septins (Fujishima et al., 2007; Peng et al., 2002). To identify possible compensatory mechanisms, we performed Western blot analysis for several septins. Indeed, Sept11, the closest homolog to Sept6, was significantly elevated 1.6 fold in myelin membranes from Sept6-deficient mice (Figure 22). The closely related homolog Sept8 or Sept2 which belongs to a different septin subgroup (see also Figure 12) were not changed. Increased incorporation of Sept11 into myelin membranes as compensatory reaction to the loss of Sept6 clearly points to a functional role of Sept6 in myelin.

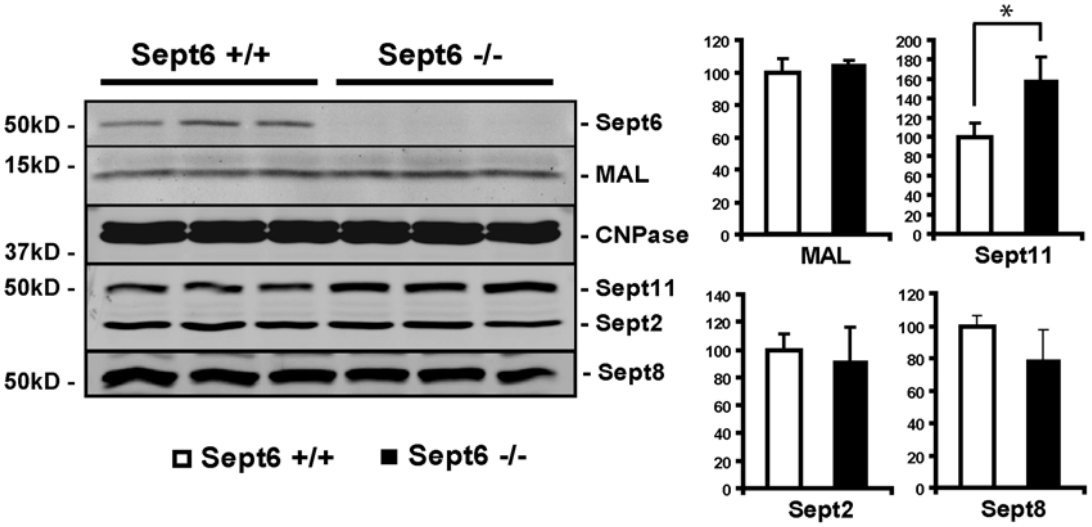

Figure 22 Sept6^{null} myelin was analyzed for alteration in protein composition. Equal protein amounts of three independent myelin preparations per genotype were loaded on SDS-PAGE gels and subjected to Western blot analysis. The protein bands were quantified with the Odyssey Software (Licor, USA) and the respective signals were normalized to the wild type level. Sept11, the closest homolog to Sept6, was significantly elevated in Sept6^{null} myelin ($p<0.001$). The protein levels of other septins were unchanged.

7.4 Oligodendrocytes express and developmentally regulate a complex septin scaffold

The analysis of Sept6^{null} mice revealed that septin function in myelinating cells might involve many different isoforms. Data from several studies identified individual septins to be incorporated into myelin fractions (Roth, 2006; Taylor et al., 2004; Werner et al., 2007). Nevertheless, there were no comprehensive data about which septins are expressed in myelinating cells. Therefore, we analyzed the expression pattern of septins in primary oligodendrocyte cultures. Mouse primary oligodendrocytes were generated from neurospheres isolated from embryonic day 13 cortical hemispheres with a protocol, which lead predominantly to the generation of oligodendrocyte precursors (Pedraza et al., 2008). The expression pattern of Sept1-12 was analyzed in oligodendrocyte precursor cells (OPCs) as well as in oligodendrocytes, which were stimulated for differentiation for 4 and 7 days. The quality of the cultures was judged by analyzing several house keeping genes as well as particular myelin genes such as MBP, CNP and MAL (Figure 23A). CNP was induced immediately after stimulation, whereas MBP expression augmented with time. As known from earlier studies, MAL expression was induced much later than the other myelin genes. Ten different septins were expressed by oligodendrocytes all of which already to some extend were expressed in the OPCs (Figure 23B). Several septins, namely Sept3, 4, 5, 7, and 8 were strongly unregulated towards the MAL-positive terminal differentiated stage, suggesting that they play a role in

oligodendrocyte differentiation and myelination. Especially, Sept4 showed an expression pattern reminiscent for a functional role in myelination since its expression was induced in a later phase of oligodendrocyte differentiation in a similar fashion as MAL. In contrast, Sept6 and Sept9 showed high expression already in OPCs and their expression levels were reduced to a steady state during the differentiation process. Still, their expression stayed high in differentiated oligodendrocytes, suggesting that those septins might play a role in OPC proliferation as well as in differentiation. Sept11, however, was transiently upregulated during the intermediate CNPase-positive stage and subsequently downregulated towards terminal differentiation, indicating a possible function during early differentiation of the progenitor cells. The absolute expression values of the septin gene family are depicted and compared to the expression pattern in sciatic nerve in Figure 25. Taken together, our data demonstrate that oligodendrocytes express a complex set of septins during all stages of differentiation.

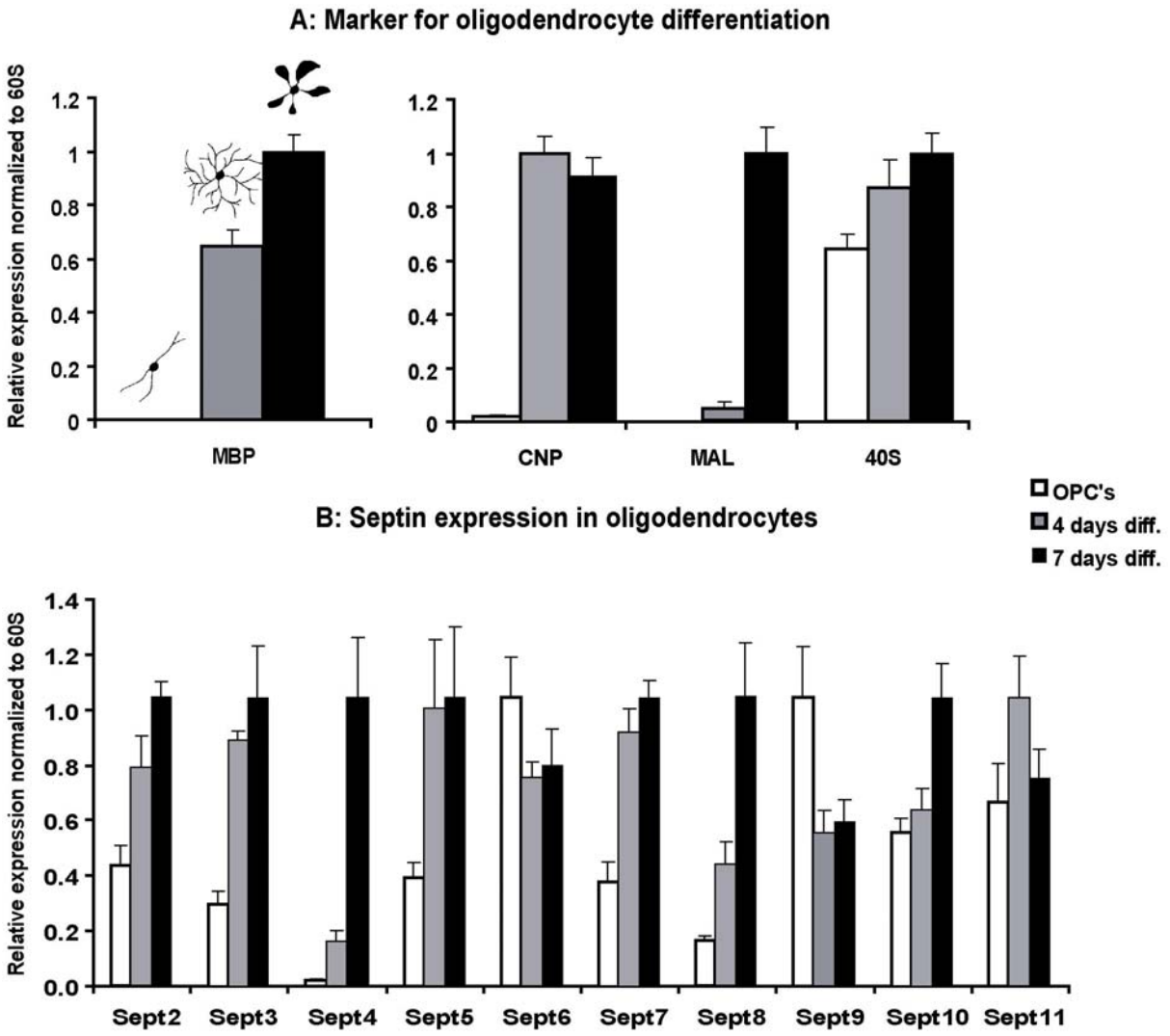

Figure 23 Oligodendrocyte precursor cells (OPCs) were generated from neurospheres and differentiated to mature oligodendrocytes (4 days diff. / 7 days diff.). Total RNA was isolated from $4x10^5$ cells per sample. Four individual plates per time point were used and separately subjected to RNA isolation, cDNA synthesis and quantitative real time PCR. The expression of the indicated genes was measured with the Light Cycler system and normalized to the 60S house keeping gene. For depiction the time point of highest expression was set to one for each gene. (A) The expression of known myelin markers was monitored. The cells reached a CNPase/MBP positive intermediate stage after 4 days in differentiation medium. After 7 days, the oligodendrocytes also expressed late myelin markers like MAL. (B) The expression pattern of the septin gene family in oligodendrocytes was determined. A complex set of septins was expressed and developmentally regulated in the oligodendrocytes.

7.5 A distinct septin scaffold is upregulated during PNS myelination

Oligodendrocytes and Schwann cells, besides being very different in regard of origin, are confronted with very similar tasks concerning membrane buildup and structuring. In line with this, both CNS and PNS internodes share basic structural features. Therefore, we also investigated the septin cytoskeleton in PNS myelination. Total RNA was isolated from sciatic nerves from postnatal day 0 (P0) to P28 to follow the developmental and myelination processes in the PNS. Schwann cell differentiation and myelination was monitored by the expression of Krox20 and Oct6 as markers for differentiation and P0, CNPase and MBP as markers for myelination (Figure 24A and B). In the sciatic nerve the expression of the same ten septins than in the oligodendrocytes was detectable (Figure 24C). Most of these septins were upregulated during the period of highest myelination activity around P14 – P21 and subsequently went down to a plateau. This pattern of expression clearly followed the expression pattern of the classic myelin proteins P0, CNPase and MBP (Figure 22A and B). Sept7 which is discussed as being crucial in most if not all septin complexes was already highly expressed around birth. Other septins like Sept3, 8, and 9 showed an upregulation of over 10fold coinciding with the peak of myelination. Sept4 in contrast was highly expressed at birth and was afterwards continuatively expressed at lower levels, indicating a role in Schwann cell proliferation. The absolute mRNA expression values are displayed in Figure 25. Interestingly, Sept7, 8 and 9 are highly expressed in both oligodendrocytes and Schwann cells. Sept4 seemed to be CNS specific whereas Sept3 was more abundant in the PNS.

In summary, these data show that multiple septins are expressed and are differentially regulated in oligodendrocytes and Schwann cells many of those clearly parallel with myelinating activity.

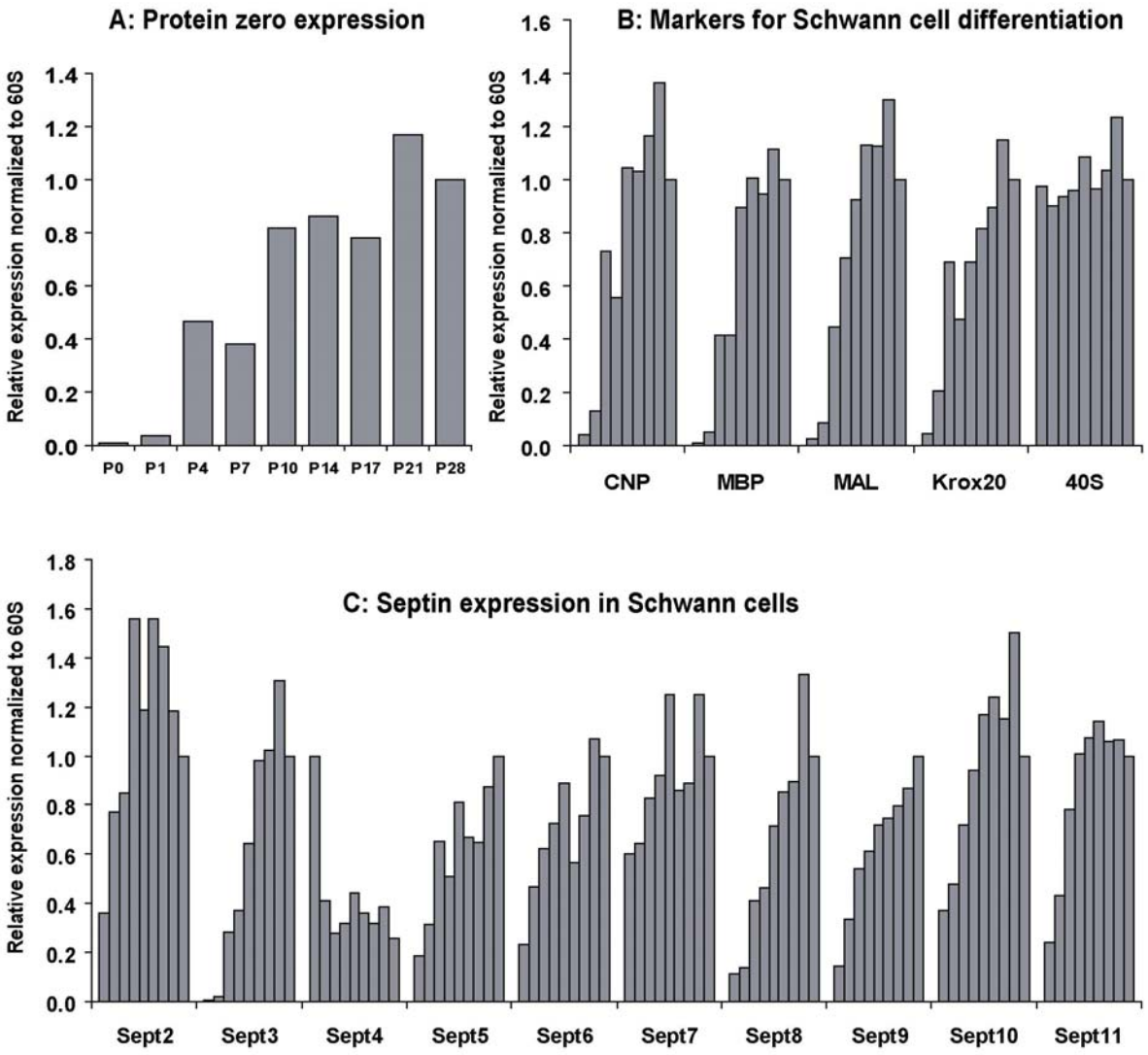

Figure 24 Total RNA was isolated from sciatic nerves from postnatal day 0 (P0) to P28. The nerves of four animals per time point were pooled. Myelination was monitored by analyzing the expression level of several myelin genes as well as differentiation markers. The P28 time point was set to one for depiction. (A/B) As expected, classic myelin markers as well as Krox20, a marker for Schwann cell differentiation, showed a peak of expression in the period of highest myelinating activity (P14 - P21). (C) The expression of multiple septins was detectable. Notably, most expressed septins were upregulated during myelination.

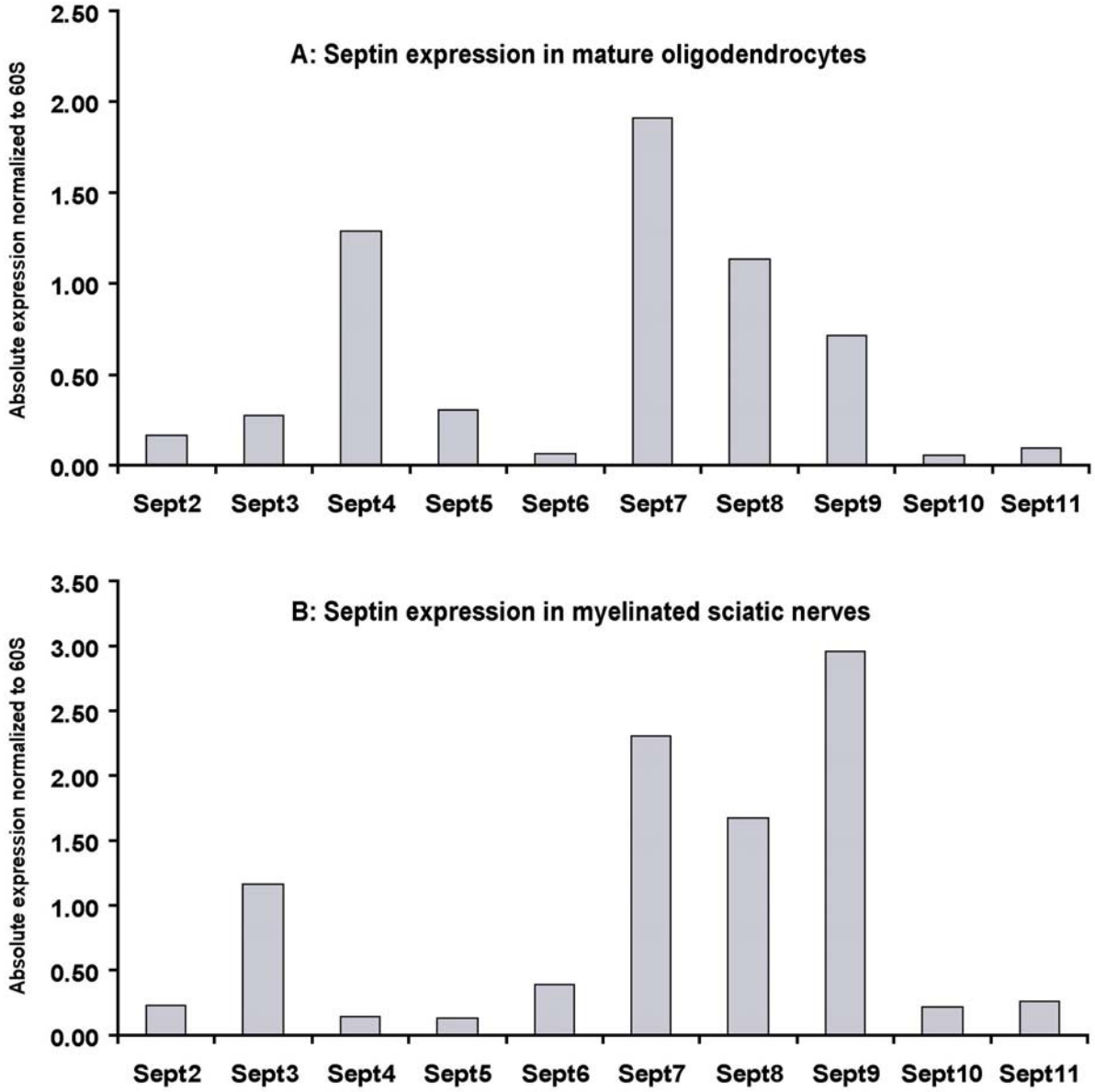

Figure 25 The measured septin mRNA levels were normalized to the 60S gene. These absolute expression values are depicted for mature oligodendrocytes and myelinated sciatic nerves. For the oligodendrocytes, the septin expression pattern after 7 days in differentiation medium is displayed (A) and compared to the septin expression pattern of the postnatal day 28 sciatic nerve sample (B).

7.6 Discrete septin complexes interact with myelin membranes

The expression analysis data showed that the septin cytoskeleton in myelinating cells is very complex. To identify septin scaffolds relevant for myelin membrane formation and maintenance, the composition of septin complexes incorporated into myelin fractions was analyzed by immunoprecipitation. Additionally, we wanted to directly verify the interaction of Sept6 and MAL in myelin fractions.

7.6.1 Sample preparation for immunoprecipitation

Myelin membrane fractions are difficult samples for immunoprecipitation since they are extremely hydrophobic. They cannot be directly used for pull down experiments due to their unspecific binding to sepharose beads. Therefore, mild detergents were used to solubilize myelin membranes without denaturing the proteins. After detergent extraction, the insoluble components were separated from soluble components by centrifugation. The supernatant was used for immunoprecipitation. Several detergents were tested for efficient solubilization of myelin proteins like MAL. Myelin membranes could be solubilized by using the detergent n-dodecyl-β-D-thiomaltopyranoside (DDTM). Being non-ionic DDTM is considered to be a mild detergent preserving the protein tertiary structure and potentially also protein/protein interactions. The presence of septins as well as a selection of myelin proteins was tested in the soluble fraction after detergent extraction. Indeed, Sept2, 6 and 7 (not shown) as well as the myelin proteins MAL, MAG, Neurofascin, MBP and PLP were detected in the detergent extract (Figure 26). This myelin membrane extract was further used for all co-immunoprecipitation assays.

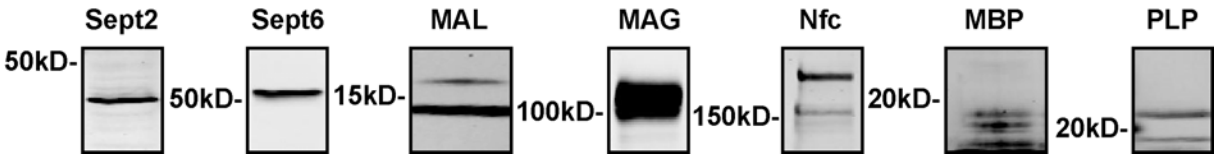

Figure 26: A myelin membrane fraction was incubated with 1% DDTM for 30'. Subsequently, insoluble components were separated by centrifugation. The supernatant was analyzed by Western blot analysis. All tested septins and myelin proteins were detected in the detergent extract.

7.6.2 Co-immunoprecipitation for Sept6 using proteinA sepharose

It was shown in this work that Sept6 interacts with the myelin protein MAL and is targeted to myelin fractions. As a next step, immunoprecipitation assays for Sept6 were performed to isolate myelin-relevant septin complexes as well as co-purifying myelin components. The Sept6 N-terminus specific antibody was immobilized on sepharose beads. A standard method for antibody immobilization is to use proteinA sepharose. ProteinA specifically interacts with the Fc portion of IgG. Cross-linking agents can then be used to covalently attach the IgG to the proteinA sepharose. Indeed, the SeizeX ProteinA Immunoprezipitation kit (Pierce, USA) lead to efficient coupling of IgG. With this system, it was possible to immunoprecipitate Sept6 from solubilized myelin membrane samples (Figure 27). However, the background level of the negative control and even of the gel itself (not shown) was considerable. This might be due to the presence of the high amount of proteinA on the sepharose which, by itself, may be unfavorable to work with complex and highly hydrophobic samples as derived from myelin fractions. Therefore, this system was not further used.

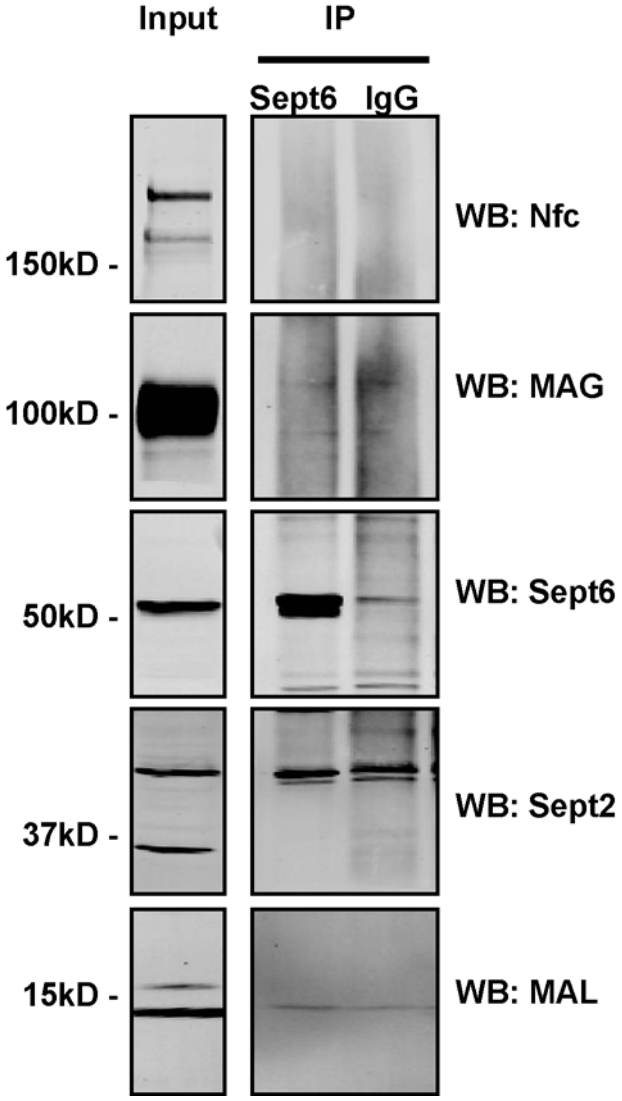

Figure 27 Sept6 specific antibodies were used to pull down septin complexes from solubilized myelin membranes. The elution fraction was analysed for Sept6 and Sept2 as well as MAL, Neurofascin (Nfc) and MAG. Sept6 could be purified from the myelin sample. However the background level on the control IgG beads was to high to specifically detect interaction partners of Sept6.

7.6.3 Co-immunoprecipitation for Sept6 using activated agarose

Another method for antibody immobilization is to couple the IgG via primary amines on aldehyde-activated beaded agarose. This results in efficient but random coupling of the IgG directly on the agarose. The ProFound Co-Immunoprecipitation kit (Pierce, USA) led to efficient immobilization of IgG and low background signals in the negative control. Indeed, Sept6 could be purified from the solubilized myelin membrane sample (Figure 28). Together with Sept6, Sept2 specifically co-purified in the IP. The elution fraction was tested for interacting myelin components. Neither MAL nor any other tested myelin protein could be co-purified. No other protein band was evident from silver stained gels. A possible explanation might be that Sept6 was to low abundant in the myelin fraction.

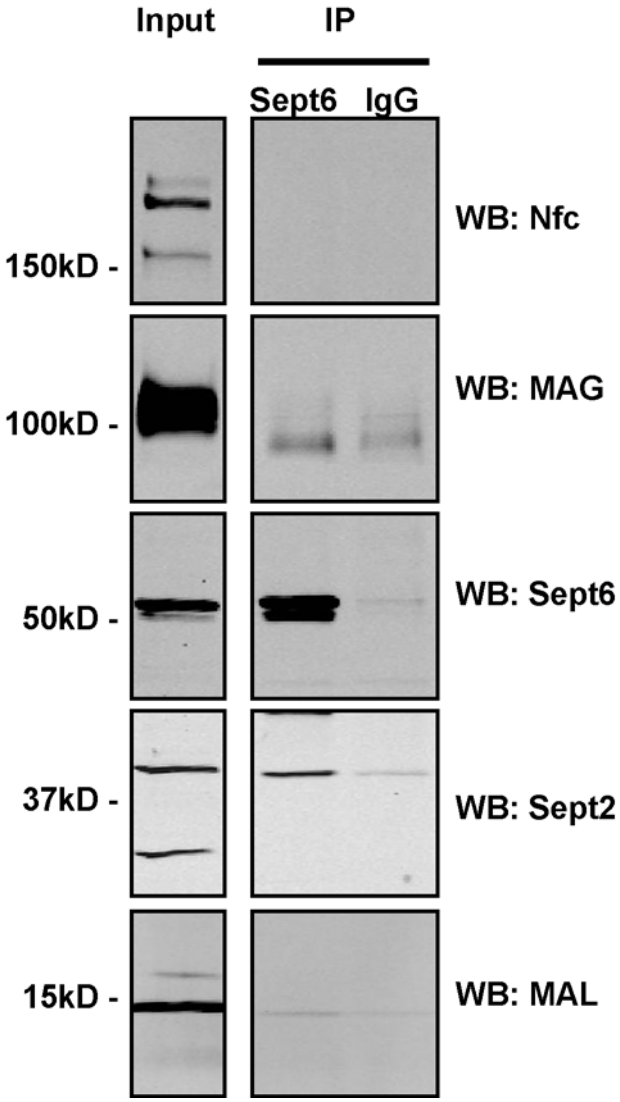

Figure 28 The ProFound activated sepharose system was used for co-immunoprecipitation assays. Solubilized myelin membranes were incubated with Sept6 or control IgG antibodies covalently coupled to sepharose. Sept6 was specifically enriched in the positive control. Sept2 co-purified with Sept6.

7.6.4 Co-immunoprecipitation for Sept2

It was not possible to co-purify myelin components or further septins with antibodies against Sept6. This might be due to the relative low abundance of Sept6 in myelin membranes. Since we co-immunoprecipitated Sept2 together with Sept6 this septin was analyzed regarding myelin relevance. Septins are known to form heteromeric complexes important for their functionality. Therefore, we wanted to use Sept2 as a lever to isolate myelin specific complexes also regarding Sept6 and MAL. Immunofluorescence analysis of Sept2, revealed strong staining of all myelinated brain structures such as corpus callosum (Figure 29A arrow) and cerebellar white matter (Figure 29B arrowhead). For this reason, further co-immunoprecipitation experiments for this septin were performed (Figure 29B and C). Since it was recognized that the coupling with activated sepharose led to a reduced affinity of the antibodies, as reported in the literature, another oriented coupling technique without proteinA was used. The Affi-Gel Hz Immunoaffinity Kit (Biorad, USA) immobilizes IgG on sepharose via carbohydrate moieties on the Fc region of the antibodies, resulting in oriented coupling. This leads to efficient coupling and high antibody activity. Indeed, this system could be used to efficiently immunoprecipitate Sept2 with low background signal (Figure 29B). First, the interaction between Sept6 and Sept2 could be verified (Figure 32). Second, a distinct septin complex could be purified from myelin membranes. This septin complex was analyzed with SDS-PAGE both for CNS and PNS myelin membranes (Figure 29C). Visible bands after Coomassie staining (CBB) were excised and subjected to trypsine digestion and protein identification by mass spectrometry (Figure 30 and Figure 31).

The presence of the identified Sept2 interactors was verified by Western blot analysis (Figure 32). From CNS myelin a distinct septin complex was co-precipitated together with Sept2. This complex contained besides Sept2 and Sept6 also Sept4, Sept7, Sept8, Sept9 and Sept11 (Figure 29C). The protein band intensities after silver staining implied that Sept2, Sept7 and Sept8 may represent a stoechiometric complex in CNS myelin. Interestingly, we were able to purify the same septin complex from a sciatic nerve homogenate with one major difference, the lack of Sept4. Sept2, Sept7 and Sept8 also represented a stoechiometric complex in the PNS (Figure 29C). Besides the septins, also actin was detected interacting with Sept2 and its complexes both in the CNS and PNS myelin fractions (Figure 29C, 30 and 31). Tubulin was not pulled down together with this complex (data not shown).
Besides septins and actin no further proteins co-precipitating with Sept2 could be detected suggesting that the interaction between septins and membrane components might be either destroyed upon detergent extraction or be to minor in respect to other complexes.

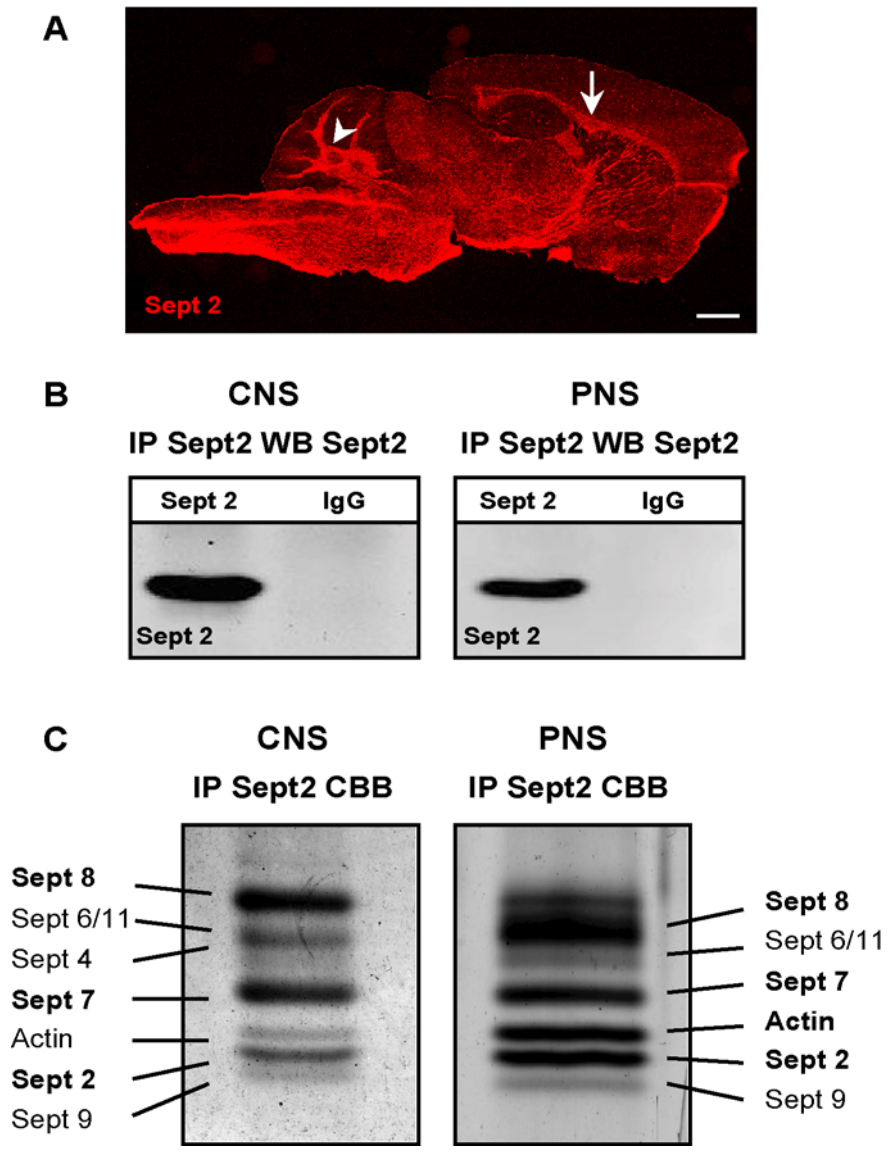

Figure 29 (A) Sept2 could be localized to myelinated fiber tracts (arrows) in the CNS by immunostaining. (B) Sept2 could be immunoprecipitated from myelin fractions both from the CNS and PNS. (C) Protein bands co-precipitating with Sept2 were isolated and identified by mass spectrometry (see also Figures 30 and 31). In CNS and PNS myelin Sept2/ 7/ 8 was the major stoechiometric septin complex. Besides this, Sept4, 6, 9 and 11 could be detected as minor components. Actin co-precipitated with the septin complex both from CNS and PNS myelin. The presence of all identified septins was verified with Western blot analysis (Figure 32). No further membrane bound or soluble proteins could be co-precipitated. Bar 1mm

Identified: Sept8	**P(pro):** 4.15E-03	**Score (XC):**	28.17
Peptides		**Hits**	
R.ISNAEPEPR.S		4	
K.VNIIPIIAK.A		1	
K.EFLSELQR.K		1	
Identified: Sept11	**P(pro):** 2.07E-08	**Score (XC):**	50.25
Peptides		**Hits**	
K.AAAQLLQSQAQQSGAQQTK.K		4	
R.SYELQESNVR.L		2	
K.FESDPATHNEPGVR.L		2	
K.RNEFLGELQK.K		2	
K.STLM*DTLFNTK.F		1	
Identified: Sept7	**P(pro):** 1.07E-06	**Score (XC):**	40.15
Peptides		**Hits**	
K.LKDSEAELQR.R		2	
K.FEDYLNAESR.V		1	
R.ILEQQNSSR.T		5	
K.DVTNNVHYENYR.S		1	
Identified: Actin	**P(pro):** 1.46E-07	**Score (XC):**	30.15
Peptides		**Hits**	
R.GYSFTTTAER.E		2	
K.AGFAGDDAPR.A		2	
K.DSYVGDEAQSKR.G		2	
Identified: Sept2	**P(pro):** 3.72E-07	**Score (XC):**	54.22
Peptides		**Hits**	
R.TVQIEASTVEIEER.G		2	
R.LTVVDTPGYGDAINSR.D		2	
R.M*QAQM*QM*QMQGGDTDSSTLGHHV.-		2	
K.ADTLTLKER.E		2	
K.ASIPFSVVGSNQLIEAK.G		1	
Identified: Sept9	**P(pro):** 4.31E-05	**Score (XC):**	28.13
Peptides		**Hits**	
K.YLQEEVNINR.K		1	
K.VVNIVPVIAK.A		2	
K.ADTLTLEER.V		1	

Figure 30 Proteins co-precipitating with Sept2 from PNS myelin were identified. Visible bands after Coomassie blue staining were excised and subjected to tryptic digest. The masses of the resulting peptides were measured by electro spray ionization and matched to the Mascot database (Matrix Science Inc., USA). The protein probability P(pro) and the cross-correlation score XC are depicted. XC scores above 2.0 are indicative of a good correlation.

Identified: Sept8	**P(pro):** 4.56E-05	**Score (XC):** 58.15
Peptides		**Hits**
K.SLDLVTMK.K		4
K.SLDLVTM*K.K		3
R.VNMEDLR.E		2
K.VNIIPIIAK.A		3
K.VKETELELK.E		2
K.EFLSELQR.K		1

Identified: Sept11	**P(pro):** 8.14E-06	**Score (XC):** 30.14
Peptides		**Hits**
R.SYELQESNVR.L		2
K.AAAQLLQSQAQQSGAQQTK.K		2

Identified: Sept7	**P(pro):** 3.48E-08	**Score (XC):** 50.20
Peptides		**Hits**
R.QFEEEKANWEAQQR.I		2
K.SPLAQMEEERR.E		2
K.FEDYLNAESR.V		2
K.DVTNNVHYENYR.S		2
K.LAAVTYNGVDNNK.N		2

Identified: Sept4	**P(pro):** 2.76E-04	**Score (XC):** 8.14
Peptides		**Hits**
R.VNIVPILAK.A		2

Identified: Actin	**P(pro):** 6.78E-05	**Score (XC):** 18.17
Peptides		**Hits**
R.VAPDEHPILLTEAPLNPK.I		2
R.SYELPDGQVITIGNER.F		1

Identified: Sept2	**P(pro):** 4.90E-11	**Score (XC):** 116.29
Peptides		**Hits**
R.M*QAQM*QM*QMQGGDTDSSTLGHHV.-		26
R.LTVVDTPGYGDAINSR.D		3
R.YLHDESGLNR.R		2
R.ILDEIEEHSIK.I		10
K.VNIVPVIAK.A		2
R.TVQIEASTVEIEER.G		1
K.ADTLTLKER.E		2

Identified: Sept9	**P(pro):** 5.97E-05	**Score (XC):** 40.15
Peptides		**Hits**
K.VVNIVPVIAK.A		2
K.YLQEEVNINR.K		1
K.STLINTLFK.S		2
K.ADTLTLEER.V		2

Figure 31 Proteins co-precipitating with Sept2 from CNS myelin were identified. Visible bands after CBB staining were excised and analyzed by mass spectroscopy. The protein probability P(pro) and the cross-correlation score XC are depicted. XC scores above 2.0 are indicative of a good correlation.

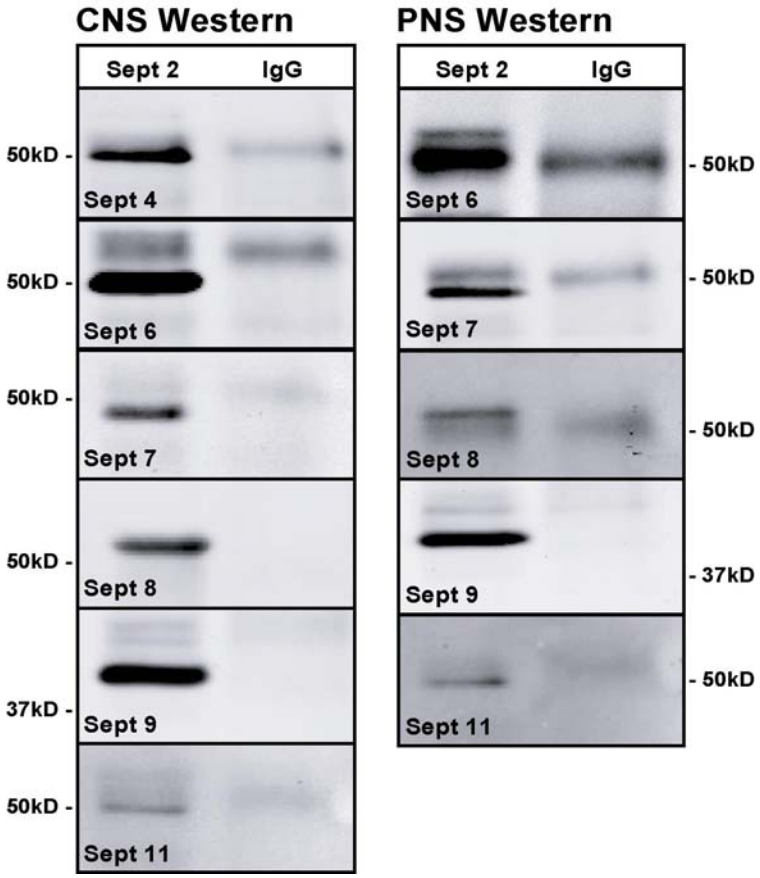

Figure 32 Septins co-precipitated together with Sept2 were identified by mass spectrometry (Figure 29C, 30 and 31). Subsequently, their specific enrichment was verified. The elution fraction after immunoprecipitation was loaded on SDS-PAGE gels and analyzed by Western blot analysis. All identified septins were specifically co-precipitated together with Sept2.

7.6.5 A septin scaffold differentially interacts with myelin membranes

In a next step, the distribution of the identified Sept2 interactors in myelin preparations from CNS samples was analyzed by Western blot. Similar to Sept2/ 6/ 7 (Figure 20) also Sept4, Sept8, Sept9 and Sept11 were highly enriched in myelin fractions of the CNS (Figure 33A). For Sept8, three splice variants were identified in the brain homogenate (Figure 33A). Interestingly two of these Sept8 isoforms were enriched in the myelin membrane fraction, whereas one in the plasma membrane fraction, which predominantly consist of neuronal/axonal and astrocytic plasma membranes. To analyze if the identified septins also interact with PNS myelin fractions, myelin membranes were isolated from sciatic nerve homogenates and analyzed for co-purifying septins. Sept2, 7 and 8 all co-purified with the myelin fraction suggesting a specific interaction between these septins and the myelin membranes (Figure 33B). Here, the plasma membrane fraction could not be isolated due to the very high abundance of myelin membranes in the sciatic nerve homogenate as indicated by the major myelin protein P0. Sept6, 9 and 11 were not detectable by direct Western blot analysis. As illustrated by actin the specific interaction with myelin membranes is unique for septins (Figure 33B).

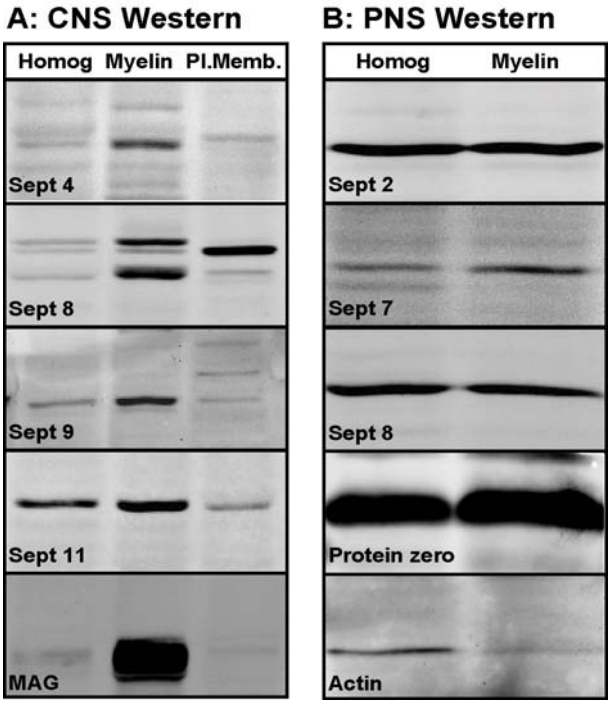

Figure 33 The septins co-precipitating with Sept2 were analyzed for interaction with myelin membranes both from CNS and PNS. (A) In the CNS all analyzed septins were clearly enriched in the myelin fraction. Interestingly, three splice isoforms of Sept8 were detected two of which were specifically enriched with myelin fractions. (B) In the PNS the major septin complex Sept2/ 7/ 8 was detectable and interacted specifically with the myelin fraction. Sept6, 9 and 11 were not detectable by direct Western blot analysis.

7.7 The incorporation of septins into myelin is not dependant on MAL

MAL is known to be involved in targeting specific elements to their respective domain. PLP and MAL are structurally related proteolipids but lead to different phenotypes in respective null mutants. A recent study of the PLP^{null} mouse demonstrated that the loss of the major myelin protein PLP results in a reduced incorporation of distinct septins into myelin fractions (Werner et al., 2007). We asked if the lack of MAL might result in a similar loss of septins from myelin membranes which might directly point to an interaction *in vivo*. Myelin preparations from MAL-deficient mice were analyzed for alterations in the level of septins by Western blot analysis (Figure 34). All tested septins such as Sept2, 4, 6, 7, 8, 9 and 11 were not altered suggesting that MAL is not crucial for localization of septins to myelin fractions or that the loss of MAL is compensated by PLP or other components of myelin.

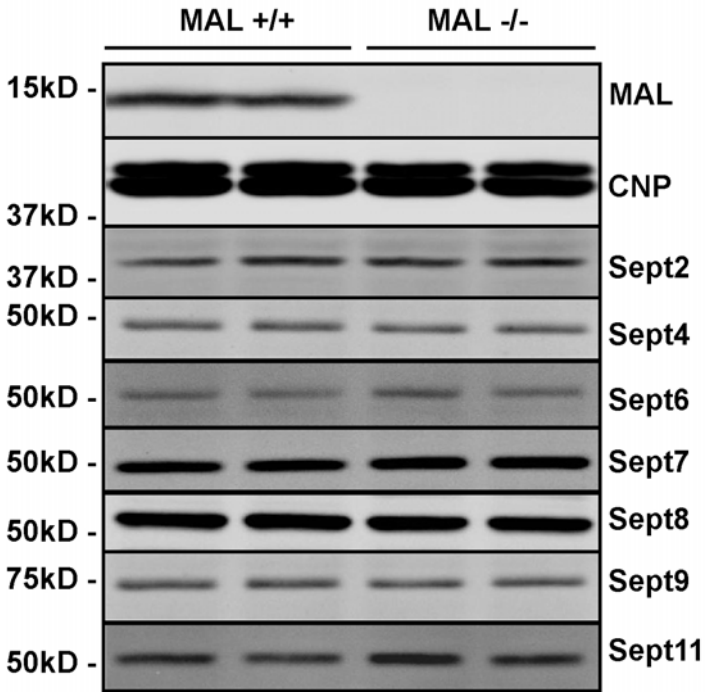

Figure 34 Myelin fractions from two MAL^{wt} mice and two mice MAL^{null} were prepared as already described. Equal amounts of proteins were loaded on SDS-PAGE gels and used for Western blot analysis. MAL deficiency did not lead to alterations in the incorporation of septins into the myelin fraction.

7.8 Accumulation of septins in non-compact myelin structures

Data from this work suggests that septins interact abundantly with myelin membranes. Still, the subcellular localization of septins in myelinated internodes was unknown. Therefore, a confocal co-localization study on teased fibers from sciatic nerves of adult mice was performed. Teased fibers from the PNS allow to reveal the precise localization of proteins in particular compartments of the myelin sheath. The subcellular distribution of the different septins was compared to the localization of Caspr, known to be specifically localized to the paranodal membrane of myelinated axons (Poliak and Peles, 2003), to MAG, which is detected in periaxonal membrane, paranodal loops and in Schmidt-Lantermann incisures (Erb et al., 2006), with Gliomedin, which is confined to microvilli (Eshed et al., 2005) and with actin localized in Cajal bands, Schmidt-Lanterman incisures and paranodal loops. Sept2 was detected in the Schwann cell cytoplasm of the Cajal bands (Figure 35A, arrow) where it co-localized with the actin cytoskeleton (Figure 35C, arrows). In addition, Sept2 was abundant in the paranodes and microvilli of the node of Ranvier (Figure 35A, asterix and Figure 35D, open arrow). Further, we identified co-localization of Sept2 with Caspr (Figure 35E, open arrows), suggesting that Sept2 may play a role in the paranodal loops. Besides this, Sept2 accumulations could be detected in the outer rim of the Schmidt-Lanterman incisures (Figure 35B, arrowheads), whereas in the cytoplasm of the incisures within the compact myelin sheath Sept2 could not be detected (Figure 35C, arrowheads). Furthermore, teased fibers were stained for all septins identified in the co-immunoprecipitation assays. Immunofluorescent analysis for Sept7, 8, 9 and 11 showed an equivalent accumulation in the microvilli at the nodes of Ranvier (Figure 35F asterix) and in Cajal bands (Figure 35F, arrows). Immunofluorescent analysis for Sept6 did not result in a specific signal in mouse sciatic nerve tissue. This might be due to the accessibility of the epitope or the affinity of the Sept6 antibody to undenatured Sept6.

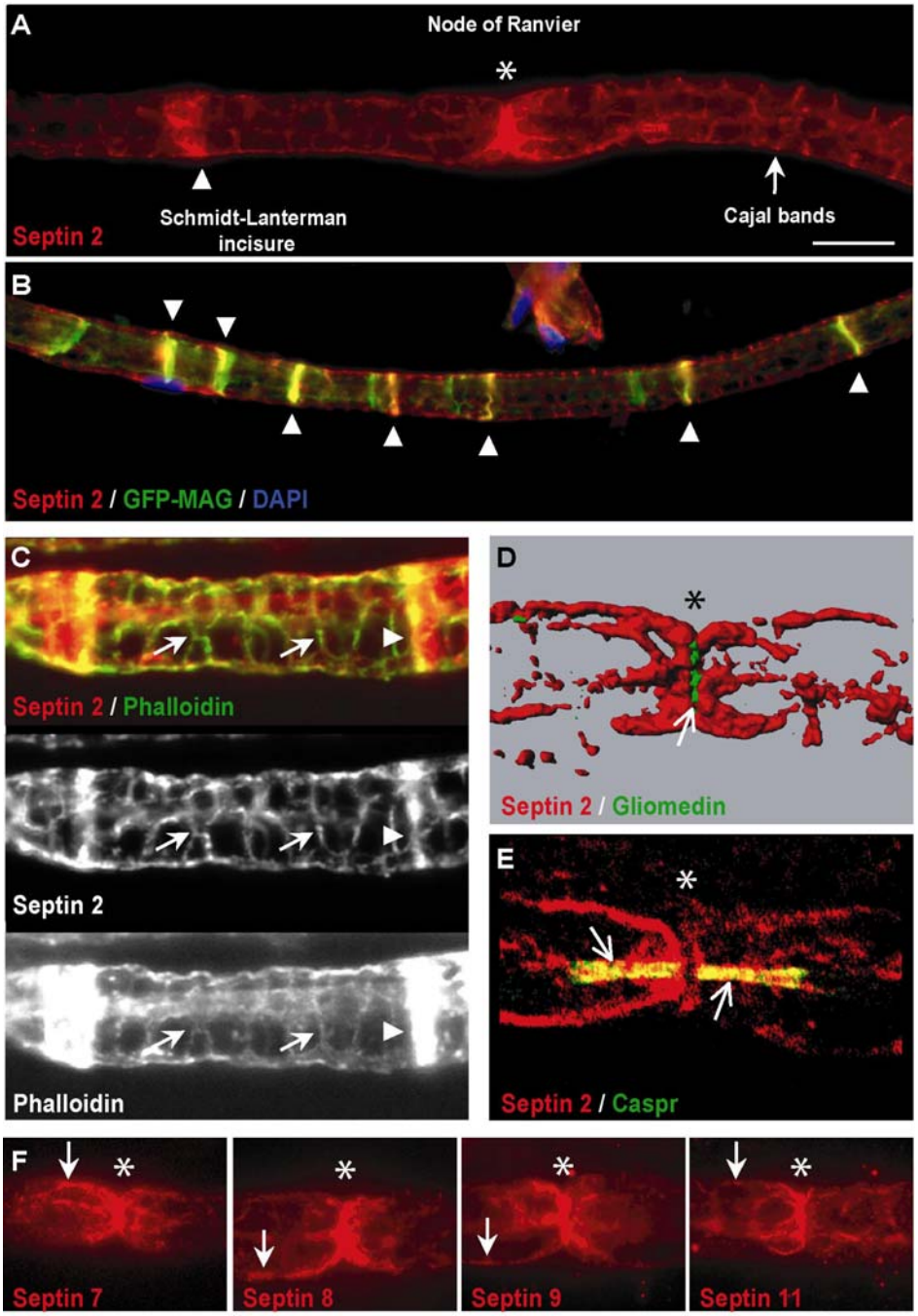

Figure 35 Teased fiber preparations from sciatic nerves were stained for septins. (A) A cytoplasmic pool of Sept2 was detectable as Cajal bands (arrows). Besides this, Sept2 accumulated in the non-compact myelin compartments, the Schmidt-Lanterman incisures (arrowheads) and at the nodes of Ranvier (asterix). (B) Sept2 co-localized with MAG at the outer rims of the Schmidt-Lanterman incisures (arrowheads). (C) The Cajal band localization was verified with co-localizing actin signal (arrows). (D/E) Sept2 highly accumulated in paranodal and microvilli regions where it co-localized with Gliomedin and Caspr (open arrows). (F) Besides Sept2, also Sept7, Sept8, Sept9 and Sept11 accumulated at the nodes of Ranvier forming a complex septin scaffold (asterix).

7.9 Sept6 and MAL co-localize in the Schwann cell cytoplasm

As mentioned, it was not possible to stain Sept6 in mouse teased fibers. Therefore, cross sections of human femoralis nerve tissues were stained to co-localize Sept6 and MAL and determine the site of a possible interaction (performed by Beat Erne, Neurobiology, Department of Biomedicine and Neurology, University Hospital Basel, Pharmacenter, Basel, Switzerland). MAL was detected in the non-compact myelin compartment where it co-localized with MAG (Figure 36A, arrowhead) as well as in the compact myelin compartment co-localizing with MBP (Figure 36B, arrowhead). Additionally, MAL was detected in the Schwann cell perykaryon (Figure 36A and B, arrows). Sept6 was strongly detected in the perikaryon of the Schwann cells (Figure 36C and D, arrow) but not in the non-compact (Figure 36C, arrowhead) and compact (Figure 36D, arrowhead) myelin compartments. These data indicate that interaction between Sept6 and MAL may take place in the cytoplasm of the Schwann cell.

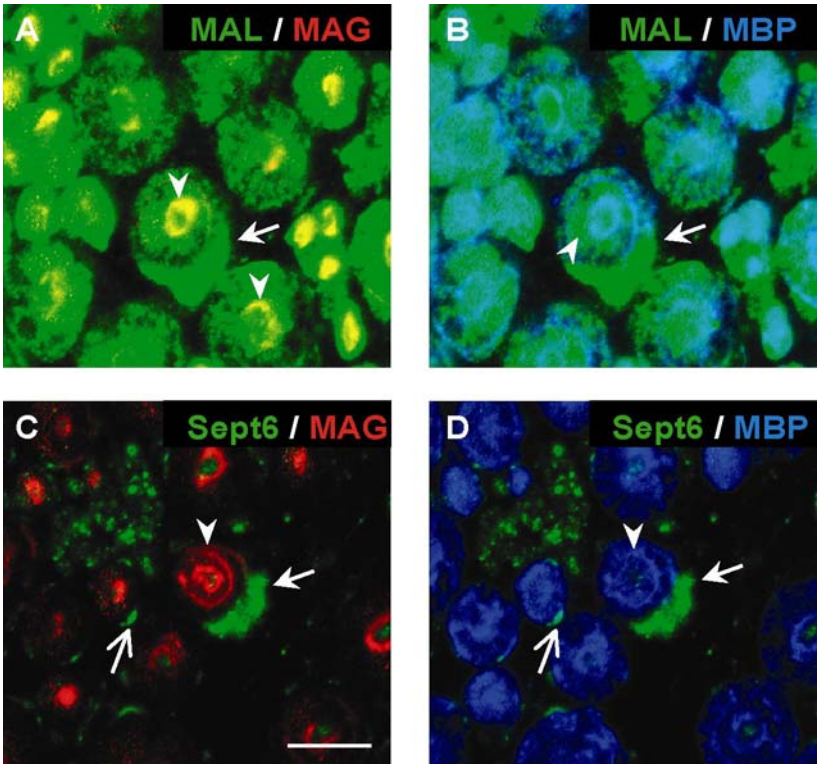

Figure 36 Human femoralis nerve autopsies were used for immunohistochemical co-localization of Sept6 and MAL. (A and B) MAL was detected in the compact (MBP+, arrowhead) and non-compact (MAG+, arrowhead) myelin compartments as reported earlier (Schaeren-Wiemers et al., 2004). In addition, MAL was detected in the Schwann cell perikaryon (arrows). (C and D) Sept6 signal was detected in the perikaryon where it co-localized with MAL (arrow). Additionally, Sept6 was found in the Cajal bands (open arrow). No Sept6 signal was detected in the abaxonal non-compact (MAG+, arrowhead) or compact (MBP+, arrowhead) myelin compartment. Bar 10μm

7.10 Disturbance of the septin cytoskeleton by RNA interference

7.10.1 Myelinating DRG/ Schwann cell co-cultures

Dorsal root ganglia (DRG)/ Schwann cell co-cultures are frequently used to study different aspects of Schwann cell biology. In this system, mechanisms like axon-glia interaction, myelination and myelin maintenance can be analyzed *in vitro*. Dorsal root ganglia from E13 mouse or E15 rat embryos are isolated and used for explant cultures. The cells are dissociated to obtain a single cell suspension of dorsal root neurons and Schwann cells. The neurons will generate extensive neurite trees. After the beginning of synapse formation some neurites will become myelinated by the Schwann cells (Figure 37). The first 2-3 days in culture, the Schwann cells are highly proliferative and can be infected by retroviruses. The retroviral vectors stably integrate into the Schwann cell genome and can be used to introduce constructs e.g. for RNA interference or expression of recombinant proteins. Then, the effect of the respective construct on myelination can be analyzed. We wanted to use this system to target the septin cytoskeleton of myelinating Schwann cells by RNA interference and analyze the impact on myelination. Therefore, myelinating DRG/ Schwann cell co-cultures were established. Published efficient RNA interference target sequences for Sept2 and Sept7 (Kinoshita et al., 2002) were from mouse and, therefore, mouse co-cultures were used in this study. A GFP reporter gene integrated in the retroviral vector was used to identify infected Schwann cells and selectively analyze the impact of the RNA interference construct on a single cell level. Myelinating DRG/ Schwann cell co-cultures were prepared as described earlier (Carenini et al., 1998). The medium was modified to increase myelination efficiency (according to personal communications Jonah Chan, Keck School of Medicine, Los Angeles, USA). Robustly myelinating cultures were obtained as judged by the formation of MBP+ internodes (Figure 37). These cultures were used to study the impact of septin loss on myelination.

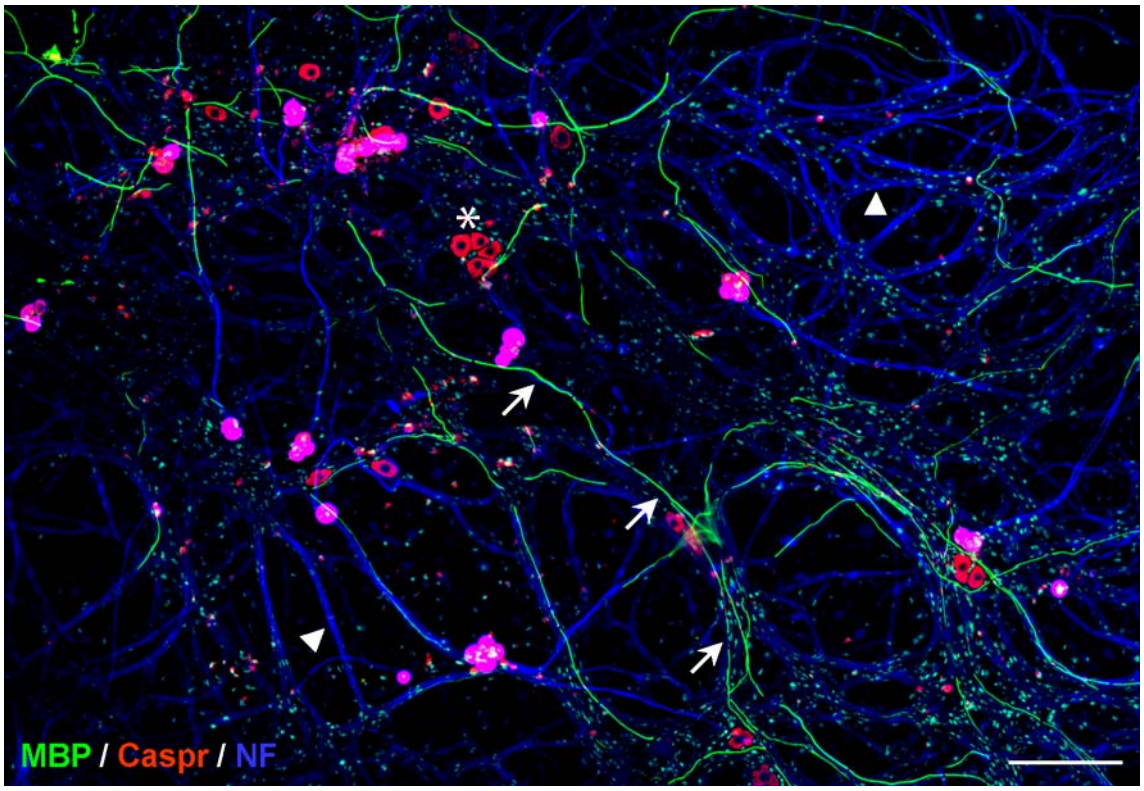

Figure 37 Dorsal root ganglia (DRG) were isolated from E13 embryos and plated on cover slips after generation of a single cell suspension. The DRG neurons (Caspr+ cell bodies, asterix) generate a network of neurites (Neurofilament+ (NF), arrowhead) and the Schwann cells proliferate until they cover the cell culture area. After 4 weeks in culture, some Schwann cells begin to myelinate and form MBP+ internodes (arrows). Bar 100μm

7.10.2 Retroviral RNAi constructs targeting Sept2 and Sept7

Reported effective RNAi target sequences for Sept2 and Sept7 (Kinoshita et al., 2002) as well as the empty vector (GFP control) were used. The functionality of the retroviral construct was evident in fibroblast frequently found in the DRG/ Schwann cell co-cultures which also expressed both Sept2 and Sept7 (Figure 38). Respective cultures and control cultures were stained for Sept2 or Sept7. Sept2 or Sept7 were specifically lost after targeting with the respective RNAi constructs (Figure 38B and D). The GFP negative control did not affect the levels of Sept2 or Sept7. In conclusion, the target sequences efficiently downregulate Sept2 and Sept7, respectively, as reported earlier (Kinoshita et al., 2002).

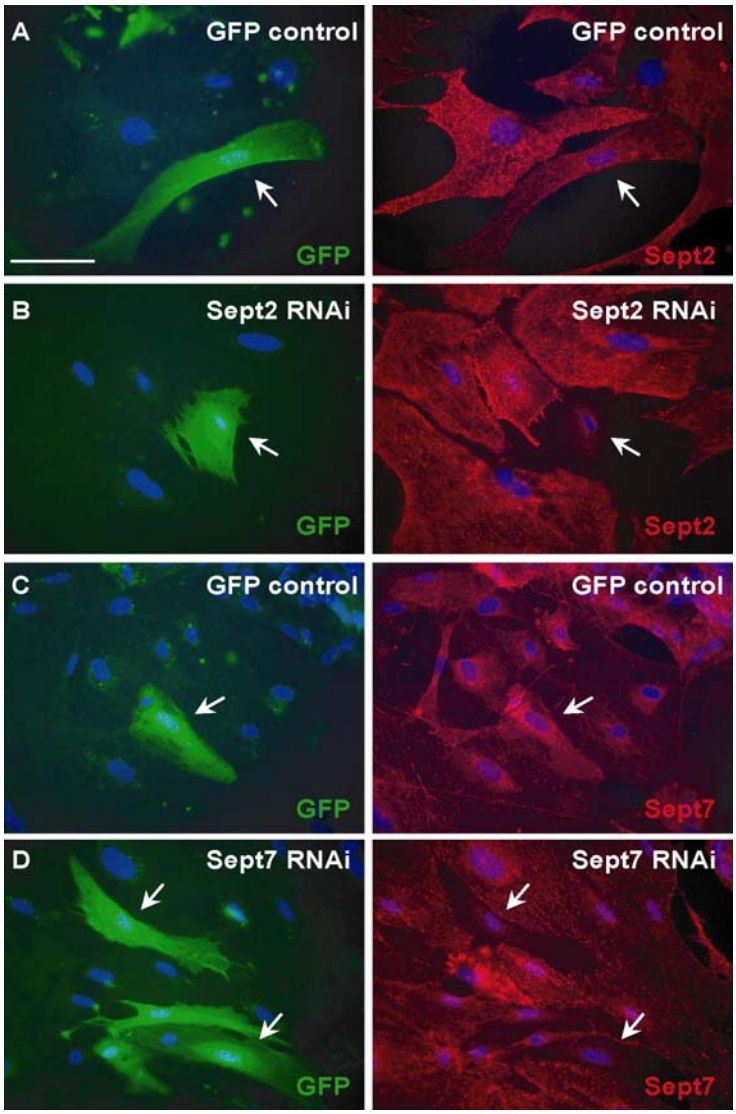

Figure 38 Infected fibroblasts were used to qualify the RNAi constructs (Kinoshita et al., 2002). In control infected fibroblasts (GFP control) the septin signal was indistinguishable from non-infected cells (A and C). The Sept2 and Sept7 RNAi constructs lead to a profound loss of Sept2 and Sept7 signal respectively (B and D). Bar 50μm

7.10.3 Control infected co-cultures myelinate normally

The established myelinating DRG/ Schwann cell co-cultures were infected with retroviral particles at day 1, 2 and 3 after plating. As a negative control for further experiments a reported construct downregulating MAG with no effect on myelination was analyzed. This construct lead to successful infection of Schwann cells (Figure 39, GFP+) which formed intact internodes of myelin (Figure 39, arrow) in a very same fashion as reported earlier (Carenini et al., 1998; Eshed et al., 2005). These data indicate that infection and the activation of the RISC complex upon RNA interference per se did not disturb normal myelination in this co-culture system.

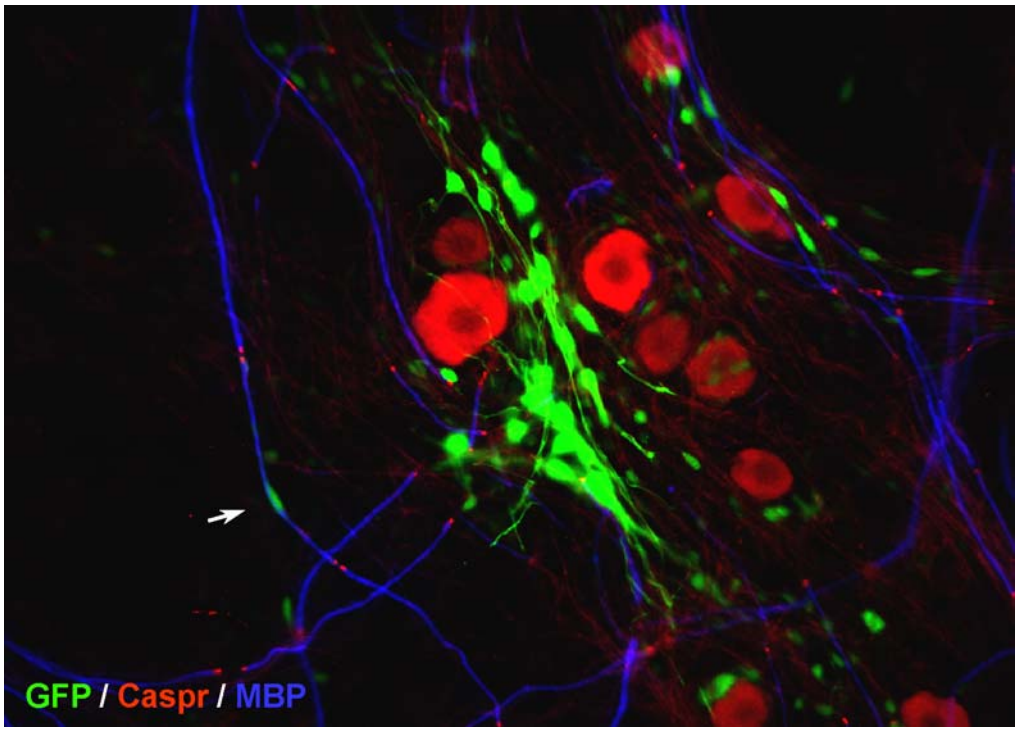

Figure 39 Myelinating DRG/ Schwann cell co-cultures were infected with a retroviral construct expressing a RNA hairpin targeting MAG. GFP was expressed under the control of a second promoter and was used as infection control. Schwann cells were infected with varying frequencies depending on the initial density of the culture. Ideally, the infection efficiency was up to 30% but frequently 10-20% of the Schwann cells were infected. The cultures were analyzed for GFP+ cells which formed MBP+ internodes (arrow). The downregulation of MAG did not impair normal myelination indicated by MBP expression and Caspr clusters.

7.10.4 Downregulation of Sept2 has no impact on myelination

The myelinating DRG/ Schwann cell co-cultures were infected with retroviral supernatants targeting Sept2. The infected Schwann cells were analyzed for myelin formation indicated by MBP and nodal integrity by the paranodal marker Caspr. Schwann cells were infected in a similar frequency than control MAG RNAi-infected cells (Figure 40A and B). Most important, they were able to form normal MBP-positive internodes with Caspr clusters (Figure 40E) indicating normal formation of the nodal and paranodal structures in absence of Sept2. These data indicate that downregulation of Sept2 in Schwann cells does not have an effect on myelination efficiency or internode integrity.

7.10.5 Downregulation of Sept7 may impair Schwann cell survival

In contrast, DRG/ Schwann cell co-cultures subjected to RNA interference for Sept7 lead not to comparable numbers of infected Schwann cells in five independent experiments (Figure 40C). After induction of myelination only few GFP-positive cells remained, probably correlating to the penetrance (infected, but not active) of the construct. As early as two days after infection, the number of GFP-positive cells was very low. These data suggest that loss of Sept7 may have an impact on Schwann cell survival. However, it was not possible to quantify this effect since it was not possible to pin down an early time point where the cells robustly expressed GFP as marker for infection but were still viable. In conclusion, Sept7 may have essential functions for Schwann cell biology and loss of Sept7 leads to death of the cells already during early differentiation stages. These cultures, therefore, cannot be used to study the function of Sept7 in myelination.

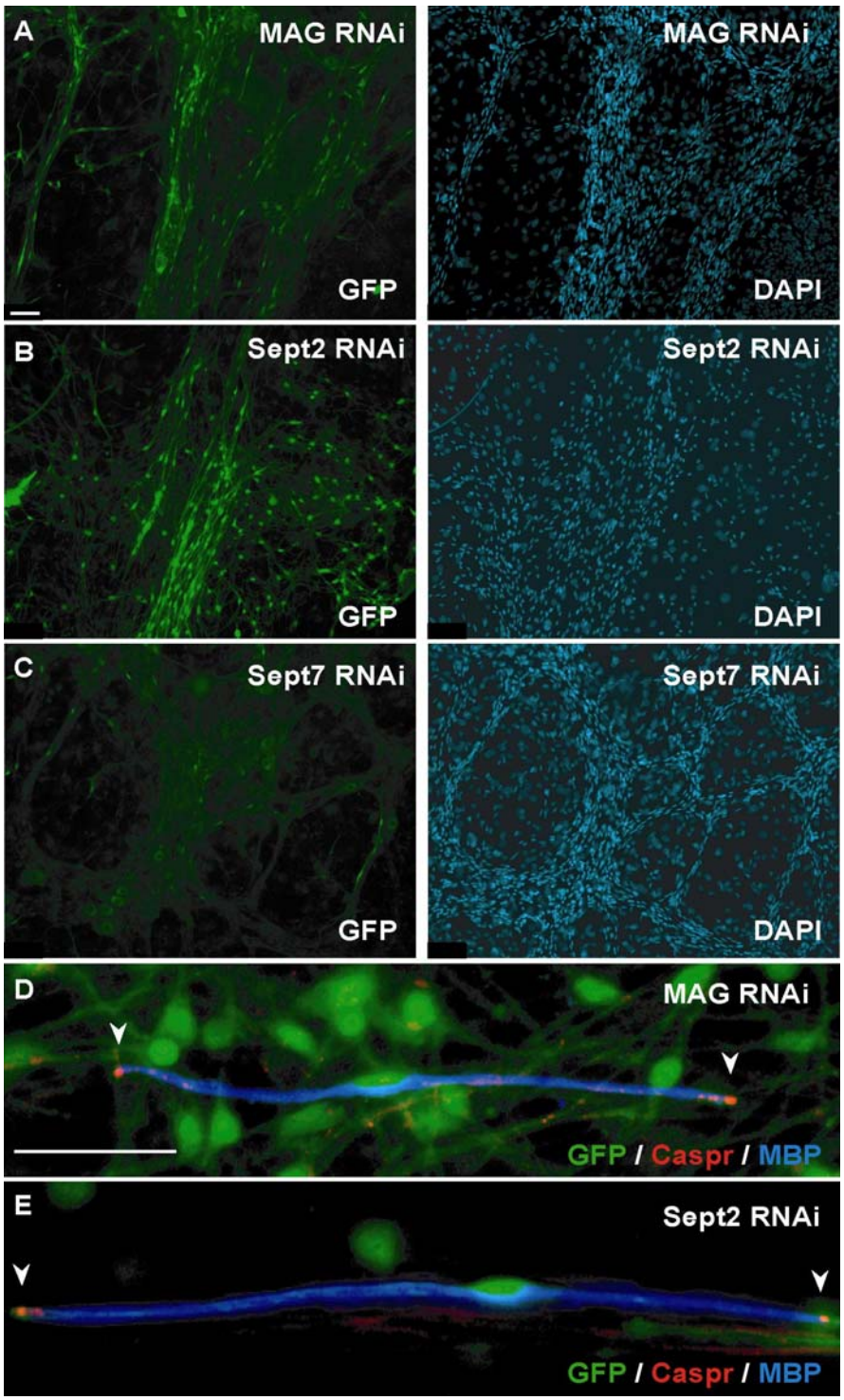

Figure 40 Myelinating DRG/ Schwann cell co-cultures were infected with retroviral particles bearing constructs downregulating Sept2 or Sept7. A RNAi construct targeting the myelin protein MAG was used as negative control. (A-C) Cultures were infected at day 1,2 and 3 after dissection. After myelination comparable numbers of infected Schwann cells (GFP+) were found for MAG RNAi and Sept2 RNAi. In contrast, only few cells were positive for the Sept7 RNAi construct and myelination could not be qualified. (D) Schwann cells downregulating MAG were able to form normal MBP+ internodes and Caspr clusters (arrowheads) as reported elsewhere. (E) Comparably, loss of Sept2 had no impact on myelination. Bars: A-C: 60μm; D-E: 32μm

7.11 A dominant negative approach to disturb the septin cytoskeleton

Several dominant negative mutants of Sept2 were described in the literature (Schmidt and Nichols, 2004; Vega and Hsu, 2003). The S51N mutation of Sept2 impaired the GTPase activity and led to aberrant neurite sprouting in PC12 cells (Vega and Hsu, 2003). Here, the effect of the dominant negative Sept2 mutation S51N on myelination was analyzed. The wild type Sept2 as well as the S51N mutant Sept2 sequences were fused C-terminally to the sequence of the red fluorescent protein mCherry (kindly provided by Prof. Tsien, UCSD, La Jolla, USA) as indicator of infection and for recombinant protein localization. The mCherry sequence as well as the respective Sept2 sequences were subcloned into the pMX retroviral vector. Accordingly to the RNAi constructs, the pMX constructs were packaged into retroviral particles. The retroviral supernatants were used to infect DRG/ Schwann cell co-cultures. The subcellular distribution of wild type Sept2-mCherry was analyzed in fibroblasts present in the co-cultures. These cells have a flat morphology and, therefore, the visualization of cytoskeleton components is straightforward. Infected cells displayed filamentous Sept2-mCherry structures (Figure 41). In addition punctuated signal was detected throughout the whole cell cytoplasm. This staining pattern is indicative for normal Sept2 distribution since Sept2 was reported to interact with actin bundles in cultured cells (Kinoshita et al., 2002). Most important, we could not detect aggregates of Sept2-mCherry. These data demonstrate that C-terminally tagged Sept2 distributes like wild type Sept2 and does not lead to impaired septin structures in cultured cell.

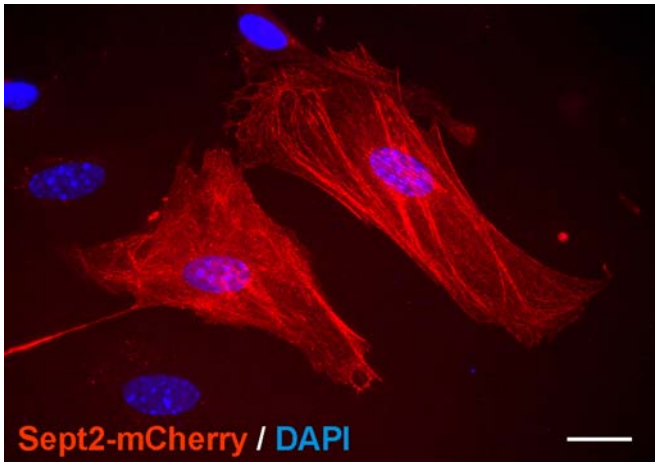

Figure 41 Cultured fibroblasts were infected with a retroviral construct expressing tagged Sept2. The red fluorescent protein mCherry was C-terminally fused to Sept2. Infected cells displayed normal morphology and Sept2-mCherry distribution. Bar 20μm

The DRG/ Schwann cell co-cultures were analyzed for mCherry positive myelinated internodes. The internodes expressing wild type Sept2-mCherry showed comparable Sept2 protein distribution as endogenous Sept2 stained by immunohistochemistry (Figure 42). These data show that Sept2-mCherry distributes similar to wild type Sept2 and, therefore, this construct could be further used to study septin dynamics by live imaging. However, the number of internodes positive for wild type Sept2-mCherry was low. Additionally, the mCherry signal was weak, which lead to difficulties to separate it from the background. A possible explanation might be that the retroviral promoter used in this construct was only weakly activated in Schwann cells.

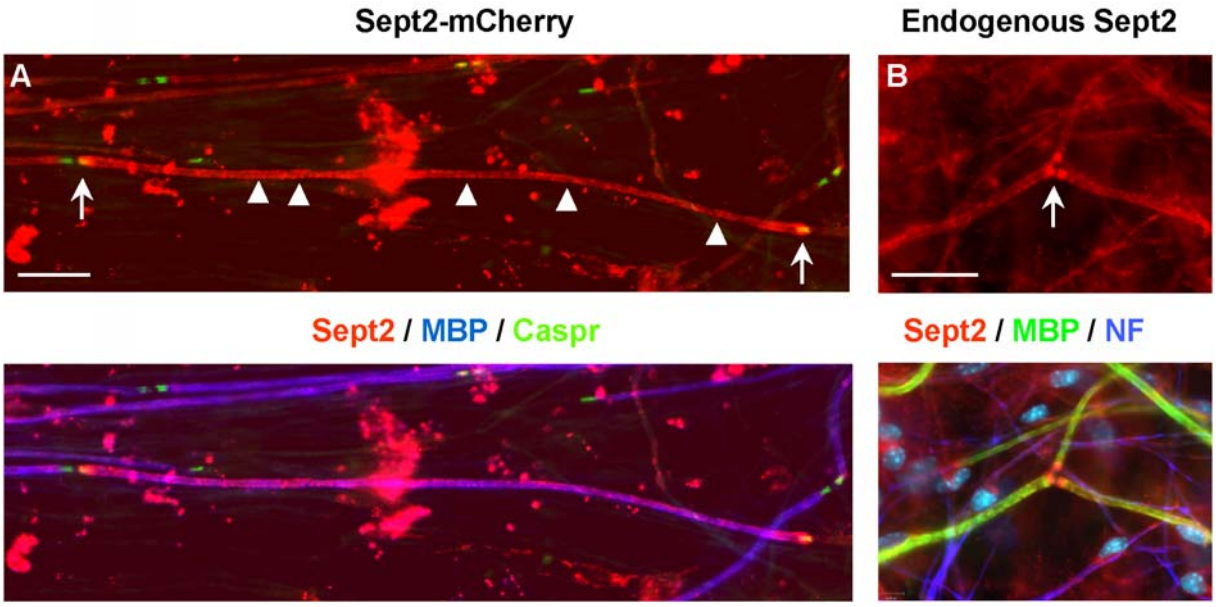

Figure 42 DRG/ Schwann cell co-cultures were infected with retroviral particles bearing the Sept2-mCherry construct. After myelination, the cultures were analyzed for mCherry positive internodes. (A) The Schwann cells expressing the Sept2-mCherry construct were able to form normal MBP+ internodes. Sept2-mCherry distributed along the entire length of the internode. At the nodes of Ranvier Sept2-mCherry accumulations co-localizing with Caspr clusters were detected. Along the internode the Sept2-mCherry signal concentrated in the tubular channels of the Cajal bands (arrowheads). (B) Immunohistological staining of endogenous Sept2 showed comparable localization as for the Sept2-mCherry. Bar 20μm

The DRG/ Schwann cell co-cultures infected with the S51N Sept2 mutant were analyzed for myelinated internodes positive for mCherry. No myelinated internode expressing the dominant negative Sept2 mutant was ever found. This might be due to vital effects on the Schwann cells as observed for the Sept7 RNA interference. Yet, it was not possible to quantify this effect since the number of internodes expressing the Sept2-mCherry negative control was already too low.

8 Discussion

Schwann cells and oligodendrocytes are the myelin forming cells in the PNS and CNS respectively. During myelination they establish and maintain an extensive membrane system with discrete domains. How compartmentalization of the myelin membranes is achieved and maintained is still not understood, yet it is clear that the integrity and function of the myelin sheath is critically dependant on correct structuring. Septins were described in many systems as membrane organizing proteins with important roles in processes like cytokinesis, protein transport and exocytosis (Kartmann and Roth, 2001; Kinoshita, 2003b). Septins have a crucial role in the organization of the cytoskeleton since they were shown to influence the actin and tubulin network under different conditions and to provide a link between these filament systems and the plasma membrane (Kinoshita et al., 2002; Kremer et al., 2005; Peng et al., 2002). Therefore, septins are interesting in the context of myelin membrane formation and compartmentalization. Recently, several studies pointed to the presence of septins in myelin membranes (Roth, 2006; Taylor et al., 2004; Werner et al., 2007), but their functional role in myelination is unknown. In this study, we show that septins are intriguing candidates for subcompartment formation and cytoskeleton regulation during myelination and maintenance.

We became interested in the septin protein family by identifying Sept6 as a binding partner of the myelin protein MAL. Sept6 interaction with the N-terminus of MAL was demonstrated in two independent experimental systems, however was not achieved with a Sept2/ 6 /7 complex. This is of interest because it suggests that the binding of septins to non-septin binding partners, here MAL, might be dependant on the composition of the septin heteromeric unit. Septin structures *in vivo* are complex and integrate many different isoforms in stoechiometric and non-stoechiometric ratios (Kinoshita, 2003a; Kinoshita et al., 2002). Septin scaffolds might, therefore, interact with binding partners in dependence of their composition. To follow this up, it would be necessary to test purified septin complexes of different composition for interaction with MAL. A parallel analysis of interactions of septin complexes with PLP might shed light on the question why distinct septins are lost in PLP^{null} myelin whereas others, like Sept7, are unchanged (Werner et al., 2007). Differences of septin interaction with PLP and MAL regarding complex composition would open up new concepts how septin scaffolds could focally interact with different membrane structures. Up to day, only few septin interaction partners have been described in mammalian systems (Table 2). In fact, despite of their abundant interaction with membranes, MAL is one of the first transmembrane proteins shown to interact with septins. Indeed, the myelin sheath might be a promising model system in which to study how septins contribute to compartmentalization of membrane structures.

Interaction partners	Subcellular structure	Presumed functions
Anillin, actin, myosin	Contractile ring, actin stress fibers	Unknown
SA-RhoGEF, rhotekin	Actin stress fibers	Organization
Borgs	Unknown	Unknown
Tubulins?	Microtubules	Unknown
MAP4	Cytoplasm	Sequestration
CENP-E	Kinetochore microtubules	Scaffold for kinetochore motors?
Syntaxins/SNARE complex	Nerve terminal, platelet granule	Scaffold, sequestration?
Glutamate transporter	Glial cortex	Regulation?
Unknown	Spermatozoon annulus	Structural support, diffusion barrier?
Hyperphosphorylated, polymerized tau	Neurofibrillary tangles	Incidental adsorption or sequestration?
Polymerized alpha-synuclein	Lewy bodies	Incidental adsorption or promoting aggregation

Table 2 Described molecular interactions and presumed functions of septin interactions are displayed. Hypothesized functions or interaction partner are indicated with a question mark (modified from Kinoshita, 2006).

To investigate whether MAL function is directly dependent on septins, the septin cytoskeleton of MAL-deficient mice was analyzed. These mice display a characteristic phenotype in the CNS, where the paranodal loops are destabilized and detached from the nodal axolemma (Schaeren-Wiemers et al., 2004). The phenotype is due to impaired transport of myelin components or local defects in the architecture of the nodal structures. In both cases, impairment of the septin cytoskeleton could contribute to some extend to this phenotype. But the composition and abundance of the septin cortex in MAL^{null} mice was not altered. To follow this up, Sept6^{null} mice were analyzed for a phenotype analogous to the MAL^{null} mice. Sept6-deficient mice were already described before (Ono et al., 2005). They have a normal lifespan and do not show obvious defects in the CNS. However, earlier studies focused mainly on neurons and much less on myelinating glia. EM analysis of optic nerves of Sept6^{null} mice showed that the paranodal loops were correctly attached to the nodal axolemma and the MAL^{null} phenotype was not evident.

One explanation for the lack of any obvious phenotype in Sept6-deficient mice could be that other components of the myelin sheath could compensate for the lack of Sept6/MAL interaction. One of the known concerns in the field is that the lack of one septin can be compensated by homologous other septins. Indeed, Sept11 - the closest homolog of Sept6 - was more abundant in myelin membranes purified from Sept6-deficient mouse brains. Increased abundance of Sept11 likely compensates for the lack of Sept6 and points to a particular role of Sept6 in myelinating cells, since increased abundance of Sept11 was not evident in Sept6^{null} whole brain homogenate

(Ono et al., 2005). As a next step, Sept11-deficient mice need to be generated and ultimately Sept6/11 double null mice to analyze the functional role of Sept6 and 11 in myelination further.

The complexity of septin scaffolds in the central nervous system has already been described (Hall et al., 2005), but which septin genes are expressed in myelinating cells has not been elucidated yet. The expression pattern of the septin gene family in myelinating cells seems to be very complex. It might not surprise that myelinating cells express many different septins, and upregulate the whole septin cytoskeleton towards differentiation and myelination since the different membrane compartments of a myelin sheath are extensive and complex. The major stoechiometric complex in both Schwann cells and oligodendrocytes seemed to be Sept2/ 7/ 8. This is in contrast to whole brain homogenate where the predominant septin complex seems to be Sept2/ 6/ 7 (Kinoshita et al., 2002). Data from other studies identified septin scaffolds of different composition in different cells (Blaser et al., 2004; Nagata et al., 2004). This might indicate that each cell type expresses a unique set of septins, which then integrate into the cytoskeleton. The role of Sept8 in myelinating glia, therefore, might be interesting since this work also demonstrated that Sept8 transcription leads to myelin specific splice isoforms.

Co-immunoprecipitation experiments for Sept6 were, first, aimed to verify the interaction of Sept6 and MAL from *in vivo* derived samples, and second, to identify further myelin components interacting with septins. But seemingly, it was not possible to pull down MAL or other membrane bound myelin proteins by immunoprecipitation for Sept6. Possibly, Sept6 was too low abundant in the myelin fractions for co-immunoprecipitation assays. Alternatively, MAL interacting septin complexes might be underrepresented in the total of Sept6 containing complexes. It has also to be considered that the interface between septins and transmembrane proteins like MAL might be lost upon detergent extraction. Here, Sept2 was the only protein co-precipitating with Sept6.

Septin function critically depends on heteromeric complex formation. Therefore, co-immunoprecipitation experiments for Sept2 were performed with the following reasoning. Sept2 was shown to interact with Sept6 in myelin fractions. The working hypothesis was that Sept6 interactors, like MAL, might be pulled down also together with Sept2 if the Sept2/ 6/ X complex was abundant and stable or if also septin complexes of other composition interacted with MAL. Sept2 turned out to be abundant in CNS myelinated fiber tracts as well as in myelinating Schwann cells. Therefore, Sept2 was a good candidate for co-immunoprecipitation assays. Indeed, immunoprecipitation for Sept2 led to the purification of multiple septins in CNS myelin and PNS homogenates. Sept6 was co-precipitated together with Sept2 verifying their interaction in myelin fractions. But, comparable to the immunoprecipitation experiments for Sept6, myelin proteins, in particular MAL, were not co-purified. An

explanation could be that the septin/membrane interface was destroyed by detergent extraction.

Immunoprecipitation for Sept2 revealed distinct septin complexes interacting with myelin membranes, and therefore, the composition of these complexes was analyzed by mass spectrometry. Complexes isolated from the CNS and PNS were identical with the exception of Sept4, which was only detected in the CNS complex. Both, in the CNS and PNS a stoechiometric complex of Sept2, 7 and 8 of relative high abundance was found. The other septins were present in non-stoechiometric quantities. Septin complexes of different composition have been reconstituted and analyzed *in vitro* and served as a model to study septin complex formation. The Sept2/ 6/ 7 complex could be expressed and isolated from E.coli (Sheffield et al., 2003) and insect cells (Kinoshita et al., 2002). This fundamental septin complex served as a model for biochemical determination of the rules for septin complexes formation. In the Sept2/ 6 /7 complex, replacement of Sept6 with Sept11 lead also to a stable complex. Sept2 could be replaced by Sept1, 4 and 5. Sept7 seemed to be irreplaceable and fundamental for all septin complexes (Kinoshita, M., C. Field, M.L. Coughlin, and T.J. Mitchison. unpublished observations (Kinoshita, 2003a)). Kinoshita and colleagues concluded from these data that one septin from the subgroup II together with one from subgroup III and Sept7 can form a stable canonical complex (see also Figure 12). The role of subgroup I needs still to be investigated. Further data suggests that septin preparations from tissue or cells may not only consist of canonical complexes but also contain sub-stoechiometric quantities of other septins. Here, in myelinating cells, Sept2/ 7/ 8 might be the predominant canonical complex both in Schwann cells and oligodendrocytes. In addition, complexes such as Sept2/ 6/ 7, Sept2/ 7/ 11 might exist. It was not possible to judge by co-immunoprecipitation if these predicted septin complexes exist as discrete entities or as mixed scaffolds. The absence of Sept4 in the PNS might point to an oligodendrocyte specific function of Sept4, which correlates well with its strong upregulation during oligodendrocyte differentiation and its abundance in CNS myelin (Werner et al., 2007).

Further characterization of the identified septins interacting with Sept2 showed that all of them were associated with myelin membrane fractions. An interesting observation was the three transcript variants of Sept8; two of which interacting specifically with myelin membranes and a third with plasma membranes either from astrocytes or from neurons. This might point to splice variant specific expression or incorporation of distinct splice isoforms into different membrane subdomains. In line with this, human Sept8 was demonstrated to generate four splice variants and these isoforms showed brain region specific expression patterns (Blaser et al., 2004). This molecular as well as structural complexity of septin scaffolds is challenging for further analysis of septin function, but the data presented in this work provide levers to specifically tackle the septin system in myelinating cells.

Several studies of the myelin proteome pointed to the presence of septins in myelin fractions (Roth, 2006; Taylor et al., 2004; Werner et al., 2007). Still, it was not known how septins distribute in oligodendrocytes and Schwann cells and in particular along the myelinated internode. In this work, confocal co-localization analysis of septins in peripheral teased nerve fiber preparations identified, besides the expected cytoplasmic localization of septins (Figure 43A), also an accumulation in particular non-compact myelin membrane compartments such as the microvilli, paranodal loops and the outer rim of the Schmidt-Lanterman incisures (Figure 43B and C). This is of interest because these compartments are believed to be important for protein turnover and maintenance of the myelin sheath. It is well-known that septins interact with components of the vesicle fusion machineries like the exocyst complex and syntaxin (Beites et al., 1999; Hsu et al., 1999; Hsu et al., 1998). It was also demonstrated that phosphorylation of Sept5 modulates exocytosis (Amin et al., 2008). In line with this, septins might have a role in vesicle targeting and incorporation into the emerging and adult myelin sheath (Figure 43A and B). Septin scaffolds of different composition might determine regions permitted for vesicle fusion or even discriminate between vesicles carrying different cargo. It was demonstrated that several myelin proteins are sorted and transported into different vesicles (Trapp et al., 1995). Septin scaffolds might discriminate between these vesicles by binding to distinct myelin proteins, like MAL, enabling fusion with the correct domain. Maybe it is worthwhile to mention that MAL was localized in all compartments of the myelin sheath in contrast to other myelin proteins which incorporate in one or the other compartment. Septins might instruct MAL containing lipid microdomains where to incorporate into myelin structures or MAL might direct septin scaffolds to sites of membrane addition and recycling. In both way septin/MAL and related complexes might be main instructors for membrane trafficking in the myelin sheath.

The localization of septins in myelinated internodes is intriguing in yet another context. In yeast, septins build up distinct membrane subcompartments by establishing diffusion barriers that restrict membrane bound structures to respective domains (Barral et al., 2000; Luedeke et al., 2005; Takizawa et al., 2000). Up to day no septin diffusion barrier was described for mammalian septins but clearly this is a major focus of current investigations. Recently, a septin complex of Sept5/ 7/ 11 was shown to form a scaffold at the spine necks of hippocampal neurons very similar to the situation at the yeast mother-bud neck (Xie et al., 2007). It remains to be demonstrated that this septin scaffold serves as a diffusion barrier, but still, these data show that septin function might be well conserved from yeast to mammals. Here, in myelinated internodes septins localized to the non-compact myelin compartment but not to the compact myelin. Therefore, septins might have a role in restricting lateral diffusion of membrane bound proteins and lipids enabling separation of the different myelin compartments.

Additionally, septins might link specialized membrane patches to other cytoskeleton elements, which might be important for the paranodal loop and microvilli organization (Figure 43C). Indeed the highest accumulation of septins was localized to the node of

Ranvier. The axonal cytoskeleton clustered at the node of Ranvier is well characterized and many key players crucial for structural integrity are known (see also Figure 7B). Yet, the counterparts in the Schwann cells are much less understood. Unfortunately, the co-immunoprecipitation assay for Sept2 did not pull down additional components of the paranodal cytoskeleton or the membrane bound interaction partners. In the future, it might be helpful to enrich nodal and paranodal components prior to immunoprecipitation to increase the chance of co-precipitating septin interaction partners from the nodal compartment.

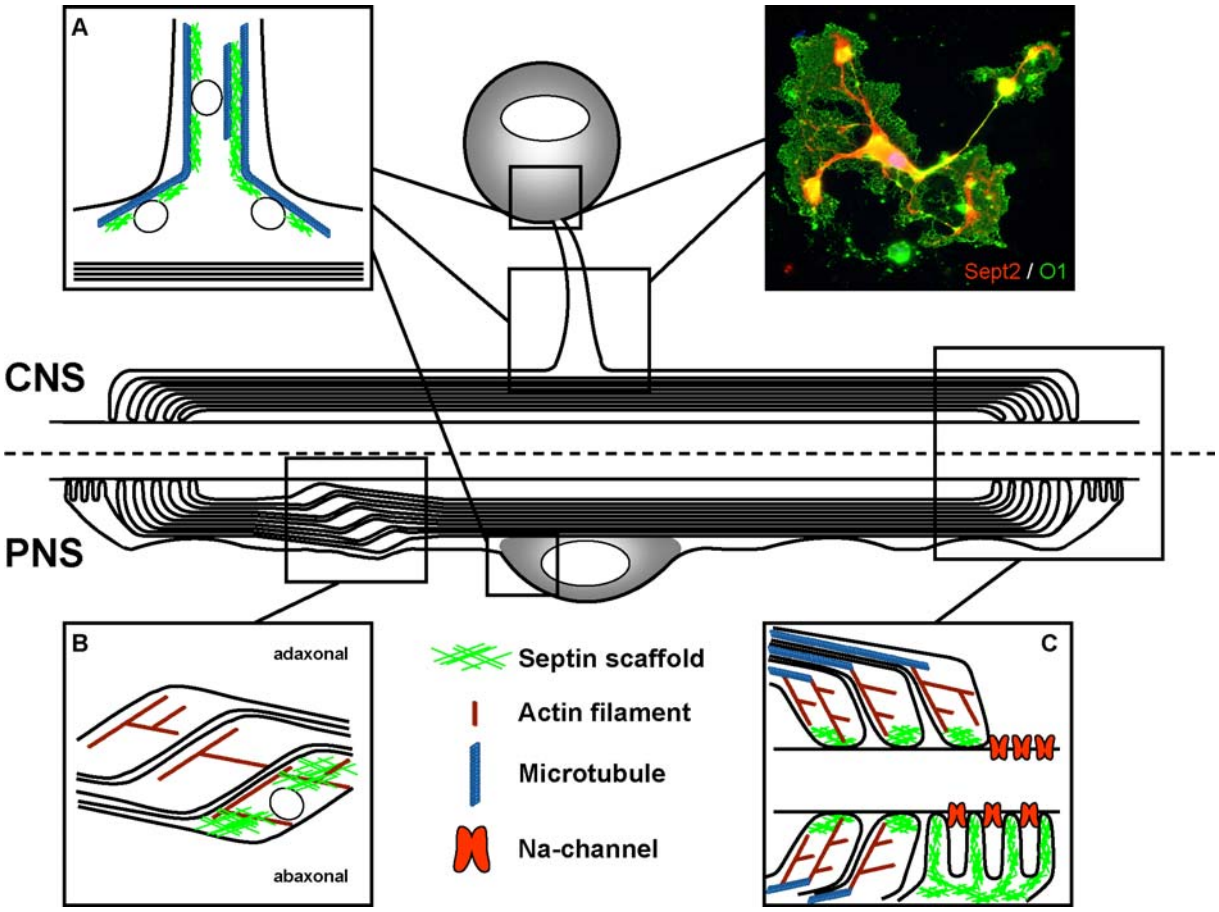

Figure 43 A schematic drawing which illustrates septin scaffolds identified in distinct subdomains of the myelin sheath. (A) The pool of septins in the perikaryon of Schwann cells as well as in the Cajal bands (not specially indicated) and the cytoplasm channels of the oligodendrocytes might have a role in sorting and targeting of myelin components to the emerging and adult myelin sheath. Furthermore, septin scaffolds are detected in the outer rim of the Schmidt-Lanterman incisures (B) as well as in the paranodal loops and the microvilli at the nodes of Ranvier (C) where they might contribute to subdomain formation and protein turnover.

The last part of this study focused on functional experiments to study the role of septins in myelinating cells. From the Sept6^{null} mice, it was evident that no phenotype on myelination was resulting from Sept6 loss. This seemed to be due to functional compensation by Sept11. Comparably, downregulation of Sept2 in the DRG/ Schwann cell co-cultures using RNA interference did not lead to a phenotype. Here, e.g. Sept5, which we showed to be expressed by Schwann cells, might compensate for the loss of Sept2. Induced downregulation of Sept7, however, led to vital effects on Schwann cell survival. This might suggest that the septin cytoskeleton is essential for glial cell development but also prevented the exact definition of the developmental step(s) at which it is required. In fact, this study demonstrated that the mouse DRG/ Schwann cell co-culture system might not be ideal to analyze effects of targeting septins. In the first place, the mouse DRG/ Schwann cell co-culture system was chosen because respective target sequences for Sept2 and Sept7 RNAi were available. Furthermore, it was planed to use myelinating co-cultures generated from GFP-MAG expressing mice. This transgenic mouse line expresses GFP-tagged MAG under the control of the MAG promoter and can be used as an elegant reporter for myelination (Erb et al., 2006). However, it became evident that the mouse co-culture system had several limitations. First, the culture had to be maintained for a long period of time until myelination takes place. Data from this work showed that the Schwann cells expressed septins in all stages of differentiation. Following infection and downregulation of the target they had to survive 4-5 weeks in culture until myelination was completed. Septins are likely involved in different aspects of Schwann cell biology, and therefore, successful targeting of the septin cytoskeleton might lead to myelin unspecific effects as seen for downregulation of Sept7. Second, the myelination efficiency in mouse cultures was low, hindering the analysis of subtle effects tremendously. Third, the infection efficiency was dependant on the rate of proliferation. Therefore, the infection efficiency varied among different cultures and even among different regions of the cover slips depending on the initial local cell density. Seemingly, it would be helpful to use rat myelinating cultures. There, Schwann cells can be isolated and cultured separately from the DRG neurons, a method which could not be established as a reliable standard protocol in the mouse system yet. The rat Schwann cells are, therefore, much easier to manipulate with retroviral constructs and much higher infection and myelination efficiencies can be obtained.

To circumvent compensation mechanisms seen both in the Sept6^{null} mouse and for Sept2 RNA interference a dominant negative mutant approach was performed on myelinating co-cultures. Several dominant negative mutants for Sept2 were already described and successfully used (Schmidt and Nichols, 2004; Vega and Hsu, 2003). Here, a dominant negative Sept2 mutant impairing the GTP binding was analyzed regarding effects on myelination. The mutant protein was tagged with the red fluorescent protein mCherry for infection control and protein visualization. The tagged wild type Sept2 protein, used as a negative control, localized analogous to

endogenous septin and no protein aggregates were formed. This is remarkable since we showed earlier that expression of GFP tagged Sept2, Sept6 or Sept7 led to aggregates in COS7 cells and in Oli-Neu cells (Buser, Masterthesis, 2003). Therefore, this new C-terminal tagged Sept2 construct seemed to be favorable in terms of protein localization. Indeed, the wild type Sept2-mCherry construct could also be further used for live imaging experiments to analyze septin dynamics in living cells. Here, DRG/ Schwann cell co-cultures were infected with constructs expressing either the wild type Sept2-mCherry or the dominant negative Sept2 mutation fused to mCherry. Unfortunately, the infection efficiency in the DRG/ Schwann cell co-cultures was highly variable comparable to the situation with the RNAi constructs. Furthermore, the expression level of tagged Sept2 in the myelinated internode was low, complicating the identification of infected cells. Therefore, it was not possible to analyze the effect of the dominant negative Sept2 mutation in myelinating Schwann cells. In the future, it might be favorable to use bicistronic vectors expressing GFP and mCherry tagged Sept2 separately to robustly identify infected cells. Comparably to the RNAi analysis, the use of rat myelinating cultures might facilitate the identification of effects of the dominant negative mutants on septin function.

In summary, this study showed that myelinating glial cells express a distinct set of septins at all stages of differentiation. Remarkably, they upregulate many components of the septin cytoskeleton in the period of high myelinating activity. It was further shown that discrete septin complexes interact with myelin membranes. Septins may form specialized scaffolds in non-compact myelin compartments (Figure 43) and the investigation of these scaffolds might reveal new cytoskeleton interactors in myelinating glia. The difficulties of tackling the septin system are well known. The redundancy among different septins complicates the analysis of septin function tremendously. All attempts to generate null-mutant animals led to very mild impairments with respect to brain development and function (Fujishima et al., 2007; Ihara et al., 2005; Kissel et al., 2005; Ono et al., 2005; Peng et al., 2002). Therefore, in the future, it may be necessary to generate inducible tissue specific mutants to circumvent compensation mechanisms.

In conclusion, septins are very intriguing in their ability to influence all other cytoskeleton systems and to organize membrane structures. Their further study will undoubtly lead to a better understanding how complex membrane structures are building up and maintained in development and in the adult.

9 Outlook

This work was the first comprehensive study of septins in oligodendrocytes and Schwann cells. The data open up new perspectives for future studies on the function of septins in myelin.

First, the expression analysis revealed which septins are expressed in myelinating cells and how they are regulated during differentiation and myelination. These data are important since the knowledge of the exact composition of the septin cortex at a given time point is crucial to understand generated phenotypes or the absence of any effect upon targeting of septins. This study indicates that the septin cortex in myelinating cells might be very robust which might be due to compensation mechanisms among homologous septins. Still, the data presented here provide levers how to overcome this redundancy. In the future, it might be promising to work with double knockouts or perform RNA interference on a double null cell culture system to completely block the expression of septins from a given subgroup. In line with this, it might be interesting to target Sept11 in the Sept6-deficient mouse either by using a Sept11-deficient mouse or by downregulating Sept11 by RNA interference. If this does not produce an effect on myelination the next step would be to target Sept8 on a Sept6/Sept11 double null background since Sept8 might compensate the loss of Sept6/11. These experiments are very complex and time consuming but, still, they might be necessary to circumvent compensation mechanisms as described in this work. Alternatively, it would be interesting to study the effect of downregulating individual septins in the rat myelinating DRG/ Schwann cell co-culture system since those cultures myelinate much more efficiently and quantitatively than the mouse system used here. There, it might be possible to detect and analyze subtle defects of myelination after septin targeting.

Another interesting route will undoubtly be the use of dominant negative septin mutants. Unfortunately, in this study we were not successful using these mutants since the expression level of the retroviral constructs was to low to generate a robust phenotype. Using a stronger promoter, such as the CMV promoter, should overcome this problem. Especially, the use of primary oligodendrocyte cultures might be very promising since these cells differentiate rapidly in culture and a dominant negative phenotype could be analyzed without generating myelin unspecific effects on cytokinesis. Analyzing an impact on the cytoskeleton or the myelin membrane structuring should be straightforward in oligodendrocyte cultures.

In line with this, it would be interesting to generate transgenic animals expressing a dominant negative septin mutant under the control of a myelin promoter like the CNPase promoter or the MAG promoter. This mouse line would start to express the septin mutant after proliferation of the Schwann cells or oligodendrocytes respectively. Therefore, it might be possible to selectively generate a phenotype on myelination or myelin maintenance avoiding unspecific cytokinesis defects.

Another very promising attempt to study septin function in myelinated internodes would be to generate a floxed Sept7 mouse. Then, Schwann cell specific myelin

promoters like the P0 promoter could be used to inactivate Sept7 by Cre recombinase after Schwann cell proliferation and migration. As mentioned, no compensation would be expected since there are no homolog's to Sept7. Additionally, using the established P0-CreERT tamoxifen inducible mouse line, Sept7 could be deleted after myelination has completed and the effect of Sept7 loss could be studied on the mature myelinated internode.

Undoubtly, it is not easy to target the septin cytoskeleton. All attempts to tackle septins by deletion mutants were either lethal or ineffective. Still, targeting septins which are known to be expressed late during differentiation like Sept4 in oligodendrocytes or controlling the timing of interference will lead to insights into septin function in myelinating cells. Septins are very intriguing in terms of their interplay with myelin membranes. Their future analysis will lead to a better understanding how the myelinating cells are able to build up one of the most complex structures in nature, the myelin sheath.

10 References

Agrawal, H.C., B.K. Hartman, W.T. Shearer, S. Kalmbach, and F.L. Margolis. 1977. Purification and immunohistochemical localization of rat brain myelin proteolipid protein. *J Neurochem*. 28:495-508.

Alonso, M.A., and S.M. Weissman. 1987. cDna cloning and sequence of Mal, a hydrophobic protein associated with human T-cell differentiation. *Proc Natl Acad Sci U S A*. 84:1997-2001.

Amin, N.D., Y.L. Zheng, S. Kesavapany, J. Kanungo, T. Guszczynski, R.K. Sihag, P. Rudrabhatla, W. Albers, P. Grant, and H.C. Pant. 2008. Cyclin-dependent kinase 5 phosphorylation of human septin SEPT5 (hCDCrel-1) modulates exocytosis. *J Neurosci*. 28:3631-43.

Anderson, R.G., and K. Jacobson. 2002. A role for lipid shells in targeting proteins to caveolae, rafts, and other lipid domains. *Science*. 296:1821-5.

Arroyo, E.J., and S.S. Scherer. 2000. On the molecular architecture of myelinated fibers. *Histochem Cell Biol*. 113:1-18.

Barman, S., and D.P. Nayak. 2000. Analysis of the transmembrane domain of influenza virus neuraminidase, a type II transmembrane glycoprotein, for apical sorting and raft association. *J Virol*. 74:6538-45.

Barral, Y., and M. Kinoshita. 2008. Structural insights shed light onto septin assemblies and function. *Curr Opin Cell Biol*. 20:12-8.

Barral, Y., V. Mermall, M.S. Mooseker, and M. Snyder. 2000. Compartmentalization of the cell cortex by septins is required for maintenance of cell polarity in yeast. *Mol Cell*. 5:841-51.

Barres, B.A., I.K. Hart, H.S. Coles, J.F. Burne, J.T. Voyvodic, W.D. Richardson, and M.C. Raff. 1992. Cell death and control of cell survival in the oligodendrocyte lineage. *Cell*. 70:31-46.

Barry, C., C. Pearson, and E. Barbarese. 1996. Morphological organization of oligodendrocyte processes during development in culture and in vivo. *Dev Neurosci*. 18:233-42.

Bartsch, S., D. Montag, M. Schachner, and U. Bartsch. 1997. Increased number of unmyelinated axons in optic nerves of adult mice deficient in the myelin-associated glycoprotein (MAG). *Brain Res*. 762:231-4.

Beites, C.L., H. Xie, R. Bowser, and W.S. Trimble. 1999. The septin CDCrel-1 binds syntaxin and inhibits exocytosis. *Nat Neurosci*. 2:434-9.

Benting, J.H., A.G. Rietveld, and K. Simons. 1999. N-Glycans mediate the apical sorting of a GPI-anchored, raft-associated protein in Madin-Darby canine kidney cells. *J Cell Biol*. 146:313-20.

Bhat, M.A., J.C. Rios, Y. Lu, G.P. Garcia-Fresco, W. Ching, M. St Martin, J. Li, S. Einheber, M. Chesler, J. Rosenbluth, J.L. Salzer, and H.J. Bellen. 2001. Axon-glia interactions and the domain organization of myelinated axons requires neurexin IV/Caspr/Paranodin. *Neuron*. 30:369-83.

Black, J.A., and S.G. Waxman. 1988. The perinodal astrocyte. *Glia*. 1:169-83.

Blaser, S., J. Horn, P. Wurmell, H. Bauer, S. Strumpell, P. Nurden, A. Pagenstecher, A. Busse, D. Wunderle, I. Hainmann, and B. Zieger. 2004. The novel human platelet septin SEPT8 is an interaction partner of SEPT4. *Thromb Haemost*. 91:959-66.

Bottenstein, J.E., and G.H. Sato. 1979. Growth of a rat neuroblastoma cell line in serum-free supplemented medium. *Proc Natl Acad Sci U S A*. 76:514-7.

Boyle, M.E., E.O. Berglund, K.K. Murai, L. Weber, E. Peles, and B. Ranscht. 2001. Contactin orchestrates assembly of the septate-like junctions at the paranode in myelinated peripheral nerve. *Neuron*. 30:385-97.

Braestrup, C., and R.F. Squires. 1977. Specific benzodiazepine receptors in rat brain characterized by high-affinity (3H)diazepam binding. *Proc Natl Acad Sci U S A*. 74:3805-9.

Britsch, S., D.E. Goerich, D. Riethmacher, R.I. Peirano, M. Rossner, K.A. Nave, C. Birchmeier, and M. Wegner. 2001. The transcription factor Sox10 is a key regulator of peripheral glial development. *Genes Dev*. 15:66-78.

Brown, D.A., and J.K. Rose. 1992. Sorting of GPI-anchored proteins to glycolipid-enriched membrane subdomains during transport to the apical cell surface. *Cell*. 68:533-44.

Brummelkamp, T.R., R. Bernards, and R. Agami. 2002a. Stable suppression of tumorigenicity by virus-mediated RNA interference. *Cancer Cell*. 2:243-7.

Brummelkamp, T.R., R. Bernards, and R. Agami. 2002b. A system for stable expression of short interfering RNAs in mammalian cells. *Science*. 296:550-3.

Brunner, C., H. Lassmann, T.V. Waehneldt, J.M. Matthieu, and C. Linington. 1989. Differential ultrastructural localization of myelin basic protein, myelin/oligodendroglial glycoprotein, and 2',3'-cyclic nucleotide 3'-phosphodiesterase in the CNS of adult rats. *J Neurochem*. 52:296-304.

Bunge, R.P. 1993. Expanding roles for the Schwann cell: ensheathment, myelination, trophism and regeneration. *Curr Opin Neurobiol*. 3:805-9.

Bunge, R.P., M.B. Bunge, and C.F. Eldridge. 1986. Linkage between axonal ensheathment and basal lamina production by Schwann cells. *Annu Rev Neurosci*. 9:305-28.

Byers, B., and L. Goetsch. 1976. A highly ordered ring of membrane-associated filaments in budding yeast. *J Cell Biol*. 69:717-21.

Cajal, R.y. 1928. Degeneration and Regeneration of the Nervous System. *Oxford University Press*.

Carenini, S., D. Montag, M. Schachner, and R. Martini. 1998. MAG-deficient Schwann cells myelinate dorsal root ganglion neurons in culture. *Glia*. 22:213-20.

Carson, J.H., K. Worboys, K. Ainger, and E. Barbarese. 1997. Translocation of myelin basic protein mRNA in oligodendrocytes requires microtubules and kinesin. *Cell Motil Cytoskeleton*. 38:318-28.

Cheong, K.H., D. Zacchetti, E.E. Schneeberger, and K. Simons. 1999. VIP17/MAL, a lipid raft-associated protein, is involved in apical transport in MDCK cells. *Proc Natl Acad Sci U S A*. 96:6241-8.

Chow, E., J. Mottahedeh, M. Prins, W. Ridder, S. Nusinowitz, and J.M. Bronstein. 2005. Disrupted compaction of CNS myelin in an OSP/Claudin-11 and PLP/DM20 double knockout mouse. *Mol Cell Neurosci*. 29:405-13.

Court, F.A., D.L. Sherman, T. Pratt, E.M. Garry, R.R. Ribchester, D.F. Cottrell, S.M. Fleetwood-Walker, and P.J. Brophy. 2004. Restricted growth of Schwann cells lacking Cajal bands slows conduction in myelinated nerves. *Nature*. 431:191-5.

Delarasse, C., P. Daubas, L.T. Mars, C. Vizler, T. Litzenburger, A. Iglesias, J. Bauer, B. Della Gaspera, A. Schubart, L. Decker, D. Dimitri, G. Roussel, A. Dierich, S. Amor, A. Dautigny, R. Liblau, and D. Pham-Dinh. 2003. Myelin/oligodendrocyte glycoprotein-deficient (MOG-deficient) mice reveal lack of immune tolerance to MOG in wild-type mice. *J Clin Invest*. 112:544-53.

della Gaspera, B., D. Pham-Dinh, G. Roussel, J.L. Nussbaum, and A. Dautigny. 1998. Membrane topology of the myelin/oligodendrocyte glycoprotein. *Eur J Biochem*. 258:478-84.

DeMarini, D.J., A.E. Adams, H. Fares, C. De Virgilio, G. Valle, J.S. Chuang, and J.R. Pringle. 1997. A septin-based hierarchy of proteins required for localized deposition of chitin in the Saccharomyces cerevisiae cell wall. *J Cell Biol*. 139:75-93.

Devor, M., R. Govrin-Lippmann, and K. Angelides. 1993. Na+ channel immunolocalization in peripheral mammalian axons and changes following nerve injury and neuroma formation. *J Neurosci*. 13:1976-92.

Dyer, C.A. 1993. Novel oligodendrocyte transmembrane signaling systems. Investigations utilizing antibodies as ligands. *Mol Neurobiol*. 7:1-22.

Dyer, C.A., and J.A. Benjamins. 1989a. Organization of oligodendroglial membrane sheets. I: Association of myelin basic protein and 2',3'-cyclic nucleotide 3'-phosphohydrolase with cytoskeleton. *J Neurosci Res*. 24:201-11.

Dyer, C.A., and J.A. Benjamins. 1989b. Organization of oligodendroglial membrane sheets: II. Galactocerebroside:antibody interactions signal changes in cytoskeleton and myelin basic protein. *J Neurosci Res*. 24:212-21.

Dyer, C.A., and J.A. Benjamins. 1990. Glycolipids and transmembrane signaling: antibodies to galactocerebroside cause an influx of calcium in oligodendrocytes. *J Cell Biol*. 111:625-33.

Dyer, C.A., and J.M. Matthieu. 1994. Antibodies to myelin/oligodendrocyte-specific protein and myelin/oligodendrocyte glycoprotein signal distinct changes in the organization of cultured oligodendroglial membrane sheets. *J Neurochem*. 62:777-87.

Dyer, C.A., T. Phillbotte, M.K. Wolf, and S. Billings-Gagliardi. 1997. Regulation of cytoskeleton by myelin components: studies on shiverer oligodendrocytes carrying an Mbp transgene. *Dev Neurosci*. 19:395-409.

Einarson, B., W. Gullick, B. Conti-Tronconi, M. Ellisman, and J. Lindstrom. 1982. Subunit composition of bovine muscle acetylcholine receptor. *Biochemistry*. 21:5295-302.

Eldridge, C.F., M.B. Bunge, R.P. Bunge, and P.M. Wood. 1987. Differentiation of axon-related Schwann cells in vitro. I. Ascorbic acid regulates basal lamina assembly and myelin formation. *J Cell Biol*. 105:1023-34.

Ellisman, M.H., and S.R. Levinson. 1982. Immunocytochemical localization of sodium channel distributions in the excitable membranes of Electrophorus electricus. *Proc Natl Acad Sci U S A*. 79:6707-11.

Erb, M., B. Flueck, F. Kern, B. Erne, A.J. Steck, and N. Schaeren-Wiemers. 2006. Unraveling the differential expression of the two isoforms of myelin-associated glycoprotein in a mouse expressing GFP-tagged S-MAG specifically regulated and targeted into the different myelin compartments. *Mol Cell Neurosci*. 31:613-27.

Erne, B., S. Sansano, M. Frank, and N. Schaeren-Wiemers. 2002. Rafts in adult peripheral nerve myelin contain major structural myelin proteins and myelin and lymphocyte protein (MAL) and CD59 as specific markers. *J Neurochem*. 82:550-62.

Eshed, Y., K. Feinberg, S. Poliak, H. Sabanay, O. Sarig-Nadir, I. Spiegel, J.R. Bermingham, Jr., and E. Peles. 2005. Gliomedin mediates Schwann cell-axon interaction and the molecular assembly of the nodes of Ranvier. *Neuron*. 47:215-29.

Fanarraga, M.L., I.R. Griffiths, M. Zhao, and I.D. Duncan. 1998. Oligodendrocytes are not inherently programmed to myelinate a specific size of axon. *J Comp Neurol*. 399:94-100.

Fawcett, J.W., and R.J. Keynes. 1990. Peripheral nerve regeneration. *Annu Rev Neurosci*. 13:43-60.

Field, C.M., O. al-Awar, J. Rosenblatt, M.L. Wong, B. Alberts, and T.J. Mitchison. 1996. A purified Drosophila septin complex forms filaments and exhibits GTPase activity. *J Cell Biol*. 133:605-16.

Field, C.M., and D. Kellogg. 1999. Septins: cytoskeletal polymers or signalling GTPases? *Trends Cell Biol*. 9:387-94.

Ford, S.K., and J.R. Pringle. 1991. Cellular morphogenesis in the Saccharomyces cerevisiae cell cycle: localization of the CDC11 gene product and the timing of events at the budding site. *Dev Genet*. 12:281-92.

Frank, M. 2000. MAL, a proteolipid in glycosphingolipid enriched domains: functional implications in myelin and beyond. *Prog Neurobiol*. 60:531-44.

Frank, M., S. Atanasoski, S. Sancho, J.P. Magyar, T. Ruelicke, M.E. Schwab, and U. Suter. 2000. Progressive segregation of unmyelinated axons in peripheral nerves, myelin alterations in the CNS, and cyst formation in the kidneys of myelin and lymphocyte protein-overexpressing mice. *J Neurochem*. 75:1927-39.

Frank, M., N. Schaeren-Wiemers, R. Schneider, and M.E. Schwab. 1999. Developmental expression pattern of the myelin proteolipid MAL indicates different functions of MAL for immature Schwann cells and in a late step of CNS myelinogenesis. *J Neurochem*. 73:587-97.

Frank, M., M.E. van der Haar, N. Schaeren-Wiemers, and M.E. Schwab. 1998. rMAL is a glycosphingolipid-associated protein of myelin and apical membranes of epithelial cells in kidney and stomach. *J Neurosci*. 18:4901-13.

Franzen, R., S.L. Tanner, S.M. Dashiell, C.A. Rottkamp, J.A. Hammer, and R.H. Quarles. 2001. Microtubule-associated protein 1B: a neuronal binding partner for myelin-associated glycoprotein. *J Cell Biol*. 155:893-8.

Frazier, J.A., M.L. Wong, M.S. Longtine, J.R. Pringle, M. Mann, T.J. Mitchison, and C. Field. 1998. Polymerization of purified yeast septins: evidence that organized filament arrays may not be required for septin function. *J Cell Biol*. 143:737-49.

Fujishima, K., H. Kiyonari, J. Kurisu, T. Hirano, and M. Kengaku. 2007. Targeted disruption of Sept3, a heteromeric assembly partner of Sept5 and Sept7 in axons, has no effect on developing CNS neurons. *J Neurochem*. 102:77-92.

Garbern, J.Y., F. Cambi, R. Lewis, M. Shy, A. Sima, G. Kraft, J.M. Vallat, E.P. Bosch, M.E. Hodes, S. Dlouhy, W. Raskind, T. Bird, W. Macklin, and J. Kamholz. 1999. Peripheral neuropathy caused by proteolipid protein gene mutations. *Ann N Y Acad Sci*. 883:351-65.

Garratt, A.N., S. Britsch, and C. Birchmeier. 2000. Neuregulin, a factor with many functions in the life of a schwann cell. *Bioessays*. 22:987-96.

Ghitescu, L., A. Fixman, M. Simionescu, and N. Simionescu. 1986. Specific binding sites for albumin restricted to plasmalemmal vesicles of continuous capillary endothelium: receptor-mediated transcytosis. *J Cell Biol*. 102:1304-11.

Greenfield, S., S. Brostoff, E.H. Eylar, and P. Morell. 1973. Protein composition of myelin of the peripheral nervous system. *J Neurochem*. 20:1207-16.

Haarer, B.K., and J.R. Pringle. 1987. Immunofluorescence localization of the Saccharomyces cerevisiae CDC12 gene product to the vicinity of the 10-nm filaments in the mother-bud neck. *Mol Cell Biol*. 7:3678-87.

Hall, P.A., K. Jung, K.J. Hillan, and S.E. Russell. 2005. Expression profiling the human septin gene family. *J Pathol*. 206:269-78.

Hall, P.A., and S.E. Russell. 2004. The pathobiology of the septin gene family. *J Pathol*. 204:489-505.

Hartman, B.K., H.C. Agrawal, D. Agrawal, and S. Kalmbach. 1982. Development and maturation of central nervous system myelin: comparison of immunohistochemical localization of proteolipid protein and basic protein in myelin and oligodendrocytes. *Proc Natl Acad Sci U S A*. 79:4217-20.

Hartwell, L.H. 1971. Genetic control of the cell division cycle in yeast. IV. Genes controlling bud emergence and cytokinesis. *Exp Cell Res*. 69:265-76.

Hazuka, C.D., D.L. Foletti, S.C. Hsu, Y. Kee, F.W. Hopf, and R.H. Scheller. 1999. The sec6/8 complex is located at neurite outgrowth and axonal synapse-assembly domains. *J Neurosci*. 19:1324-34.

Hirokawa, N. 1998. Kinesin and dynein superfamily proteins and the mechanism of organelle transport. *Science*. 279:519-26.

Hjelmstrom, P., J.E. Penzotti, R.M. Henne, and T.P. Lybrand. 1998. A molecular model of myelin oligodendrocyte glycoprotein. *J Neurochem*. 71:1742-9.

Howe, J.R., and J.M. Ritchie. 1990. Sodium currents in Schwann cells from myelinated and non-myelinated nerves of neonatal and adult rabbits. *J Physiol*. 425:169-210.

Hsu, S.C., C.D. Hazuka, D.L. Foletti, and R.H. Scheller. 1999. Targeting vesicles to specific sites on the plasma membrane: the role of the sec6/8 complex. *Trends Cell Biol*. 9:150-3.

Hsu, S.C., C.D. Hazuka, R. Roth, D.L. Foletti, J. Heuser, and R.H. Scheller. 1998. Subunit composition, protein interactions, and structures of the mammalian brain sec6/8 complex and septin filaments. *Neuron*. 20:1111-22.

Ichimura, T., and M.H. Ellisman. 1991. Three-dimensional fine structure of cytoskeletal-membrane interactions at nodes of Ranvier. *J Neurocytol*. 20:667-81.

Ihara, M., A. Kinoshita, S. Yamada, H. Tanaka, A. Tanigaki, A. Kitano, M. Goto, K. Okubo, H. Nishiyama, O. Ogawa, C. Takahashi, S. Itohara, Y. Nishimune, M. Noda, and M. Kinoshita. 2005. Cortical organization by the septin cytoskeleton is essential for structural and mechanical integrity of mammalian spermatozoa. *Dev Cell*. 8:343-52.

Jessen, K.R., A. Brennan, L. Morgan, R. Mirsky, A. Kent, Y. Hashimoto, and J. Gavrilovic. 1994. The Schwann cell precursor and its fate: a study of cell death and differentiation during gliogenesis in rat embryonic nerves. *Neuron*. 12:509-27.

Jessen, K.R., and R. Mirsky. 1999. Schwann cells and their precursors emerge as major regulators of nerve development. *Trends Neurosci*. 22:402-10.

John, C.M., R.K. Hite, C.S. Weirich, D.J. Fitzgerald, H. Jawhari, M. Faty, D. Schlapfer, R. Kroschewski, F.K. Winkler, T. Walz, Y. Barral, and M.O. Steinmetz. 2007. The Caenorhabditis elegans septin complex is nonpolar. *Embo J*. 26:3296-307.

Kamal, A., and L.S. Goldstein. 2000. Connecting vesicle transport to the cytoskeleton. *Curr Opin Cell Biol*. 12:503-8.

Kartmann, B., and D. Roth. 2001. Novel roles for mammalian septins: from vesicle trafficking to oncogenesis. *J Cell Sci*. 114:839-44.

Kidd, G.J., S.B. Andrews, and B.D. Trapp. 1994. Organization of microtubules in myelinating Schwann cells. *J Neurocytol*. 23:801-10.

Kim, H.B., B.K. Haarer, and J.R. Pringle. 1991. Cellular morphogenesis in the Saccharomyces cerevisiae cell cycle: localization of the CDC3 gene product and the timing of events at the budding site. *J Cell Biol*. 112:535-44.

Kim, T., K. Fiedler, D.L. Madison, W.H. Krueger, and S.E. Pfeiffer. 1995. Cloning and characterization of MVP17: a developmentally regulated myelin protein in oligodendrocytes. *J Neurosci Res*. 42:413-22.

Kim, T., and S.E. Pfeiffer. 1999. Myelin glycosphingolipid/cholesterol-enriched microdomains selectively sequester the non-compact myelin proteins CNP and MOG. *J Neurocytol*. 28:281-93.

Kinoshita, M. 2003a. Assembly of mammalian septins. *J Biochem (Tokyo)*. 134:491-6.

Kinoshita, M. 2003b. The septins. *Genome Biol*. 4:236.

Kinoshita, M. 2006. Diversity of septin scaffolds. *Curr Opin Cell Biol*. 18:54-60.

Kinoshita, M., C.M. Field, M.L. Coughlin, A.F. Straight, and T.J. Mitchison. 2002. Self- and actin-templated assembly of Mammalian septins. *Dev Cell*. 3:791-802.

Kinoshita, M., S. Kumar, A. Mizoguchi, C. Ide, A. Kinoshita, T. Haraguchi, Y. Hiraoka, and M. Noda. 1997. Nedd5, a mammalian septin, is a novel cytoskeletal component interacting with actin-based structures. *Genes Dev*. 11:1535-47.

Kinoshita, N., K. Kimura, N. Matsumoto, M. Watanabe, M. Fukaya, and C. Ide. 2004. Mammalian septin Sept2 modulates the activity of GLAST, a glutamate transporter in astrocytes. *Genes Cells*. 9:1-14.

Kirschner, D.A., and A.L. Ganser. 1980. Compact myelin exists in the absence of basic protein in the shiverer mutant mouse. *Nature*. 283:207-10.

Kissel, H., M.M. Georgescu, S. Larisch, K. Manova, G.R. Hunnicutt, and H. Steller. 2005. The Sept4 septin locus is required for sperm terminal differentiation in mice. *Dev Cell*. 8:353-64.

Kondo, T., and M. Raff. 2000. Oligodendrocyte precursor cells reprogrammed to become multipotential CNS stem cells. *Science*. 289:1754-7.

Kordeli, E., J. Davis, B. Trapp, and V. Bennett. 1990. An isoform of ankyrin is localized at nodes of Ranvier in myelinated axons of central and peripheral nerves. *J Cell Biol*. 110:1341-52.

Kremer, B.E., T. Haystead, and I.G. Macara. 2005. Mammalian septins regulate microtubule stability through interaction with the microtubule-binding protein MAP4. *Mol Biol Cell*. 16:4648-59.

Kroepfl, J.F., and M.V. Gardinier. 2001. Identification of a basolateral membrane targeting signal within the cytoplasmic domain of myelin/oligodendrocyte glycoprotein. *J Neurochem*. 77:1301-9.

Kroepfl, J.F., L.R. Viise, A.J. Charron, C. Linington, and M.V. Gardinier. 1996. Investigation of myelin/oligodendrocyte glycoprotein membrane topology. *J Neurochem*. 67:2219-22.

Kuhlenbaumer, G., M.C. Hannibal, E. Nelis, A. Schirmacher, N. Verpoorten, J. Meuleman, G.D. Watts, E. De Vriendt, P. Young, F. Stogbauer, H. Halfter, J. Irobi, D. Goossens, J. Del-Favero, B.G. Betz, H. Hor, G. Kurlemann, T.D. Bird, E. Airaksinen, T. Mononen, A.P. Serradell, J.M. Prats, C. Van Broeckhoven, P. De Jonghe, V. Timmerman, E.B. Ringelstein, and P.F. Chance. 2005. Mutations in SEPT9 cause hereditary neuralgic amyotrophy. *Nat Genet*. 37:1044-6.

Kursula, P., V.P. Lehto, and A.M. Heape. 2001. The small myelin-associated glycoprotein binds to tubulin and microtubules. *Brain Res Mol Brain Res*. 87:22-30.

Kusumi, A., and Y. Sako. 1996. Cell surface organization by the membrane skeleton. *Curr Opin Cell Biol*. 8:566-74.

Li, C., M.B. Tropak, R. Gerlai, S. Clapoff, W. Abramow-Newerly, B. Trapp, A. Peterson, and J. Roder. 1994. Myelination in the absence of myelin-associated glycoprotein. *Nature*. 369:747-50.

Linington, C., S. Izumo, M. Suzuki, K. Uyemura, R. Meyermann, and H. Wekerle. 1984. A permanent rat T cell line that mediates experimental allergic neuritis in the Lewis rat in vivo. *J Immunol*. 133:1946-50.

Lisanti, M.P., Z. Tang, P.E. Scherer, E. Kubler, A.J. Koleske, and M. Sargiacomo. 1995. Caveolae, transmembrane signalling and cellular transformation. *Mol Membr Biol*. 12:121-4.

Longtine, M.S., D.J. DeMarini, M.L. Valencik, O.S. Al-Awar, H. Fares, C. De Virgilio, and J.R. Pringle. 1996. The septins: roles in cytokinesis and other processes. *Curr Opin Cell Biol*. 8:106-19.

Luedeke, C., S.B. Frei, I. Sbalzarini, H. Schwarz, A. Spang, and Y. Barral. 2005. Septin-dependent compartmentalization of the endoplasmic reticulum during yeast polarized growth. *J Cell Biol*. 169:897-908.

Lunn, K.F., P.W. Baas, and I.D. Duncan. 1997. Microtubule organization and stability in the oligodendrocyte. *J Neurosci*. 17:4921-32.

Magyar, J.P., C. Ebensperger, N. Schaeren-Wiemers, and U. Suter. 1997. Myelin and lymphocyte protein (MAL/MVP17/VIP17) and plasmolipin are members of an extended gene family. *Gene*. 189:269-75.

Martin-Belmonte, F., L. Kremer, J.P. Albar, M. Marazuela, and M.A. Alonso. 1998. Expression of the MAL gene in the thyroid: the MAL proteolipid, a component of glycolipid-enriched membranes, is apically distributed in thyroid follicles. *Endocrinology*. 139:2077-84.

Martin-Belmonte, F., R. Puertollano, J. Millan, and M.A. Alonso. 2000. The MAL proteolipid is necessary for the overall apical delivery of membrane proteins in the polarized epithelial Madin-Darby canine kidney and fischer rat thyroid cell lines. *Mol Biol Cell*. 11:2033-45.

Martin, S.W., and J.B. Konopka. 2004. Lipid raft polarization contributes to hyphal growth in Candida albicans. *Eukaryot Cell*. 3:675-84.

Martinez, C., and J. Ware. 2004. Mammalian septin function in hemostasis and beyond. *Exp Biol Med (Maywood)*. 229:1111-9.

Matter, K., and I. Mellman. 1994. Mechanisms of cell polarity: sorting and transport in epithelial cells. *Curr Opin Cell Biol*. 6:545-54.

Meier, C., E. Parmantier, A. Brennan, R. Mirsky, and K.R. Jessen. 1999. Developing Schwann cells acquire the ability to survive without axons by establishing an autocrine circuit involving insulin-like growth factor, neurotrophin-3, and platelet-derived growth factor-BB. *J Neurosci*. 19:3847-59.

Mesleh, M.F., N. Belmar, C.W. Lu, V.V. Krishnan, R.S. Maxwell, C.P. Genain, and M. Cosman. 2002. Marmoset fine B cell and T cell epitope specificities mapped onto a homology model of the extracellular domain of human myelin oligodendrocyte glycoprotein. *Neurobiol Dis*. 9:160-72.

Millan, J., R. Puertollano, L. Fan, C. Rancano, and M.A. Alonso. 1997. The MAL proteolipid is a component of the detergent-insoluble membrane subdomains of human T-lymphocytes. *Biochem J*. 321 (Pt 1):247-52.

Minuk, J., and P.E. Braun. 1996. Differential intracellular sorting of the myelin-associated glycoprotein isoforms. *J Neurosci Res*. 44:411-20.

Mitic, L.L., and J.M. Anderson. 1998. Molecular architecture of tight junctions. *Annu Rev Physiol*. 60:121-42.

Montag, D., K.P. Giese, U. Bartsch, R. Martini, Y. Lang, H. Bluthmann, J. Karthigasan, D.A. Kirschner, E.S. Wintergerst, K.A. Nave, and et al. 1994. Mice deficient for the myelin-associated glycoprotein show subtle abnormalities in myelin. *Neuron*. 13:229-46.

Mostov, K., G. Apodaca, B. Aroeti, and C. Okamoto. 1992. Plasma membrane protein sorting in polarized epithelial cells. *J Cell Biol*. 116:577-83.

Munro, S. 2003. Lipid rafts: elusive or illusive? *Cell*. 115:377-88.
Nagarajan, R., J. Svaren, N. Le, T. Araki, M. Watson, and J. Milbrandt. 2001. EGR2 mutations in inherited neuropathies dominant-negatively inhibit myelin gene expression. *Neuron*. 30:355-68.
Nagata, K., T. Asano, Y. Nozawa, and M. Inagaki. 2004. Biochemical and cell biological analyses of a mammalian septin complex, Sept7/9b/11. *J Biol Chem*. 279:55895-904.
Nakatsuru, S., K. Sudo, and Y. Nakamura. 1994. Molecular cloning of a novel human cDNA homologous to CDC10 in Saccharomyces cerevisiae. *Biochem Biophys Res Commun*. 202:82-7.
Nave, K.A., and J.L. Salzer. 2006. Axonal regulation of myelination by neuregulin 1. *Curr Opin Neurobiol*. 16:492-500.
Neufeld, T.P., and G.M. Rubin. 1994. The Drosophila peanut gene is required for cytokinesis and encodes a protein similar to yeast putative bud neck filament proteins. *Cell*. 77:371-9.
Niggli, V., and M.M. Burger. 1987. Interaction of the cytoskeleton with the plasma membrane. *J Membr Biol*. 100:97-121.
NIGMS. 2005. Inside the cell.
Nottenburg, C., W.M. Gallatin, and T. St John. 1990. Lymphocyte HEV adhesion variants differ in the expression of multiple gene sequences. *Gene*. 95:279-84.
Omlin, F.X., H.D. Webster, C.G. Palkovits, and S.R. Cohen. 1982. Immunocytochemical localization of basic protein in major dense line regions of central and peripheral myelin. *J Cell Biol*. 95:242-8.
Ono, R., M. Ihara, H. Nakajima, K. Ozaki, Y. Kataoka-Fujiwara, T. Taki, K. Nagata, M. Inagaki, N. Yoshida, T. Kitamura, Y. Hayashi, M. Kinoshita, and T. Nosaka. 2005. Disruption of Sept6, a fusion partner gene of MLL, does not affect ontogeny, leukemogenesis induced by MLL-SEPT6, or phenotype induced by the loss of Sept4. *Mol Cell Biol*. 25:10965-78.
Pan, F., R.L. Malmberg, and M. Momany. 2007. Analysis of septins across kingdoms reveals orthology and new motifs. *BMC Evol Biol*. 7:103.
Parkinson, D.B., K. Langner, S.S. Namini, K.R. Jessen, and R. Mirsky. 2002. beta-Neuregulin and autocrine mediated survival of Schwann cells requires activity of Ets family transcription factors. *Mol Cell Neurosci*. 20:154-67.
Pedraza, C.E., M. R., Q. Hao, and W.B. Macklin. 2008. Production, characterization and efficient transfection of highly pure oligodendrocyte precursor cultures from mouse embryonic neural progenitors. *Glia*. in press.
Peng, X.R., Z. Jia, Y. Zhang, J. Ware, and W.S. Trimble. 2002. The septin CDCrel-1 is dispensable for normal development and neurotransmitter release. *Mol Cell Biol*. 22:378-87.
Pfeiffer, S.E., A.E. Warrington, and R. Bansal. 1993. The oligodendrocyte and its many cellular processes. *Trends Cell Biol*. 3:191-7.
Pike, L.J. 2006. Rafts defined: a report on the Keystone symposium on lipid rafts and cell function. *Journal of Lipid Research*. 47.
Poliak, S., and E. Peles. 2003. The local differentiation of myelinated axons at nodes of Ranvier. *Nat Rev Neurosci*. 4:968-80.
Pringle, N.P., H.S. Mudhar, E.J. Collarini, and W.D. Richardson. 1992. PDGF receptors in the rat CNS: during late neurogenesis, PDGF alpha-receptor expression appears to be restricted to glial cells of the oligodendrocyte lineage. *Development*. 115:535-51.
Puertollano, R., S. Li, M.P. Lisanti, and M.A. Alonso. 1997. Recombinant expression of the MAL proteolipid, a component of glycolipid-enriched membrane

microdomains, induces the formation of vesicular structures in insect cells. *J Biol Chem*. 272:18311-5.
Quarles, R.H. 1983. Myelin-associated glycoprotein in development and disease. *Dev Neurosci*. 6:285-303.
Raff, M.C., R. Mirsky, K.L. Fields, R.P. Lisak, S.H. Dorfman, D.H. Silberberg, N.A. Gregson, S. Leibowitz, and M.C. Kennedy. 1978. Galactocerebroside is a specific cell-surface antigenic marker for oligodendrocytes in culture. *Nature*. 274:813-6.
Raff, M.C., B.P. Williams, and R.H. Miller. 1984. The in vitro differentiation of a bipotential glial progenitor cell. *Embo J*. 3:1857-64.
Raine, C.S. 1982. Differences between the nodes of Ranvier of large and small diameter fibres in the P.N.S. *J Neurocytol*. 11:935-47.
Rasband, M.N., J.S. Trimmer, T.L. Schwarz, S.R. Levinson, M.H. Ellisman, M. Schachner, and P. Shrager. 1998. Potassium channel distribution, clustering, and function in remyelinating rat axons. *J Neurosci*. 18:36-47.
Revel, J.P., and D.W. Hamilton. 1969. The double nature of the intermediate dense line in peripheral nerve myelin. *Anat Rec*. 163:7-15.
Richter-Landsberg, C., and M. Gorath. 1999. Developmental regulation of alternatively spliced isoforms of mRNA encoding MAP2 and tau in rat brain oligodendrocytes during culture maturation. *J Neurosci Res*. 56:259-70.
Riethmacher, D., E. Sonnenberg-Riethmacher, V. Brinkmann, T. Yamaai, G.R. Lewin, and C. Birchmeier. 1997. Severe neuropathies in mice with targeted mutations in the ErbB3 receptor. *Nature*. 389:725-30.
Rios, J.C., M. Rubin, M. St Martin, R.T. Downey, S. Einheber, J. Rosenbluth, S.R. Levinson, M. Bhat, and J.L. Salzer. 2003. Paranodal interactions regulate expression of sodium channel subtypes and provide a diffusion barrier for the node of Ranvier. *J Neurosci*. 23:7001-11.
Rodal, A.A., L. Kozubowski, B.L. Goode, D.G. Drubin, and J.H. Hartwig. 2005. Actin and septin ultrastructures at the budding yeast cell cortex. *Mol Biol Cell*. 16:372-84.
Rodriguez-Boulan, E., and A. Gonzalez. 1999. Glycans in post-Golgi apical targeting: sorting signals or structural props? *Trends Cell Biol*. 9:291-4.
Rosenbluth, J., J.L. Dupree, and B. Popko. 2003. Nodal sodium channel domain integrity depends on the conformation of the paranodal junction, not on the presence of transverse bands. *Glia*. 41:318-25.
Roth, A.D. 2006. New ovservations on the compact myelin proteome. *Neuron Glia Biology*. 2:15-21.
Salzer, J.L. 2003. Polarized domains of myelinated axons. *Neuron*. 40:297-318.
Saraste, M., P.R. Sibbald, and A. Wittinghofer. 1990. The P-loop--a common motif in ATP- and GTP-binding proteins. *Trends Biochem Sci*. 15:430-4.
Schachner, M., and R. Martini. 1995. Glycans and the modulation of neural-recognition molecule function. *Trends Neurosci*. 18:183-91.
Schaeren-Wiemers, N., A. Bonnet, M. Erb, B. Erne, U. Bartsch, F. Kern, N. Mantei, D. Sherman, and U. Suter. 2004. The raft-associated protein MAL is required for maintenance of proper axon--glia interactions in the central nervous system. *J Cell Biol*. 166:731-42.
Schaeren-Wiemers, N., D.M. Valenzuela, M. Frank, and M.E. Schwab. 1995. Characterization of a rat gene, rMAL, encoding a protein with four hydrophobic domains in central and peripheral myelin. *J Neurosci*. 15:5753-64.
Scherer, S.S. 1996. Molecular specializations at nodes and paranodes in peripheral nerve. *Microsc Res Tech*. 34:452-61.

Schmidt, K., and B.J. Nichols. 2004. Functional interdependence between septin and actin cytoskeleton. *BMC Cell Biol*. 5:43.

Scolding, N.J., S. Frith, C. Linington, B.P. Morgan, A.K. Campbell, and D.A. Compston. 1989. Myelin-oligodendrocyte glycoprotein (MOG) is a surface marker of oligodendrocyte maturation. *J Neuroimmunol*. 22:169-76.

Shapiro, L., J.P. Doyle, P. Hensley, D.R. Colman, and W.A. Hendrickson. 1996. Crystal structure of the extracellular domain from P0, the major structural protein of peripheral nerve myelin. *Neuron*. 17:435-49.

Sheffield, P.J., C.J. Oliver, B.E. Kremer, S. Sheng, Z. Shao, and I.G. Macara. 2003. Borg/septin interactions and the assembly of mammalian septin heterodimers, trimers, and filaments. *J Biol Chem*. 278:3483-8.

Simons, K., and E. Ikonen. 1997. Functional rafts in cell membranes. *Nature*. 387:569-72.

Simons, M., E.M. Kramer, C. Thiele, W. Stoffel, and J. Trotter. 2000. Assembly of myelin by association of proteolipid protein with cholesterol- and galactosylceramide-rich membrane domains. *J Cell Biol*. 151:143-54.

Simpson, P.B., and R.C. Armstrong. 1999. Intracellular signals and cytoskeletal elements involved in oligodendrocyte progenitor migration. *Glia*. 26:22-35.

Singer, S.J., and G.L. Nicolson. 1972. The fluid mosaic model of the structure of cell membranes. *Science*. 175:720-31.

Sirajuddin, M., M. Farkasovsky, F. Hauer, D. Kuhlmann, I.G. Macara, M. Weyand, H. Stark, and A. Wittinghofer. 2007. Structural insight into filament formation by mammalian septins. *Nature*. 449:311-5.

Sollner, T., S.W. Whiteheart, M. Brunner, H. Erdjument-Bromage, S. Geromanos, P. Tempst, and J.E. Rothman. 1993. SNAP receptors implicated in vesicle targeting and fusion. *Nature*. 362:318-24.

Song, J., B.D. Goetz, P.W. Baas, and I.D. Duncan. 2001. Cytoskeletal reorganization during the formation of oligodendrocyte processes and branches. *Mol Cell Neurosci*. 17:624-36.

Squires, R.F., and C. Brastrup. 1977. Benzodiazepine receptors in rat brain. *Nature*. 266:732-4.

Sternberger, N.H., R.H. Quarles, Y. Itoyama, and H.D. Webster. 1979. Myelin-associated glycoprotein demonstrated immunocytochemically in myelin and myelin-forming cells of developing rat. *Proc Natl Acad Sci U S A*. 76:1510-4.

Stossel, T.P. 1982. The structure of cortical cytoplasm. *Philos Trans R Soc Lond B Biol Sci*. 299:275-89.

Surka, M.C., C.W. Tsang, and W.S. Trimble. 2002. The mammalian septin MSF localizes with microtubules and is required for completion of cytokinesis. *Mol Biol Cell*. 13:3532-45.

Tada, T., A. Simonetta, M. Batterton, M. Kinoshita, D. Edbauer, and M. Sheng. 2007. Role of Septin cytoskeleton in spine morphogenesis and dendrite development in neurons. *Curr Biol*. 17:1752-8.

Takahashi, N., A. Roach, D.B. Teplow, S.B. Prusiner, and L. Hood. 1985. Cloning and characterization of the myelin basic protein gene from mouse: one gene can encode both 14 kd and 18.5 kd MBPs by alternate use of exons. *Cell*. 42:139-48.

Takizawa, P.A., J.L. DeRisi, J.E. Wilhelm, and R.D. Vale. 2000. Plasma membrane compartmentalization in yeast by messenger RNA transport and a septin diffusion barrier. *Science*. 290:341-4.

Taylor, C.M., C.B. Marta, R.J. Claycomb, D.K. Han, M.N. Rasband, T. Coetzee, and S.E. Pfeiffer. 2004. Proteomic mapping provides powerful insights into functional myelin biology. *Proc Natl Acad Sci U S A*. 101:4643-8.

Tran, D., J.L. Carpentier, F. Sawano, P. Gorden, and L. Orci. 1987. Ligands internalized through coated or noncoated invaginations follow a common intracellular pathway. *Proc Natl Acad Sci U S A*. 84:7957-61.

Trapp, B.D., S.B. Andrews, A. Wong, M. O'Connell, and J.W. Griffin. 1989. Co-localization of the myelin-associated glycoprotein and the microfilament components, F-actin and spectrin, in Schwann cells of myelinated nerve fibres. *J Neurocytol*. 18:47-60.

Trapp, B.D., G.J. Kidd, P. Hauer, E. Mulrenin, C.A. Haney, and S.B. Andrews. 1995. Polarization of myelinating Schwann cell surface membranes: role of microtubules and the trans-Golgi network. *J Neurosci*. 15:1797-807.

Trapp, B.D., T. Moench, M. Pulley, E. Barbosa, G. Tennekoon, and J. Griffin. 1987. Spatial segregation of mRNA encoding myelin-specific proteins. *Proc Natl Acad Sci U S A*. 84:7773-7.

Trapp, B.D., A. Nishiyama, D. Cheng, and W. Macklin. 1997. Differentiation and death of premyelinating oligodendrocytes in developing rodent brain. *J Cell Biol*. 137:459-68.

Trapp, B.D., R.H. Quarles, and K. Suzuki. 1984. Immunocytochemical studies of quaking mice support a role for the myelin-associated glycoprotein in forming and maintaining the periaxonal space and periaxonal cytoplasmic collar of myelinating Schwann cells. *J Cell Biol*. 99:594-606.

Trotter, J.L., L. Lieberman, F.L. Margolis, and H.C. Agrawal. 1981. Radioimmunoassay for central nervous system myelin-specific proteolipid protein. *J Neurochem*. 36:1256-62.

Vallen, E.A., J. Caviston, and E. Bi. 2000. Roles of Hof1p, Bni1p, Bnr1p, and myo1p in cytokinesis in Saccharomyces cerevisiae. *Mol Biol Cell*. 11:593-611.

van Meer, G. 1989. Lipid traffic in animal cells. *Annu Rev Cell Biol*. 5:247-75.

van Meer, G., and K. Simons. 1988. Lipid polarity and sorting in epithelial cells. *J Cell Biochem*. 36:51-8.

Vega, I.E., and S.C. Hsu. 2003. The septin protein Nedd5 associates with both the exocyst complex and microtubules and disruption of its GTPase activity promotes aberrant neurite sprouting in PC12 cells. *Neuroreport*. 14:31-7.

Warf, B.C., J. Fok-Seang, and R.H. Miller. 1991. Evidence for the ventral origin of oligodendrocyte precursors in the rat spinal cord. *J Neurosci*. 11:2477-88.

Waxman, S.G. 1980. Determinants of conduction velocity in myelinated nerve fibers. *Muscle Nerve*. 3:141-50.

Waxman, S.G., and J.M. Ritchie. 1993. Molecular dissection of the myelinated axon. *Ann Neurol*. 33:121-36.

Weber, I., J. Niewohner, and J. Faix. 1999. Cytoskeletal protein mutations and cell motility in Dictyostelium. *Biochem Soc Symp*. 65:245-65.

Weimbs, T., S.H. Low, S.J. Chapin, and K.E. Mostov. 1997. Apical targeting in polarized epithelial cells: There's more afloat than rafts. *Trends Cell Biol*. 7:393-9.

Werner, H.B., K. Kuhlmann, S. Shen, M. Uecker, A. Schardt, K. Dimova, F. Orfaniotou, A. Dhaunchak, B.G. Brinkmann, W. Mobius, L. Guarente, P. Casaccia-Bonnefil, O. Jahn, and K.A. Nave. 2007. Proteolipid protein is required for transport of sirtuin 2 into CNS myelin. *J Neurosci*. 27:7717-30.

Wight, P.A., C.S. Duchala, C. Readhead, and W.B. Macklin. 1993. A myelin proteolipid protein-LacZ fusion protein is developmentally regulated and targeted to the myelin membrane in transgenic mice. *J Cell Biol*. 123:443-54.

Wilson, R., and P.J. Brophy. 1989. Role for the oligodendrocyte cytoskeleton in myelination. *J Neurosci Res*. 22:439-48.

Xie, Y., J.P. Vessey, A. Konecna, R. Dahm, P. Macchi, and M.A. Kiebler. 2007. The GTP-binding protein Septin 7 is critical for dendrite branching and dendritic-spine morphology. *Curr Biol*. 17:1746-51.

Zacchetti, D., J. Peranen, M. Murata, K. Fiedler, and K. Simons. 1995. VIP17/MAL, a proteolipid in apical transport vesicles. *FEBS Lett*. 377:465-9.

Zorick, T.S., D.E. Syroid, E. Arroyo, S.S. Scherer, and G. Lemke. 1996. The Transcription Factors SCIP and Krox-20 Mark Distinct Stages and Cell Fates in Schwann Cell Differentiation. *Mol Cell Neurosci*. 8:129-45.

Zorick, T.S., D.E. Syroid, A. Brown, T. Gridley, and G. Lemke. 1999. Krox-20 controls SCIP expression, cell cycle exit and susceptibility to apoptosis in developing myelinating Schwann cells. *Development*. 126:1397-406.

11 Curriculum vitae

Name: Andres Michael Buser

Address: Güterstrasse 124
4053 Basel
Switzerland

Phone: +41-61-267 15 40
E-mail: Andres.Buser@unibas.ch

Native place: Känerkinden BL, Switzerland
Date of birth: October 30th 1979

Education:

May 2004 – now	PhD studies in Neurobiology, Postgraduate Program Biocenter, University of Basel
2003	Master in Neurobiology, Graduate Program Biocenter, University of Basel
1999 – 2003	Studies in Biology II, Graduate Program Biocenter, University of Basel
1998	Matura, focus Mathematics
1986 - 1998	Schools in Switzerland

Languages:
German (mother tongue)
English (Certificate in Advanced English Grade A)
French (Matura)

Professional experience:

2004 – Now	PhD thesis in the Neurobiology Laboratory, Department of Biomedicine, University Hospital Basel, supervisor Prof. N. Schaeren-Wiemers “The septin cytoskeleton is associated with distinct myelin structures of the central and peripheral nervous system”
2003/2004	Temporary employment, 5 months in the Department of Biotechnical Operations CH, Novartis Pharma AG, Basel “Modification of an operation protocol for BiotechOPs Switzerland”
2002/2003	Master thesis in the Neurobiology Laboratory, Department of Biomedicine, University Hospital Basel, supervisor Dr. N. Schaeren-Wiemers, co-examiners Prof. M. Rüegg and Dr. T. Meyer “Characterization of septin6 as a potential intracellular binding partner of MAL”
2002	Internship, 2 months in the Department of Neurobiology, UCLA Medical Center, Los Angeles “RNAi mediated downregulation of Parkin in hippocampal neurons”
2000	Temporary employment, 2 months in the Clinical Research UNIT, Swiss Pharma Contract, Basel Assistant Clinics and Laboratory
1999	Internship, 3 months in the Department of Biotechnology Development and Production, Novartis Pharma AG, Basel “Inducible expression of anti-apoptotic genes in SP2/0 transfectoma cell lines”

Publications:

Andres Buser et al., Nicole Schaeren-Wiemers. (2008). The septin cytoskeleton is associated with distinct myelin structures of the central and peripheral nervous system. Manuscript submitted

Andres Buser et al., Nicole Schaeren-Wiemers. (2008). MAL gene dosage determines the expression level of p75 neurotrophic receptor and thus regulates the progress of myelination in the peripheral nervous system. Manuscript in preparation. Submission planned June/July 2008

Presentations:

Mai 2008	Gordon Research Conference on Myelin, Il Ciocco, Italy Poster session "A complex scaffold of septin cytoskeleton proteins is expressed and developmentally regulated in myelinating cells and differentially interacts with myelin subcompartments" Andres Buser, Hauke Werner, Klaus-Armin Nave and Nicole Schaeren-Wiemers
November 2007	37th annual meeting of the Society for Neuroscience, San Diego Slide session 330.7 "Septin function in myelinating cells" Andres Buser and Nicole Schaeren-Wiemers
September 2007	8th European meeting on glial cells in health and disease, London Poster session Myelin B22 "The role of septins in myelinating cells" Andres Buser and Nicole Schaeren-Wiemers
May 2007	2nd International Meeting on septin biology, Monte Verita, Switzerland Poster session "The role of septins in myelinating cells" Andres Buser and Nicole Schaeren-Wiemers
January 2006	Joint Meeting Swiss Society for Neuroscience – Swiss Society for Neuroradiology, Basel Poster session "Are septins involved in trafficking of myelin proteins?" Andres Buser and Nicole Schaeren Wiemers
August 2005	7th Bi-annual ISN Satellite Meeting on Myelin Biology, Irsee, Germany Poster session "Are septins involved in trafficking of myelin proteins?" Andres Buser, Hauke Werner, Klaus-Armin Nave and Nicole Schaeren-Wiemers
February 2005	Joint Meeting Swiss Sociey for Neuroscience – Union of the Swiss Societies for Experimental Biology, Zurich, Switzerland Poster session "Are septins involved in trafficking of myelin proteins?" Andes Buser and Nicole Schaeren-Wiemers

PhD program related oral presentations:

October 2007	TGIF, Postgraduate Program Biocenter "Septin function in myelinating cells"
January 2007	Journal Club, Novel Literature in Neurobiology, Postgraduate Program Biocenter "A neurovascular niche for neurogenesis after stroke" J Neuroscience, 2006 26(50)

June 2004	Journal Club, Novel Literature in Neurobiology, Postgraduate Program Biocenter "Multiple spotlights of attentional selection in human visual cortex" Neuron, 2004 42(4), 677-686

Personal awards and grants:

Mai 2008	Travel Award of the International Society for Neurochemistry
August 2007	Travel Award of the Union of the Swiss Societies for Experimental Biology
Mai 2007	Travel Award of the Swiss Society for Neuroscience
April 2006	Stipend of the Swiss National Foundation: Three year PhD full-funding
March 2005	Stipend of the Roche Research Foundation: One year PhD full-funding

Expertise and Techniques:

Standard Cell Culture:
- Culturing of standard cell lines (COS7, NIH3T3, 293) and glial cell lines (Olineu, S16)
- Transfection, infection, immunohistochemical and morphological analysis

Primary Cell Cultures:
- Neonatal oligodendrocyte cultures
- Neurospheres including generation of OPCs and mature oligodendrocytes
- Schwann cell cultures
- Myelinating mouse DRG-Schwann cell co-cultures
- Myelinating mouse DRG-oligodendrocyte cell co-cultures

Retroviral Infection:
- Generation of retroviral constructs
- Culturing and transfection of the phoenix helper cell line
- Titration of retroviral supernatants
- Infection of cell lines and primary cells

Molecular Biology:
- Molecular cloning including database searches, subcloning, sequencing
- Quantitative real time PCR (Light Cycler) including RNA isolation, cDNA synthesis, data analysis
- Fusion protein constructs (GFP, mCherry, Myc, GST) including construct design and generation
- RNAi constructs including target sequence selection, transfection/infection, verification of knockdown

Biochemistry:
- Immunohistochemistry (cell cultures, tissue sections, teased nerve fibers)
- Western Blot analysis including ECL and fluorescent detection (Odyssey infrared imaging system)
- Northern Blot analysis including generation of DIG labeled riboprobes
- In situ hybridisation
- Recombinant protein production (GST fusion proteins)
- Antibody production including target selection, antibody purification, determination of specificity
- Immunoprecipitation
- Sample preparation for Mass Spectrometry
- GST pull down

Animal Work:
- Education: FELASA category B (mouse, rat, guinea pig, rabbit)
- Routine handling, intraperitoneal injections, perfusions etc
- Screening, breeding, maintenance and analysis of transgenic mice